THE DOMINANCE OF THE MANITOBA TYPE1 STRAIN: EXAMINING THE STRAIN-RELATED VIRULENCE OF A *MYCOBACTERIUM TUBERCULOSIS* ISOLATE.

BY

DENNIS P. PETRELLI

A Thesis
Submitted to the Faculty of Graduate Studies
In Partial Fulfillment of the Requirements for the Degree of

MASTER OF SCIENCE

Department of Medical Microbiology and Infectious Diseases
University of Manitoba
Winnipeg, Manitoba

THE UNIVERSITY OF MANITOBA

FACULTY OF GRADUATE STUDIES

*****

COPYRIGHT PERMISSION

THE DOMINANCE OF THE MANITOBA TYPE1 STRAIN: EXAMINING THE STRAIN-RELATED VIRULENCE OF A *MYCOBACTERIUM TUBERCULOSIS* ISOLATE.

BY

DENNIS P. PETRELLI

A Thesis/Practicum submitted to the Faculty of Graduate Studies of The University of Manitoba in partial fulfillment of the requirement of the degree

OF

MASTER OF SCIENCE

Table of Contents

Acknowledgements

I thank my supervisor, Dr. Amin Kabani, for being so patient, understanding and encouraging during my time under his supervision. Throughout my studies, his help, time and confidence in my ability have been invaluable in allowing me to succeed. I wish to thank him for not only providing me with access to state of the art technology and facilities to strengthen my growth as a microbiologist but also for allowing me to experience the other side of research through attending major microbiology conferences. I also thank him for all the hours he spent treating me like a colleague rather than his student even during difficult times when my research wasn't progressing well.

I thank the members of my committee, Dr. Grant McClarty, Dr. Xi Yang and Dr. Steven J. Jones for serving on my committee and for providing valuable suggestions, criticism and guidance during my studies.

I thank my family and close friends for their understanding and encouragement during my educational adventure, for sticking with me through my frustration, disappointment and excitement over many aspects of this project. I thank Alison Trethart, for her numerous morning wake-up calls, reminders and constant nagging, especially during the writing of this thesis in an attempt to keep me on track.

I owe thanks to each member, both past and present, of the National Reference Centre for Mycobacteriology for their incredible willingness to help trouble shoot or even just listen to my daily rants over my experiments. In particular, I thank Dr. Meenu Sharma for taking so much time from her own studies to take me under her wing and help me learn the basics so that I could succeed. I also thank Kym Blackwood-Antonation, whose patience in answering the millions of molecular questions I posed was exceptional and kind-hearted. I was truly fortunate to be able to "pick your mind" on a daily basis. Thanks to the ladies of the NCRM and HSC's superstar Nancy Smart for every small thing they did for me in containment and for understanding when I forgot or was delayed in doing my weekly duties. Your help was always appreciated.

I thank the staff and students of the Department of Medical Microbiology as well as the DNA Core Facility staff for all of their technical help and insightful discussions. In particular I would like to thank Steven Theriault for offering technical suggestions and research ideas and Nina Kuzenko for the hours of proof-reading and advice she gave me on so many papers and presentations.

I wish to express my special thanks to Cathy Whitelam, for going beyond the call of duty and helping me out immensely with everything from scheduling meetings to tracking down Dr. Kabani.

Lastly, I would like to thank everyone not specifically mentioned by name for helping me be the best grad student I could possibly be and for making this experience one I will always remember.

...Veni, vidi, vici...

- excerpt from Roman general Julius Caesar's message to the Roman senate describing his recent victory over Pharnaces II of Pontus in the Battle of Zela, 47 BC.

...I came, I saw, I conquered...

- excerpt from Encore by Jay-Z from his album, The Black Album, 2003.

List of Figures

List of Tables

List of Abbreviations

~	approximately
β	beta
δ	delta
°C	degrees Celsius
γ	gamma
∞	infinity
μ	micro
#	number
ϕ	phi
2DBGD	two-dimensional bacterial genome display
A	adenine
ABI	Applied Biosystems
ADC	albumin-dextrose-catalase
AFB	acid-fast bacilli
ANOVA	Analysis of Variance
ATCC	American Type Culture Collection
BD	Becton Dickinson
BCG	bacille Calmette-Guérin
BLAST	basic local alignment search tool
bp	base pair
C	cytosine
cc	cubic centimetre
CL3	containment level 3
CO_2	carbon dioxide
CSCHAH	Canadian Science Centre for Human and Animal Health
CTAB	cetyltrimethyl ammonium bromide
CFU	colony forming unit
DAP	Meso-diaminopimelic acid
DEPC	diethyl pyrocarbonate
dH_2O	distilled water
ddH_2O	double distilled water
DNA	deoxyribonucleic acid
dNTP	deoxynucleotide triphosphate
ECL	enhanced chemiluminescence
E. coli	*Escherichia coli*
EDTA	ethylenediamine tetraacetic acid
ESAT	early secretory antigenic target
FA	formaldehyde agarose
FasL	Fas ligand
FP	fingerprint pattern
g	gram
G	guanine
GI	growth index (radiometric)

Glu	glutamic acid
Gp	group
H_2O_2	hydrogen peroxide
HRP	horseradish peroxidase
HSC	Health Sciences Centre
IFN-γ	interferon gamma
IL	interleukin
IPTG	isopropyl-ß-D-thiogalactopyranoside
Kb	kilobases
IS	insertion sequence
L	litre
LB	Luria-Bertani
m	metre
M	Molarity
Mg^{2+}	magnesium ion
M. tb	*Mycobacterium tuberculosis*
M. tuberculosis	*Mycobacterium tuberculosis*
MAP Complex	mycolic acid-arabinogalactan-peptidoglycan complex
MB	Manitoba
min	minute
MOPS	3-(N-morpholino) propane-sulfonic acid
mRNA	messenger ribonucleic acid
n	nano
NaCl	sodium chloride
NaOH	sodium hydroxide
NCBI	National Center for Biotechnology Information
NK	natural killer cell
NML	National Microbiology Laboratory
NO	nitric oxide
NRCM	National Reference Centre for Mycobacteriology
NTM	Nontuberculous mycobacteria
ORF	open reading frame
PBS	phosphate buffered saline
PCR	polymerase chain reaction
Pro	proline
RFLP	restriction fragment length polymorphism
ROI	reactive oxygen intermediates
RNA	ribonucleic acid
RNI	reactive nitrogen intermediates
rRNA	ribosomal RNA
RT-PCR	reverse-transcriptase polymerase chain reaction
SCOTS	selective capture of transcribed sequences
SD	standard deviation
SDS	sodium dodecyl sulfate
sec	second
SH	subtractive hybridization

SOP	standard operating procedures
SSC	salt sodium citrate
SSH	suppression subtractive hybridization
T	thymine
TAE	tris acetate ethylene diamine tetraacetic acid
TB	tuberculosis
TBE	tris borate ethylenediamine tetraacetic acid
TE	tris ethylenediamine tetraacetic acid
Th1	Type 1 T-helper cells
Th2	Type 2 T-helper cells
TIGR	The Institute for Genomic Research
Tris	2-Amino-2-(hydroxymethyl)-1,3-propanediol
Tris-HCl	hydroxymethyl aminomethane hydrochloride
TNF-α	tumor necrosis factor alpha
U	unit
UV	ultraviolet
V	volts
X-Gal	5-bromo-4-chloro-3-indoyl-ß-D-galactopyranoside

ABSTRACT

Mycobacterium tuberculosis is one of the most prolific pathogens in the world, estimated to have caused infection in one-third of the world's population and accounting for 3 million annual deaths. IS*6110* RFLP analysis conducted on all Manitoban isolates from 1992-99, identified a single dominant fingerprint pattern, designated Type1, which accounted for 25.8% of the total TB cases reported and caused a significant clinical impact on the treaty-status population of the province. The predominance and widespread occurrence of this isolate has been speculated to be as a result of a hypervirulent nature of the organism brought about by strain-specific virulence factors, which affect the manifestation and progression of disease in the host.

In order to investigate the predominant and hypervirulent nature of the Type1 strain, survival studies in 3 mouse models of differing genetic make-up, immunity and tolerance to challenge by *M. tuberculosis* were performed and confirmed that Type1 is hypervirulent in comparison to other common clinical isolates encountered within the province. Histological analysis of lung sections revealed that when comparing the granulomatous response in C3H and BALB/c mice, two distinct patterns of inflammation were observed. A semi-quantitative RT-PCR approach was employed with the purpose of correlating the observed granulomatous responses with cytokine mRNA levels from lung homogenates with regard to establishing a conclusive linkage.

The search for a plausible explanation for the overwhelming dominance of the Type1 strain was initiated using a suppression subtractive hybridization strategy in an attempt to identify strain-specific virulence factors present within the Type1 genome, which potentially may be the source of the hypervirulence of this strain.

1. INTRODUCTION

1.1 *Mycobacterium tuberculosis*

Mycobacterium tuberculosis is one of the most prolific and poorly understood pathogens in the history of mankind. Evidence from ancient mummies, has shown that this bacterium and its associated disease have been plaguing humans for at least 4000 years (*Tuberculosis,* 1996). Not surprisingly, *Mycobacterium tuberculosis* is the most common cause of death among adults due to a single bacterial organism. It is estimated that one-third of the world population is infected with *Mycobacterium tuberculosis* and that each year 3 million deaths are attributed to its associated disease (Kochi, 1991; Sudre, *et al.*, 1992; Dolin, *et al.*, 1994; Raviglione, *et al.*, 1995).

Within the family *Mycobacteriaceae*, *Mycobacterium tuberculosis* belongs to the same genus as several other mycobacteria, collectively known as Nontuberculous mycobacteria (NTM), of which most are capable of causing pulmonary disease. However, this bacterium can best be described taxonomically as a member of the *Mycobacterium tuberculosis* complex. This complex consists of several members who are capable of causing a similar type of disease but are associated with a specific primary host (Cousins, *et al.*, 2003). Members include: *M. bovis* (cattle), *M. microti* (voles), *M. caprae* (goat) and *M. pinnipedii* (seal). Although other members of the complex such as *M. canettii* and *M. africanum* are responsible for human infections (the latter typically in Africa), *M. tuberculosis* is the major human pathogen.

In 1882, Robert Koch demonstrated that this pathogen is the etiological agent responsible for causing the disease tuberculosis (Fenton and Vermeulen, 1996). Tuberculosis (TB) can best be characterized as a chronic, infectious disease that primarily

attacks the lungs but in reality can attack almost any part of the body. Typically, individuals who are simply infected with the bacterium will show no symptoms but an individual with active disease may display symptoms which appear to consume people from within or waste them away, such as: weight loss, fatigue, loss of appetite, fever and coughing up blood.

1.2 The Bacterium

Mycobacterium tuberculosis is a slow growing aerobic, intracellular pathogen. Typically, the generation time for this bacterium is extremely slow in comparison to other bacteria ranging from 12-20 hours depending on growth conditions. Visible colonies can be detected 3-4 weeks post-inoculation when grown on appropriate media under optimal conditions. The tubercle bacilli are slender, slightly curved or straight, non-spore forming and non-motile rods measuring 0.2-0.7 X 1.0-10 μm (*Bergey's Manual of Determinative Bacteriology*, 1993). The distinguishing characteristics of *Mycobacterium tuberculosis* are the complexity and composition of its cell wall, which essentially differentiates mycobacteria from other prokaryotes. Although mycobacteria may be classified as gram-positive organisms as they produce a weakly positive response to the gram stain, the composition of the mycobacterial cell wall contains properties of both gram-positive and gram-negative bacteria. The basic structure of the cell wall is typical of gram-positive bacteria but also includes meso-diaminopimelic acid (DAP) and an outer lipid barrier, common features of gram-negative bacteria (*Tuberculosis*, 1996). Additionally, the most important features of the mycobacterial cell wall are the unique waxy and lipid rich mycolic acids, which make up 60% of the cell wall components. The mycolic acids are

the backbone of the MAP complex, a mixture of mycolic acids, arabinogalactan and peptidoglycan which form the protective lipid barrier that the organism utilizes for endogenous resistance to common antibiotics and detergents which allows it to survive even in a desiccated state (*Tuberculosis*, 1996; Crick, *et al.*, 2001). Therefore, based on this compositional complexity, staining techniques used to identify *Mycobacterium tuberculosis,* such as Ziehl-Nielsen staining, use certain stains that are retained following treatment with acidic solution and accordingly tubercle bacilli are referred to as acid-fast bacilli (AFB).

1.3 Course of Infection and Disease

1.3.1 Transmission

Mycobacterium tuberculosis infections are primarily acquired via aerosol transmission of infectious bacilli. Specifically, transmission occurs through droplet nuclei, 5 μm in size, which may contain up to 10 bacilli (*Tuberculosis*, 1996). When an individual with active TB comes in close contact with another person, these droplets are expelled during coughing, sneezing, spitting or even just casual talking. During these encounters, a single organism may be enough to cause an infection, but in reality, a dose of 5-200 bacilli is required for a human infection to occur (Dannenberg, 1989). The probability that such an exposure will result in a transmission and consequently, an infection depends on several factors including: the infectiousness of the person, the duration and environment of the exposure along with the relative virulence of the *M. tuberculosis* strain involved. It is believed that left untreated, an individual with active TB, can annually infect between 10-20 additional people. In addition, *M. tuberculosis*

infections can also be acquired through accidental or direct inoculation, typically in a laboratory setting.

1.3.2 Primary Infection

Approximately 5-10% of individuals infected with *Mycobacterium tuberculosis* will develop active disease while for the remainder, either the bacilli will simply be cleared with no evidence of infection or a latent infection with no disease manifestation will occur (Comstock, 1982). In those individuals who do go on to develop the disease, the tubercle bacilli once inhaled, eventually reach the pulmonary alveoli where they clump together on the host tissue and are internalized by alveolar macrophages. Within the macrophages, the bacilli are able to replicate and the initial infection foci continues to expand as more macrophages and lymphocytes home towards the infection site. This cell-mediated response generally can take from 2 to 8 weeks to occur and this aggregation of immune cells along with fibroblasts and epithelioid cells produces the granulomatous inflammatory conditions typically observed in tuberculosis cases (*Tuberculosis*, 1996). The recruitment of these cells and the formation of the tubercle or granuloma serve to seal off the bacteria and functions to prevent the metastasis of the infection throughout the body (Figure 1). At this point, the granuloma is transformed into scar tissue, the bacilli become dormant and the rest of the body is spared any further damage.

1.3.3 Dormancy and Reactivation

Although the granuloma serves as an area for cell-to-cell communication and to prevent the dissemination of the infection, the granuloma also seems to protect the bacilli from the destructive power of the immune system and supports limited growth. This apparent shielding of the bacilli is potentially the reason why *M. tuberculosis* is capable of entering a latent state and persisting within the granuloma for many years or even decades.

Provided that an individual's immune system remains strong and uncompromised, *Mycobacterium tuberculosis* will persist within the granuloma in its latent state and have little to no effect on the host. However, when there is deterioration in host immune status as a result of factors such as old age, malnutrition, chemotherapy and simultaneous infection with the human immunodeficiency virus, reactivation of disease can occur. In such a situation, the granuloma caseates and spills its bacilli filled pus, producing additional tubercles and infecting other regions of the lungs and body. Further scarring, cavity formation and destruction of bronchial walls takes place as lung tissue destruction and necrosis is observed as the bacilli multiply in the extracellular environment. This active form of disease provides the perfect conditions for the bacilli to be transmitted via aerosols as the newly infectious individual coughs up the bloody sputum released from the numerous necrotic material containing cavities.

1.4 Host Responses to *Mycobacterium tuberculosis* Infection

The host-pathogen interaction is a delicate balance that determines whether an infection with *Mycobacterium tuberculosis* progresses onto active disease or is controlled

by the host's immune response (Barnes, *et al.*, 1992a, 1992b). The host response must attempt to counteract the various evasion and defence mechanisms employed by the TB bacilli while regulating its own response to prevent excess harmful tissue damage when contributing to the elimination of bacilli (Barnes, *et al.*, 1993b). Cell-mediated immunity forms the backbone of protection against TB disease, particularly macrophages and T-lymphocytes whose production of specific cytokines early during infection, play a vital role in the outcome of the infection. Although the belief exists that the induction of certain cytokines, either of a Th1 or Th2 nature, exert potent immunoregulatory effects during TB disease (*Tuberculosis*, 1996), recent work performed by Kevin Urdahl (Seattle, Washington) has highlighted a new theory which suggests the potential role of T regulatory cells in suppressing optimal immune responses and thus shaping the clinical manifestations observed during disease (Kaufmann, *et al.*, 2005)

Following ingestion of bacilli by macrophages, production of IL-2, a Th1 cytokine responsible for T-cell growth and increased macrophage activation (*Tuberculosis*, 1996), leads to increased numbers of T-Lymphocytes. The numerous T-lymphocytes then produce macrophage activating factors that in conjunction with the autocrine activity of IL-2, stimulate macrophages to aggregate in order to form the granuloma but also to carry out effector mechanisms on the ingested bacilli. Macrophages, once activated in this manner, use reactive oxygen and nitrogen intermediates (ROI and RNI respectively) in an attempt to eliminate the bacilli. Although the activated macrophages utilize mechanisms to clear the bacilli, the bacilli also seem to be able to survive and grow within the macrophages by inhibiting macrophage function. In addition, recent evidence describing clinical *M. tuberculosis* isolates prevalent within

the human population who are resistant to RNI (Firmani and Riley, 2002), indicate that the interaction between the bacilli and the host response is not simply one-sided.

IL-12 is another important cytokine produced by activated macrophages and dendritic cells that plays an important role in the protection and subsequent clearance of *M. tuberculosis* (Wozniak, *et al.*, 2006). IL-12, primarily has two functions in tuberculosis protection. First, IL-12 may act on precursor T-cells to favour their development into Th1 cells, which are critical in the protective response. Secondly, IL-12 enhances the production of interferon gamma (IFN-γ) as well as enhancing the cytolytic effector function of Natural Killer (NK) and CD8+ T-cells (Gazzinelli, *et al.*, 1993; Fulton, *et al.*, 1996). CD1 restricted CD8+ T-cells, which recognize glycolipids present within the mycobacterial cell wall, have also been implicated in the protective response against TB but their role remains not completely understood (Kaufmann, 2004; Raja, 2004). Additionally, toll-like receptors play a critical part in the innate response by activating cells through recognition and signalling (Raja, 2004; Ryffel *et al.,* 2005) so that cells of the innate immune response can provide an initial defense until adaptive responses like CD4+ T-cells who function as effector cells using the Fas-FasL mechanism (Stenger and Modlin, 1999) and γδ T-cells who function as cytolytic killer cells, can occur.

Besides their role as cytolytic effectors, NK and T-cells are also major sources of IFN-γ, a cytokine that has a critical role in tuberculosis protection (Fenton, *et al.*, 1997). IFN-γ works in synergy with another factor, TNF-α, in the formation of both the granuloma and RNI. In addition, studies involving GKO mice, which fail to produce IFN-γ, have revealed how critical this cytokine is with respect to *M. tuberculosis* infection as

these knockout mice suffer severe disease and fail to develop any resistance to infection (Flynn, *et al.*, 1993).

Although many of the host responses seen following infection with *M. tuberculosis* seem to deal with the activation of effector cells, perhaps more importantly is the production of factors such as TNF-α and chemokines such as IL-8 and RANTES which are responsible for the aggregation and migration of cells to form the granuloma (Raja, 2004).

Even though the host is capable of mounting all of these activities during the host response, the outcome of a *M. tuberculosis* infection does not always result in clearance as the bacilli also influences the host response. As well as inhibiting microbicidal activity of macrophages, TB bacilli also induce the production of certain cytokines that act to inhibit, down-regulate and prevent activities of the protective response. IL-10, an anti-inflammatory cytokine produced by macrophages, down-regulates IL-12 and prevents lymphocyte proliferation (Raja, 2004). Additionally, IL-5, which can also be induced and produced by Th2 cells, can support B-cell growth and differentiation thus swaying the immune reaction away from the protective cell-mediated response and more towards a humoral response (*Tuberculosis: Pathogenesis, Protection, and Control*, 1994). It has been shown that the upregulation of IL-5, IL-10 and IL-13 occurs in macrophages infected with virulent strains of *M. tuberculosis* (Freeman *et al,* 2006).

Although newly described cytokines have added to the insight of the pathogen-host interaction, the complexity of the interaction remains great as new discoveries challenge the original Th1/Th2 paradigm of TB control and protection. IL-15, a pro-inflammatory cytokine, produced by monocytes and macrophages, induces T-cell

proliferation and the induction of other pro-inflammatory cytokines such as IL-12 and IL-17 (Abebe *et al.,* 2005). Based on the Th1/Th2 paradigm, it would be assumed that IL-15 would be protective but in fact since IL-15 is an important trigger for IL-17 mediated pulmonary inflammation and due to the overexpression of other pro-inflammatory cytokines mediated by IL-15, it has been shown that IL-15 fails to resolve *M. tuberculosis* infection in mice via a Th1-mediated immunity (Abebe *et al.,* 2005).

Other cytokines such as IL-23 and IL-27 have recently been brought into focus with regard to TB. These cytokines induce T-cell proliferation and cytokine production as well as mediating inflammatory responses and have been shown to contribute to protection against TB disease and control mycobacterial growth but again are not entirely essential to the process as their absence does not make knockout mice more susceptible to progressive disease (Happel *et al.,* 2005; Khader *et al.,* 2005; Wozniak *et al.,* 2006). Therefore despite new information on the host response, the complex relationship between TB control or disease progression remains a discovery in progress.

1.5 TB Genetics

In 1998, scientists at the Sanger Center achieved perhaps the most important development in TB research since Koch's discovery of *M. tuberculosis* as the causative agent responsible for TB disease. The complete DNA sequencing and annotation of the H37Rv genome revolutionized the field of TB genetics which had previously been neglected due to the difficulty of working with *M. tuberculosis* and the lack of adequate tools (Smith, 2003).

Originally, the H37Rv genome was reported to contain 4,411,529 base pairs of which the G+C content was 65.6%. Annotation of the sequence revealed 3924 open reading frames (ORF) from which 50 genes coded for functional RNA molecules present within the genome (Cole, *et al.*, 1998). Initial investigation proposed that 40% of predicted proteins matched proteins of known function, 44% matched hypothetical unknown proteins and 16% had no homology match to known proteins. Since the release of the original sequence, re-annotation of the genome has identified an additional 82 protein-coding sequences and currently it is possible to assign a function to 52% of predicted proteins (Camus, *et al.*, 2002). Additionally, two prophages have been located within the genome although no plasmids have been detected (Cole and Barrell, 1998).

Several unique features have been observed within the H37Rv genome. A large portion of the coding capacity of the genome is devoted to the production of enzymes involved in fatty acid metabolism. In fact, 250 genes have been described within the *M. tuberculosis* genome, nearly five times the amount seen in *Escherichia coli* (Cole, *et al.*, 1998; Manabe, *et al.*, 2002). Another unique feature of the H37Rv genome is the presence of two unrelated groups of glycine-rich proteins. The PE and PPE proteins, named respectively due to the presence of Pro-Glu and Pro-Pro-Glu sequences found in conserved N-terminal regions, together make up approximately 4% of the genes in *M. tuberculosis* (Smith, 2003). Although the function of these proteins is still unknown, it has been speculated that these proteins may be a potential source of antigenic variation (Cole and Barrell, 1998).

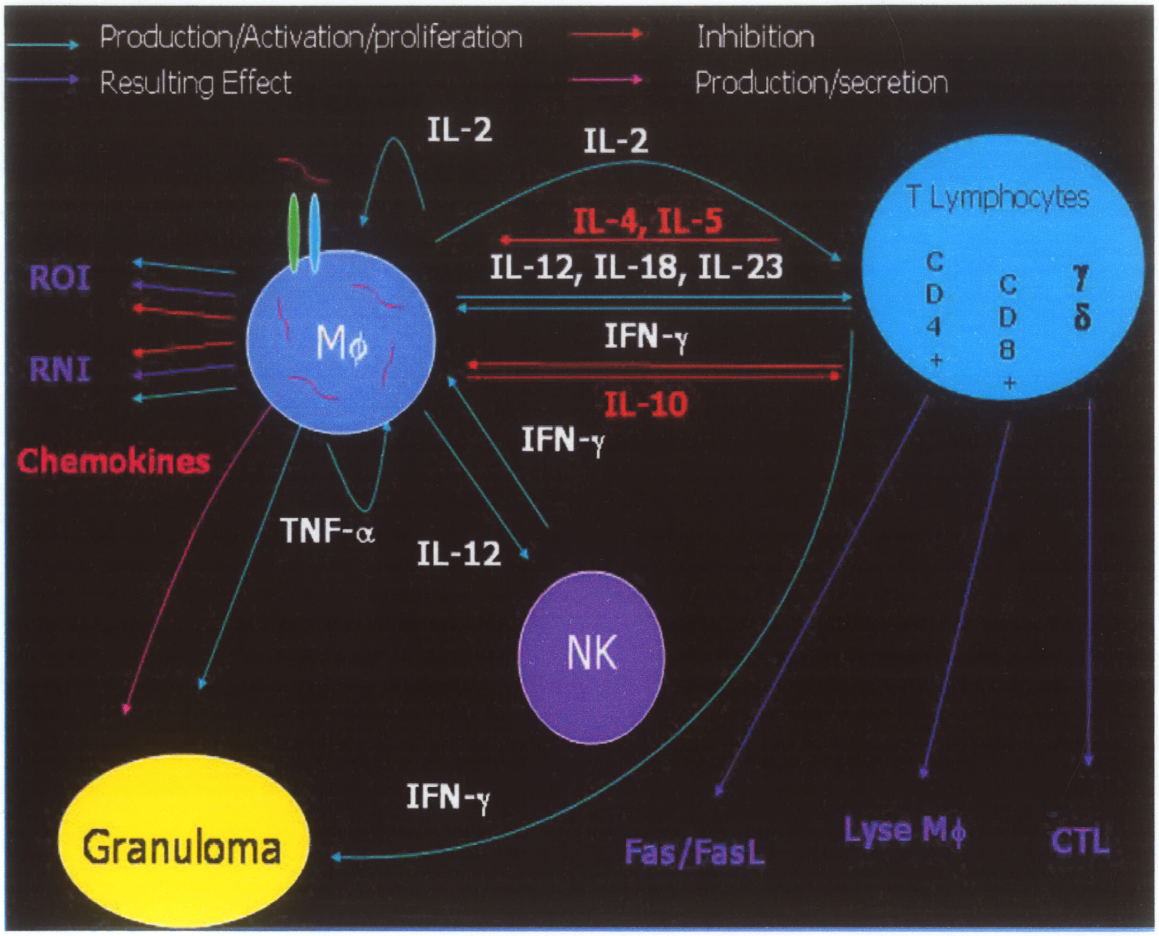

Figure 1. Nature of the host response following infection with *M. tuberculosis*. The complex yet delicate balance between activation and inhibition of the host response determines either the successful clearance or progression onto active TB disease following infection.

The most interesting discovery made from the completion of the *M. tuberculosis* genome was the remarkable lack of diversity observed at the nucleotide level, an aspect that potentially can be exploited for future vaccine development. In reality, the primary source of polymorphisms within the *M. tuberculosis* genome stem from insertion or deletion events caused by the numerous insertion sequences present (Cole and Barrell, 1998; Brosch, *et al.*, 2001). In addition to IS*6110* and IS*1081*, 32 different insertion sequences have been identified within the genome (Cole, *et al.*, 1998). This striking lack of diversity has even led to the proposition that the *M. tuberculosis* genome is either uncommonly inert or is relatively young with respect to evolution (Kapur, *et al.*, 1994; Sreevatsan, *et al.*, 1997).

Comparative genomics have also revealed information about *M. tuberculosis* in terms of the virulence of the organism. Comparative studies involving BCG vaccines or *M. tuberculosis* isolates have demonstrated that the accumulation of deletions generally reduces the virulence of the strain (Behr, *et al.*, 1999; Behr, 2001; Kato-Maeda. *et al.*, 2001). Currently, these observations fit with respect to the sizes of the three strains of *M. tuberculosis,* H37Rv, CDC1551 and 210, that have already been completely or partially sequenced where 210, a more virulent strain compared to H37Rv and CDC1551, is estimated to be slightly larger in terms of base pairs (Cole, *et al.*, 1998; Fleischmann, *et al.*, 2002).

Table 1. Genome Information of three *Mycobacterium tuberculosis* isolates

Strain	Sequence Info	Length (bp)	TIGR assigned genes	TIGR genes assigned a role	Reference
H37Rv	1998 by Sanger Institute	4411529	4220	2867	Cole *et al.* Nature 393,537-544
CDC1551	2001 by TIGR	4403837	4245	2583	Fleischmann *et al.* J Bacteriol 184, 5479-90
210	*2004 by TIGR	~4447000	Unknown	Unknown	N/A

* Data for the 210 strain is preliminary from 2004 with the completion of the entire sequence estimated for 2006.

1.6 Mouse Model of TB Infection

Throughout the history of TB research, various animal models have been employed in an attempt to understand several aspects of TB disease including pathogenesis, virulence and host immune responses. Three main animal models: rabbits, guinea pigs and mice, have primarily been used although models utilizing rats and monkeys have also been attempted (*Tuberculosis*, 1996). Although each of the main animal models have their own advantages and disadvantages, the use of mice has become the preferred model and a wealth of knowledge concerning tuberculosis has been gained over the past several decades. Even though the guinea pig model is the best choice for examining a progressive infection which resembles active TB disease in humans (*Tuberculosis*, 1996) and the rabbit model provides the best comparison to humans when evaluating granulomas in active disease (Smith, 2003), mice still provide researchers with an excellent model that compares well to humans who generate a strong immune

response against *M. tuberculosis* infection and do not go on to develop active disease (*Tuberculosis*, 1996). The availability of inbred mice with well defined genetics along with the newer knockout versions have made mice vital in immunological studies involving *M. tuberculosis*. Additionally, the relatively cheap purchase and maintenance price, the ease at which mice can be worked with, along with the availability of immunology-based reagents, such as monoclonal antibodies, for the mouse model provide further reasoning for mice being the most frequently used model (*Tuberculosis: Pathogenesis, Protection, and Control*, 1994; Smith, 2003).

In terms of virulence studies, the mouse model has one major advantage over all other models. Various inbred mice, which differ in both their genetic make-up and susceptibility to challenge by *M. tuberculosis,* can be purchased in order to study infection *in vivo* (Medina and North, 1998; Talaat, *et al.*, 2004). The advantage of being able to use strains with a wide range of susceptibilities, including sensitive C3H or resistant C57BL/6 mice not only allows the virulence of the organism to be investigated but also permits the examination of the host-pathogen interaction (Smith, 2003).

1.7 Epidemiology of Tuberculosis in Manitoba

Despite worldwide improvements in both the surveillance and treatment of tuberculosis during the past century, the ultimate goal of global TB control and the eventual eradication of the disease have yet to be achieved. Throughout the history of Canada, tuberculosis has been a major cause of concern in terms of morbidity and mortality for Canadians. In the Canadian province of Manitoba, epidemiological analysis has revealed that in terms of numbers and population distribution, TB does not see the

large impact of immigration on disease seen in other provinces although the burden of disease on aboriginals remains high. From January 1, 1992 to December 31, 1999, 855 cases of TB were reported in the province. Unlike the majority of the nation, where most cases are generally associated with foreign-born individuals (Health Canada, Population and Public Health Branch, 1998), only 29.4% of the cases in Manitoba were classified as foreign-born, meaning the bulk of TB cases (70.6%) were native to Canada (Blackwood, *et al.*, 2003). Even more striking is the fact that almost half (44.4%) of the total patients in the province were treaty status individuals (Blackwood, *et al.*, 2003). TB incidence rates in Manitoba are higher than in the majority of the country. During the period from 1992-99, the provincial incidence rate was 9.2 per 100,000, higher in comparison to the national rate of 5.9 per 100,000 in 1998 (Health Canada, Population and Public Health Branch, 1998; Blackwood, *et al.*, 2003). A more extensive examination of incidence rates within particular subgroups of the population reveals the true nature of the disease in Manitoba. The incidence rate for tuberculosis for Canadian-born treaty status individuals was 48.4 per 100,000, a value more than ten times higher than among Canadian-born non-treaty status individuals (3.3 per 100,000) and more than double compared to foreign-born individuals (22.0 per 100,000). Interestingly, the rate for Canadian-born treaty status individuals in selected northern communities soars to greater than 490 per 100,000 (Blackwood, *et al.*, 2003).

From the 855 cases of tuberculosis documented between 1992-99, 629 isolates (73.6%) were available for IS*6110* RFLP (IS*6110* Restriction Fragment Length Polymorphism) analysis yielding 249 different fingerprint patterns. The four most common fingerprints (Type1: 25.8%, Type2: 5.1%, Type5: 4.8%, and Type72: 3.5%)

account for 39.2% of the cases studied. The dominant or most commonly encountered isolate, the Type1 strain, accounted for 162 of the total cases in Manitoba. In addition to its overall presence in the province, Type1 is also over-represented in the treaty status population, accounting for 75.3% (122 of 162) of the cases (Blackwood, *et al.*, 2003). Within the province, individual isolates encountered tend to be situated around a particular area. When the geographical distribution of Type1 is examined, the trend of localization around a certain site is not observed; rather this strain tends to have a ubiquitous distribution (NRCM unpublished data).

Recent data has demonstrated that even though the incidence rate in Canada continues to decrease, 5.5 per 100,000 in 2001, the incidence of TB in Manitoba has experienced an opposite effect and has increased to 10.0 per 100,000 (Health Canada, Population and Public Health Branch, 2001). In the years following the initial data analysis of the molecular typing of isolates from Manitoba, new data has shown that a few of the most commonly encountered isolates within the province from 1992-1999 no longer rank within the top five most prevalent strains. However, in the case of FP1, preliminary data has revealed that not only has this strain remained the most dominant and widely encountered isolate in the province but an increase in the percentage of cases associated with this strain has also been observed (NRCM unpublished data).

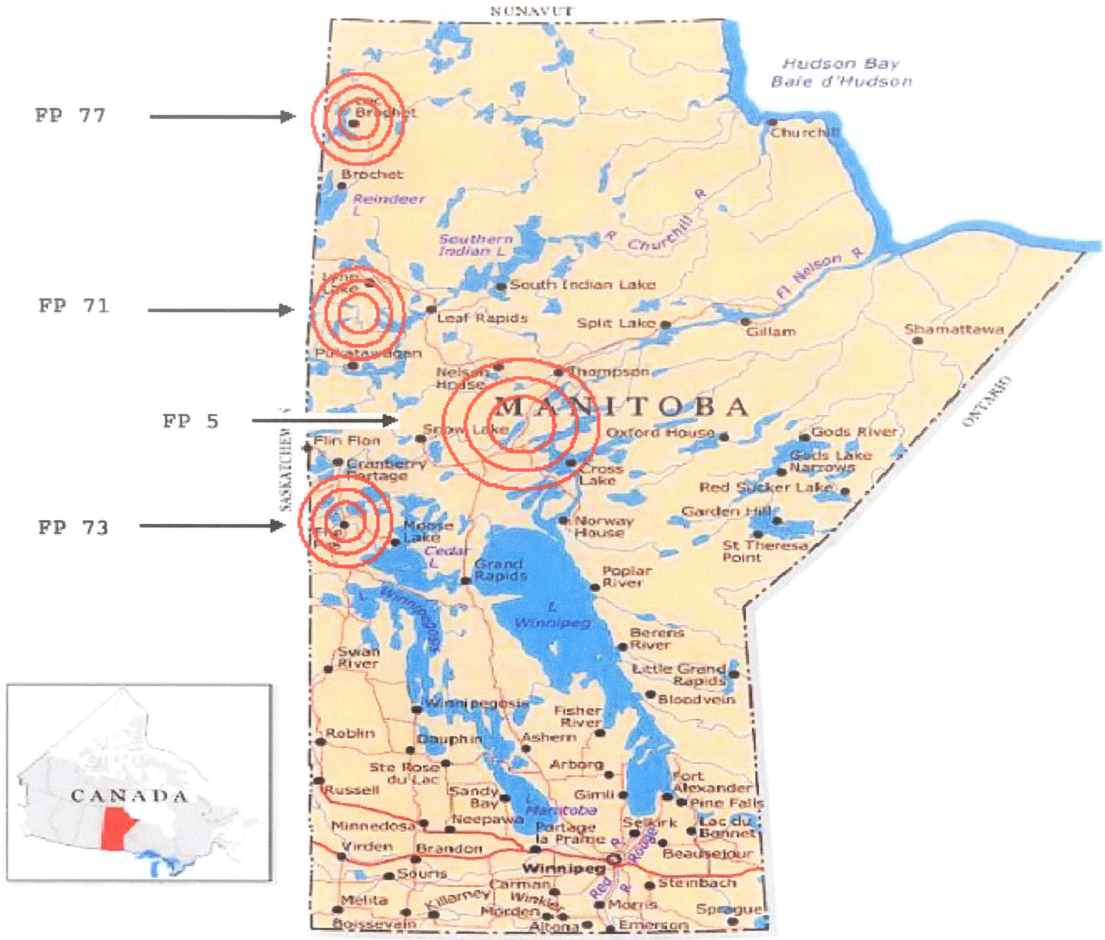

Figure 2. Geographical localization of *M. tuberculosis* isolates in Manitoba. Individual *M. tuberculosis* isolates from Manitoba usually bunch around a particular locale. However, FP1, the most commonly encountered strain in the province does not tend to localize but rather has a ubiquitous distribution.

Table 2. Comparison of the Top 5 most prevalent strains in Manitoba

1992-1999			1992-2003		
Strain	**# of Cases**	**%**	**Strain**	**# of Cases**	**%**
FP1	162	25.8	FP1	317	28.8
FP2	32	5.1	FP2	59	5.3
FP5	30	4.8	FP5	57	5.2
FP72	22	3.5	FP77	37	3.4
FP71	15	2.3	FP15	32	2.9

1.8 Strain-Related Virulence

The analysis of molecular typing data from the province of Manitoba has revealed the highly successful nature of a particular isolate, the Type1 strain. Although socio-economic factors, such as poverty, malnutrition and over-crowding, which occur throughout the province, especially in selected northern communities and on reserves, play a role in the spread of Type1, the exact reason for the widespread occurrence and overwhelming dominance remains unknown. Several potential suggestions have been proposed in an attempt to explain the prevalence of Type1 in order to facilitate the improvement of therapy and treatments as well as gaining new insight towards vaccine development.

It was speculated that perhaps the dominance of Type1 was simply a case of this strain being the first to be introduced into the Manitoban population. However, without sufficient typing data, such an assumption is difficult at best to justify. Another thought

of reasoning was that the prevalence of Type1 stemmed from natural selection. The idea suggested that administration of the BCG vaccine to treaty status infants may have increased protection against other susceptible strains through selective immunity, thus allowing Type1 to more readily establish itself within the province (Blackwood, *et al.*, 2003). Although these two explanations are plausible, the case numbers and population distribution of Type1 indicates that a possible unique interaction between the host and pathogen may be a more feasible theory. If an interaction between the bacilli that are trying to colonize and the host trying to eliminate them is taking place, then an imbalance in this interaction must be occurring for one strain to be so dominant. Accordingly, the genetic make-up of the host and bacterial virulence factors provide the most logical and probable rationales to the dominance of Type1 in Manitoba.

In the late 1990s, the research focus of strain-related virulence became prominent in tuberculosis pathogenesis studies. The introduction and characterization of two putative hypervirulent outbreak strains from the United States, CDC1551 and HN878, in the literature (Valway, *et al.*, 1998; Manca, *et al.*, 1999, 2001), provided the basis to suggest that strain-related virulence may be occurring in this Manitoban strain. Initial *in vitro* infections of monocyte cell lines performed by Dr. Meenu Sharma at the National Reference Centre for Mycobacteriology, demonstrated that pro-inflammatory cytokine secretion is suppressed in Type1 infected cultures compared to H37Rv and H37Ra infected cultures (Sharma, *et al.*, 2003). Additional animal survival data from the BALB/c mouse model has also shown that Type1 infected mice displayed an early mortality and a more rapid transition from a Th1 to Th2-type immune response in the lungs in comparison to H37Rv infected mice (NRCM unpublished data). Presented with

these suggestions of hypervirulence in other clinical isolates along with initial Type1 results, the highly successful pathogenesis of the Type1 strain may be dependant on unknown strain-specific virulence factors that interact with the host. In addition, these factors may modulate the host immune response and confer strain related advantages such as increased transmissibility, infectivity or the ability to replicate longer and to greater numbers that allow for greater prevalence of the Type1 strain in Manitoba.

1.9 Hypothesis

The widespread occurrence and overwhelming dominance of the Type 1 strain is a result of strain-specific bacterial virulence factors.

1.10 Thesis Objectives

The overall goal of this project was to provide an explanation for the spread and dominance of the Type1 strain throughout the province of Manitoba. Specifically, the concept of strain-related virulence was targeted as the primary research focus as it had recently emerged in the literature as a viable explanation in tuberculosis pathogenesis (Manca, *et al.*, 1999, 2001). To meet this goal, specific objectives were outlined:

- To confirm the putative hypervirulence observed in *Mycobacterium tuberculosis* Type1 strain in comparison to other common clinical isolates from Manitoba by conducting survival studies in three mouse models that differ in genetic make-up, immunity and tolerance to challenge by *M. tuberculosis*.

· To determine whether the enhanced virulence of Type1 can be attributed to a higher growth rate by evaluating the growth of this strain in the lungs compared to other isolates.

· To assess lung pathology using histological analysis in order to further characterize the progression and disease manifestation of pulmonary tuberculosis caused by this strain.

· To investigate the relationship between the manifestation of disease caused by Type1 and the extent of the host immune response by evaluating cytokine mRNA levels from lung homogenates.

· To identify strain-specific bacterial virulence factors that may be a potential source of the apparent hypervirulence of Type1 using the suppression subtractive hybridization (SSH) method.

2. MATERIALS AND METHODS

2.1 Bacterial Strains and Growth Conditions

Handling of all *Mycobacterium tuberculosis* strains was performed under Containment Level 3 (CL3) conditions at the National Microbiology Laboratory in Winnipeg, Manitoba, Canada as outlined in an in-house Standard Operating Procedures (SOP) from the National Reference Centre for Mycobacteriology. Additional CL3 handling procedures that were implemented are outlined in the Health Canada Laboratory Biosafety Guidelines 2nd Edition, 1996 (http://www.phac-aspc.gc.ca/publicat/lbg-ldmbl-96/index.html).

2.1.1 Preparation of Bacterial Cultures for Aerosol Infections

M*ycobacterium tuberculosis* isolates were obtained from the Health Sciences Centre (Winnipeg, MB). *Mycobacterium tuberculosis* strains H37Rv (ATCC 27294), Manitoba Type1 (#2950), Type2 (#2936), Type5 (#2739) and Type72 (#1367) were initially grown in Middlebrook 7H12 broth in 12B vials (BD Diagnostics) at 37°C until reaching a radiometric growth index (GI) of 999. For each strain, 0.1 cc of 12B broth was plated on Middlebrook 7H10 media plates (Appendix 2) and grown for 3-4 weeks or until sufficient growth had occurred at 37°C with 5% CO_2. Single colonies for each strain were picked and placed in water with beads, then vortexed for 1-2 minutes. Three to four drops of bacterial suspension was added to Middlebrook 7H9 broth with ADC enrichment (Appendix 2) and grown at 37°C with 5% CO_2 for 2-3 weeks. Additionally, in order to confirm that each strain was pure, separate blood agar plates containing 5% sheep blood were inoculated with either 2 drops of culture from the initial water with beads

suspension or from the Middlebrook 7H9 broth cultures. Blood agar plates were incubated at 37°C and checked for growth daily for up to 72 hours. To ensure that bacilli were as close as possible to their initial compositional state as when they were obtained in the clinical setting, frozen cultures were thawed then grown in the absence of Tween 80 since this detergent has been shown to effect the composition of the cell wall, specifically by causing a decrease in the surface expression of arabinomannan (Schwebach, *et al.*, 2001). In addition, Tween 80 does not totally alleviate the challenge of bacterial clumping and may cause a reduction in virulence of mycobacteria (Collins, 1984; Masaki, *et al.*, 1990). To assure that clumping was not an issue, cultures were subjected to daily agitation and smears of the inoculum were prepared to visually check for excessive clumping. Cultures were centrifuged, washed twice in phosphate buffered saline (PBS) and matched in turbidity to a McFarland Standard #1 suspension.

2.1.2 Maintenance of Cultures for DNA and RNA Manipulations

To guard against any potential attenuation due to repeated passages or alterations of possible virulence factors, cultures of *Mycobacterium tuberculosis* H37Rv and Type1 were inoculated into Middlebrook 7H12 broth in 12B vials and then maintained at 37°C for up to 10 weeks before being freshly subbed into new vials. For all DNA and RNA manipulations, cultures were prepared by spreading 0.2 cc of organism containing 12B broth onto Middlebrook 7H10 agar plates and incubating them at 37°C with 5% CO_2 for 2-3 weeks prior to any extractions procedures.

2.2 IS*6110* Restriction Fragment Length Polymorphism

2.2.1 Concept

In order to differentiate various strains of *Mycobacterium tuberculosis*, Restriction Fragment Length Polymorphism analysis, a procedure where extracted DNA is digested with restriction enzymes, separated by gel electrophoresis, southern blotted onto a membrane and then probed with a specific labelled fragment, has been employed to generate highly polymorphic patterns based upon a repetitive DNA element present within the *M. tuberculosis* genome. RFLP analysis in *M. tuberculosis* is based on IS*6110*, a 1,355 bp insertion sequence widely found within the *M. tuberculosis* complex and present within the *M. tuberculosis* genome ranging from 1 to 20 copies (*Tuberculosis*, 1996). The success of the IS*6110* RFLP procedure in *M. tuberculosis* analysis can be attributed to the use of *Pvu* II as the restriction enzyme since it cleaves the insertion sequence in only one spot and permits the use of a DNA probe that hybridizes to the right side of the cleavage site thus minimizing the number of bands to be analyzed (Tuberculosis, 1996; van Soolingen, *et al.*, 1994).

2.2.2 Isolation of Genomic DNA from *Mycobacterium tuberculosis*

For each *M. tuberculosis* strain, once sufficient growth was obtained as described in section 2.1.2, two heaping loopfuls of cells were added to 500 µl of 1X TE (Appendix 2), heated to 80°C for 20 minutes and then allowed to cool to room temperature. To break down the bacteria cell wall, cells were then mixed with 50 µl of 10 mg/ml lysozyme, incubated at 35°C for 1 hour and then treated with 70 µl 10% sodium dodecyl sulphate (SDS) and 6 µl of 10 mg/ml proteinase K, followed by incubation for 10 minutes at 65°C.

Another 10 minute incubation at 65°C following the addition of 100 µl of 5M NaCl and 80 µl of pre-warmed CTAB/NaCl, was performed prior to standard chloroform/isoamyl alcohol extraction and isopropanol/ethanol precipitation of the DNA pellet. Pellets were then resuspended in 40 µl of 1X TE and stored at -20°C until needed.

2.2.3 *Pvu* II Digestion of *M. tuberculosis* Genomic DNA

For each *M. tuberculosis* and RIVM reference strain (Mt.14323), 4.5 µg of genomic DNA was digested in a total reaction mixture of 50 µl which was prepared as follows: 5 µl 10X M Digestion Buffer, 2 µl *Pvu* II restriction endonuclease (added last) and varying amounts of DNA and sterile ddH_2O. Samples were incubated in a 37^0C water bath for at least 6 hours.

2.2.4 Gel Electrophoresis of Digested Products

DNA fragments were electrophoretically separated on 0.8% agarose gels made with and run using 1X Tris Borate EDTA (TBE) buffer (Appendix 2) and containing ethidium bromide (3 µl of 10 mg/ml stock solution) for DNA staining. For each sample and the RIVM standard, 5.0 µl of the internal marker (Supercoiled DNA Ladder-PvuII/PhiX174 Internal Marker Mix), and 20 µl of the digested sample or standard were combined. An external marker (lambda-*Hind*III/PhiX174-*Hae*III mix) was loaded in the first lane (22 µl) followed by two RIVM standards encompassing the digested samples. Electrophoresis was carried out for approximately 20 minutes at 100 volts (V) and then decreased to 40V and run overnight for at least 20 hours or until the 2.0 kilobase lambda-*Hind*III band reached 7.0 cm ± 0.4 cm from the wells.

2.2.5 Southern Blot Assay – IS*6110* Probe

Following electrophoresis, the gel was photographed and then exposed to UV light for five minutes. The gel was then soaked three times with gentle shaking, each for 20 minutes, in 0.5M NaOH/1.5M NaCl, then rinsed in distilled water for 5 minutes followed by two 20 minute washes in 0.5M TRIS pH 7.5/1.5M NaCl and an additional 5 minute rinse in distilled water. A capillary blotting assembly was constructed with all the layers of the stack, from the bottom to the top, being as follows: wick 3MM Chromatagraphy paper (Whatman), 2 pieces of 3MM Chromatagraphy paper soaked in 10X salt sodium citrate (SSC), gel with bottom side up, Hybond N^{+} ^{TM} membrane (Amersham), a "border" of pieces of parafilm surrounding the membrane, another two pieces of 3MM Chromatography paper soaked in 10X SSC, and a large stack of paper towels. All pieces of the chromatography paper were cut to the size of the gel (normally 1 cm larger) and all air bubbles between the various layers were pressed out. The pool of 10X SSC transfer buffer and the entire assembly were wrapped in plastic wrap and a weight was added to the top. The transfer was allowed to proceed overnight at room temperature.

Following the transfer, the apparatus was disassembled and 1 µl of marker mix was added to each corner of the membrane prior to it being subjected to UV crosslinking for 3 minutes. Finally, the membrane was soaked for three minutes in 2X SSC, baked at 80°C in a vacuum oven for 2 hours on a piece of crinkled aluminium foil and stored in a plastic bag at room temperature.

2.2.6 IS*6110* Probe Labelling, Hybridization and Detection

The probe was prepared by performing PCR to amplify a 505 bp amplicon from within the IS*6110* element. PCR was carried out using Taq Polymerase (Amersham) and a MJ DNA Engine® (PTC-200™) thermal cycler. A 100 µl reaction was prepared and contained the following: 10 µl 10X PCR buffer (with Mg^{2+}), 10.0 µl dNTP mix [2.0 mM each dNTP] (Invitrogen), 10 µl Primer TB#1 (50 ng/µl), 10 µl Primer TB#2 (50 ng/µl), 5 µl of 20 ng/µl IS*6110* containing genomic DNA from a *Mycobacterium* strain, 0.5 µl Taq polymerase [5 units/µl] (Amersham) and 54.5 µl sterile dH_2O. Sequences of forward and reverse primers were: Primer TB#1 5'-TCAGCCGCGTCCACGCCGCCA-3' and Primer TB#2 5'-CCGACCGCTCCGACCGACGGT-3'. PCR cycling conditions were as follows: 94°C for 2 minutes, then 40 cycles of 94°C for 30 seconds, 60°C for 30 seconds and 72°C for 30 seconds followed by 72°C for 10 minutes and left at 4°C forever. The PCR product was run on 2% low-melting point agarose gel and purified using Wizard mini columns (Wizard PCR Preps DNA Purification System, Promega) as per manufacturer's instructions.

Labelling, hybridization and detection were carried out with an ECL Direct™ Nucleic Acid Labelling and Detection System (Amersham) as per manufacturer's instructions. Following a 20 minute exposure, detection of the chemiluminescent signal was captured on Hyperfilm™ ECL™ (Amersham) and developed using a Feline 14 Automatic X-Ray Film Processor (Fischer Industries Inc., Geneva, Ill).

2.2.7 IS*6110* RFLP Analysis Using Bionumerics 2.0

Film images were scanned and saved as .tif files and loaded into Bionumerics version 2.0 (Applied Maths, Kortrijk, Belgium). In order to confirm the identity for each of the *Mycobacterium tuberculosis* strains to be used in aerosol infections for the animal survival studies, IS*6110* fingerprint banding patterns were compared with an existing RFLP database, created and maintained by the National Reference Centre for Mycobacteriology, Winnipeg, Manitoba.

2.3 Mouse Model of *Mycobacterium tuberculosis* Infection

2.3.1 Preparation of Inoculums

Preparation of *Mycobacterium tuberculosis* cultures was conducted as described in section 2.1.1. Prior to exposing the mice to aerosols of the five *M. tuberculosis* strains, confirmation of the bacterial concentration was performed by plating serial dilutions of the prepared inoculum. Middlebrook 7H10 plates were incubated at 37°C with 5% CO_2 and colonies were counted after 21 days. An inoculum range from 1.0-2.6 x 10^7 bacilli per ml in PBS was observed. Inoculum values for each strain were as follows: 1.52 x 10^7 CFU/ml *M. tuberculosis* Type1, 2.6 x 10^7 CFU/ml Type2, 1 x 10^7 CFU/ml Type5, 2.24 x 10^7 CFU/ml Type72 and 1.28 x 10^7 CFU/ml H37Rv. For each strain 5 ml of inoculum was used for aerosol infections.

2.3.2 Mice

Female BALB/c, C57BL/6 and C3H mice were obtained from Charles River Canada (Saint-Constant, PQ) and transported to the Canadian Science Centre for Human

and Animal Health (CSCHAH) in Winnipeg, MB, where they were maintained in an environment free of common pathogens. All mice used in experiments were 6-8 weeks of age.

2.3.3 Aerosol Infection

Aerosol infections for the experimental model of pulmonary tuberculosis were carried out under CL3 conditions at the National Microbiology Laboratory (NML) in Winnipeg, Manitoba, Canada. All procedures were carried out by a Level III trained Animal Health Technician. All the protocols were approved by the Animal Care Committee of the NML, CSCHAH.

Infections were carried out inside an aerosol exposure chamber (plexiglass or polycarbonate plastic chamber with the dimensions of 10" W x 19"D x 9"W) with an inlet for aerosols and oxygen as well as a Hepa-filter exhaust. The chamber was placed within a class-II, B2 biological safety cabinet. Individual *M. tuberculosis* strains were suspended using a nebulizer and an air source and introduced into the chamber from the top, so that the inoculum descended over the animals. A total of 324 mice were used for this study (3 mouse strains X 6 experimental groups X 18 mice per group). Each strain of mouse, BALB/c, C57BL/6 and C3H, was divided into 6 different experimental groups. For each experimental group, consisting of 18 animals each, mice were exposed to aerosols of either PBS, Type1, Type2, Type5, Type72 or H37Rv. Twenty seven mice (9 from each mouse strain) were placed inside the inhalation chamber and the nebulizer was started in order to deliver the dose. This was done twice for a total of 18 mice (9+9) for each mouse strain. One chamber was used for the control group and one test group,

Table 3. Animals used for *Mycobacterium tuberculosis* aerosol infections

Species & Strain	Age	Sex	Exposure Groups and Total Mice
Mus musculus BALB/c	6-8 weeks	Female	6 groups of 18 mice - 108 Mice
Mus musculus C57BL/6	6-8 weeks	Female	6 groups of 18 mice - 108 Mice
Mus musculus C3H	6-8 weeks	Female	6 groups of 18 mice - 108 Mice
TOTAL NUMBER OF MICE			**324 MICE**

Table 4. Distribution of animals among experimental groups

Group	Total mice	# of mice	BALB/c mice	C57BL/6 mice	C3H mice
Gp 1 Saline (PBS) - exposure 1	54	27	9	9	9
Gp 1 Saline (PBS) - exposure 2		27	9	9	9
Gp 2 M. tb Type1 - exposure 1	54	27	9	9	9
Gp 2 M. tb Type1 - exposure 2		27	9	9	9
Gp 3 M. tb Type2 - exposure 1	54	27	9	9	9
Gp 3 M. tb Type2 - exposure 2		27	9	9	9
Gp 4 M. tb Type5 - exposure 1	54	27	9	9	9
Gp 4 M. tb Type5 - exposure 2		27	9	9	9
Gp 5 M. tb Type72 - exposure 1	54	27	9	9	9
Gp 5 M. tb Type72 - exposure 2		27	9	9	9
Gp 6 M. tb H37Rv - exposure 1	54	27	9	9	9
Gp 6 M. tb H37Rv - exposure 2		27	9	9	9
TOTAL		**324**	**108**	**108**	**108**

and then a different chamber was utilized for each experimental group. The contact time for whole body exposure to the *M. tuberculosis* aerosols (1-2.6 x 10^7 bacilli per ml in 5 ml of PBS) was 30 minutes, after which time the nebulizer was stopped. The inoculum was allowed to settle inside the chamber for an additional 30 minutes. In preliminary experiments, this range of inoculum and duration of exposure had reproducibly resulted in the delivery of 100 to 250 viable CFU of *M. tuberculosis* into the lungs. Chambers were opened within the biological safety cabinet, the mice were removed with forceps, placed inside the micro-isolator cages whose exteriors were surface decontaminated with 2% phenolic S7 and then placed within the incubators. Six mice were housed per small micro-isolator cage and 12 mice per large micro-isolator cage.

2.3.4 Data and Sample Collection

Mice were monitored daily to ensure that they were all eating and drinking well in addition to displaying normal grooming and behaviour patterns. Cages and water bottles were changed twice a week. Animals were weighed once a week for first month. For the duration of the experiment, animals were weighed regularly, particularly the ones showing any clinical manifestations of the disease. Clinical symptoms and endpoint data were recorded as per the Humane Endpoint Chart.

Once the designated time point was reached or upon reaching criteria outline in the Humane Endpoint Chart (Table 5), animals were cervically dislocated in the biological safety cabinet, by the Animal Health Technologist. Lung samples were harvested aseptically from every animal and immediately frozen on dry ice before being

stored at -80°C. Carcasses were autoclaved out of the CL3, then rendered as per the CSCHAH guidelines.

2.3.5 Survival Study

Following aerosol exposure, 12 mice from each of the 6 experimental groups (per mouse strain) were used for the survival study and allowed to progress from initial infection through active disease. Each day, animals were observed and those showing symptoms were scored daily as per Humane Endpoint Criteria derived from standards previously established by the Canadian Council on Animal Care, based on three categories: body weight changes, physical appearance and respiratory distress. When a total score of greater than three using all three categories was reached, the Animal Health Supervisor was notified and a consensus decision was made whether or not to euthanize the animal for ethical reasons. Animals were euthanized by trained Animal Health Technologists.

2.3.6 Colony Forming Unit (CFU) Assay

To evaluate the bacterial growth of each *Mycobacterium tuberculosis* strain, 6 mice per experimental group from each strain of mouse were euthanized at 15 days post-exposure. The lungs were harvested aseptically, placed into cryo vials and immediately frozen. Homogenates of 100 mg of lung tissue were prepared and 10-fold serial dilutions were plated on Middlebrook 7H10 plates, incubated for 3 weeks at 37°C with 5% CO_2 and colonies were then counted (Manca, *et al.*, 1999).

Table 5. The Humane Endpoint Scoring checklist

A. Body weight changes

Score	Variables
0	Normal
1	0-10% weight loss
2	10-15% weight loss
3	15% or more weight loss

B. Physical appearance

Score	Variables
0	Normal
1	Rough coat (indicates animal is ill)
2	Abnormal posture (indicates animal is not breathing normally), nasal/ocular discharge

C. Respiratory Distress

Score	Variables
0	Normal
1	Abnormal breathing

Endpoint Scoring: When a total score >3 using all three categories was obtained, based on the above checklist for a chronic infectious respiratory disease in Mice, as approved by the Animal Care Committee, the Animal Health Supervisor was notified and a decision to euthanize the animal was reached.

2.3.7 Histological Analysis of Lung Samples

To assess lung pathology, histological analysis of lung samples was conducted using a protocol previously described by Hernandez-Pando (1997). Lungs from 6 mice per experimental group for the BALB/c and C3H strains of mouse were aseptically removed at day 15 post-exposure and one randomly selected lobe was fixed in 10% formalin for at least 72 hours (Hernandez-Pando, *et al.*, 1997). Parasaggittal sections of 5 μm thickness were processed by stretching out sections onto slides using warm water then subjected to gradient concentrations of ethanol and stained using haematoxylin-eosin staining methodology (*Carleton's Histological Technique*, 1967). The average number of nodules per section, the average size of a nodule (diameter) along with the total area of the lungs involved in granulomatous inflammation was evaluated by examining and analyzing 25 random 100X fields for each mouse. Images were captured using the SPOT RT camera and software v3.2 (Sterling Heights, MI) and analyzed using Image-Pro Plus v4.5 (Media Cybernetics, Silver Spring, MD). The presence of AFB at the infection site was studied using Ziehl-Nielsen counter-stained sections (*Manual of Histological Staining Methods of the Armed Forces Institute of Pathology*, 1968). Analysis was conducted blinded where both the mouse strain and experimental infection group were unknown at the time of observation and analysis.

2.3.8 Statistical Analysis of Survival Data

Survival analysis estimating survival curves with Kaplan-Meier estimates and comparing the curves with a log-rank test was conducted. The data was statistically analyzed using a two-way ANOVA analysis where histological variables and survival data were compared between 5 *M. tuberculosis* strains, adjusting for 3 mouse strains. The

ANOVA was followed by a least square mean comparisons where the interaction term was significant. The effect of these TB strains between 3 mouse strains was calculated and studied using SAS v8.2 (Statistical Analysis System of Cary, NC).

2.4 Quantification of Cytokine mRNA Expression Profiles

In order to investigate the relationship between the manifestation of disease caused by Type1 and the extent of the host immune response, cytokine mRNA levels from mouse lung homogenates were evaluated in duplicate by conducting semi-quantitative RT-PCR. Lung samples were obtained 15 days post-exposure from 6 mice per experimental group for the BALB/c and C3H strains and immediately frozen at -80°C until RNA isolation was conducted.

2.4.1 Isolation of Total RNA Using TRIzol

All isolations of total RNA were carried out using TRIzol reagent (Invitrogen) as per manufacturer's instructions. Briefly, for each sample, 100 mg of frozen lung tissue was cut from the original lung sample and homogenized in 1 ml of TRIzol using a small tissue grinder (VWR). To facilitate the homogenization, 0.5 ml of TRIzol was initially added to the frozen tissue then homogenized prior to the addition of the remaining 0.5 ml. Once homogenized, samples were incubated at room temperature for 5 minutes prior to the addition of 0.2 ml of chloroform. Samples were then vigorously shaken by hand for 15 seconds, incubated for another 2-3 minutes and then centrifuged at 12,000 x g for 15 minutes at 4°C. Precipitation of RNA was performed by gently mixing the aqueous top phase with 0.5 ml of isopropanol by inverting, followed by incubation for 10 minutes at

room temperature and then centrifugation at 12,000 x g for 10 minutes at 4°C. The visible RNA pellet was then washed in 1 ml of 75% ethanol, vortexed and centrifuged at 7500 x g for 5 minutes at 4°C. The ethanol was then decanted, the RNA pellet briefly air dried and resuspended in 50 µl of RNase-free water. Finally, the redissolved RNA was incubated at 55-60°C and stored at -20°C until further use. All centrifugation steps were carried out using an Eppendorf® 5415 R Microcentrifuge.

2.4.2 RNA Integrity Check

Prior to treatment with DNase I, random RNA samples were run on denaturing formaldehyde agarose gels to check the integrity of the isolated RNA as per general guidelines (Qiagen Literature General Molecular Biology Protocols, 2003). Visualization of RNA was performed by 1% Formaldehyde Agarose gel electrophoresis where 100 ml gels were made with 10X FA buffer (Appendix 2), containing 1 µl of a 10 mg/ml ethidium bromide stock solution and 1.8 ml of 37% (12.3 M) formaldehyde, and run in 1X FA buffer. RNA samples, 1 µg in total, were added to 5X RNA loading buffer (Appendix 2) in a 1:5 ratio, prior to being loaded on a gel. Electrophoresis was run for 50 minutes at 50 volts. The 1X FA buffer between the anode and cathode buffer chambers was changed every 20 minutes. A molecular weight marker, 0.24-9.5 Kb RNA Ladder™ (Invitrogen, Appendix 3), was also included on the gels. RNA bands were visually observed using UV light and gel images were captured using AlphaImager® Imaging System (Alpha Innotech Corporation, San Leandro, CA).

2.4.3 DNase I Treatment of RNA

In order to eliminate the occurrence of contaminating DNA within the isolated RNA prior to any RNA amplification procedures, samples were subjected to DNase I treatment. For each sample, RNA was quantified using the NanoDrop (NanoDrop Technologies, Inc., Rockland, DE) and then at least 2 µg of RNA per sample was treated with DNase I. A typical treatment reaction for 2 µg of RNA was prepared on ice as follows: 2 µl 10X DNase I Reaction Buffer, 2 µl DNase I, Amplification Grade [1 U/µl] (Invitrogen) and varying amounts of RNA and DEPC-treated water, up to a total reaction volume of 20 µl. Reaction tubes were incubated at room temperature for 15 minutes followed by the addition of 1 µl of EDTA (25 mM) to the mixture to inactivate the DNase I. The RNA was then heated at 65°C for 10 minutes and then stored at -20°C until used in reverse transcription procedures.

2.4.4 Reverse Transcription and Amplification of RNA Samples

All RT-PCR reactions were performed using a QIAGEN One-Step RT-PCR™ kit. Each reaction was prepared as follows: 10 µl 5X OneStep RT-PCR buffer, 2 µl deoxynucleotide triphosphate (dNTP) mix solution (10 mM of each dNTP), 1.0 µl (200 ng final concentration) of each forward and reverse primers, 1.0 µl RNaseOUT™ Ribonuclease Inhibitor [10U/µl] (Invitrogen), 2 µl One-Step RT-PCR Enzyme Mix™, a varying amount of RNA, and sterile, RNase-free dH_2O (provided in kit), up to a total reaction volume of 50 µl. To ensure quality control, negative water controls were employed where the amount of RNA added was substituted by additional RNase-free dH_2O. RT-PCR reactions using general cycling conditions outlined in Table 6 were

performed using Techne TC-512 Gradient Thermocyclers. Five different primer sets were used to examine the cytokine profile within infected lungs. Sequences for the following primer sets: ß-actin, IFN-γ, IL-5, IL-10 and IL-12 p40, were obtained courtesy of Dr. Xi Yang, Department of Medical Microbiology, University of Manitoba and synthesized by the DNA Core Facility, National Microbiology Laboratory.

Table 6. General RT-PCR cycling conditions

Number of Cycles	Time	Temperature	Cycle Type
1	30 min	50°C	Reverse transcription
1	15 min	95°C	Initial PCR activation step
25-40	30 sec 30 sec 30 sec	94°C 50-68°C 72°C	Denaturation Annealing Extension
1	5 min	72°C	Final Extension
1	∞	4°C	Cooling

Table 7. List of primers used in RT-PCR reactions

Name	Sequence	Predicted Band Size
Murine ß-actin 5'	5' GTG GGG CGC CCC AGG CAC CA 3'	539
Murine ß-actin 3'	5' CTC CTT AAT GTC ACG CAC GAT TTC 3'	
Murine IFN-γ 5'	5' AAC GCT ACA CAC TGC ATC T 3'	397
Murine IFN-γ 3'	5' TGC TCA TTG TAA TGC TTG G 3'	
Murine IL-5 5'	5' GCA CAG TGG TGA AAG AGA CC 3'	273
Murine IL-5 3'	5' TAA TCC AGG AAC TGC CTC GT 3'	
Murine IL-10 5'	5' CTG AGG CGC TGT CAT CGA TT 3'	213
Murine IL-10 3'	5' AGG TCC TGG AGT CCA GCA GA 3'	
Murine IL-12 p40 5'	5' CTC ACC TGT GAC ACG CCT GA 3'	431
Murine IL-12 p40 3'	5' CAG GAC ACT GAA TAC TTC TC 3'	

Prior to the running of experimental samples, gradient RT-PCR was performed to optimize both the number of cycles and the annealing temperatures for each of the sets of primers used. Additionally, three different concentrations of RNA template, 1.0 μg, 0.5 μg and 0.1 μg, were tested under optimized conditions to determine the ideal concentration to generate the best possible amplification product. Optimization determined that 0.5 μg of RNA template produced the most consistent and sound bands upon visualization of the products and therefore, all reactions that were performed for experimental samples used 5 μl (0.1 μg/μl) of RNA template.

Table 8. Optimized RT-PCR annealing temperatures and cycle numbers

Primer Set	**Number of Cycles (Denaturation, Annealing and Extension)**	**Anneal Temperature**
Murine ß-actin	23	65°C
Murine IFN-γ	30	55°C
Murine IL-5	40	65°C
Murine IL-10	35	56°C
Murine IL-12 p40	30	55°C

2.4.5 Visualization and Imaging of RT-PCR Products

RT-PCR products were run on 1.5% agarose gels, made with and run in 1x Tris Acetate EDTA (TAE) buffer (Appendix 2). Gels were prepared with 4 μl ethidium bromide (10 mg/ml stock solution) in order to visualize the bands using UV light. For each sample, 22 μl of product was mixed with 3 μl of 10X Ficoll DNA tracking dye. To confirm the size of observed products, a 100 bp DNA Ladder (Invitrogen, Appendix 3) was also loaded on the gel. Electrophoresis was performed for 30 minutes at 125 volts.

Gel images were captured using the AlphaImager® Imaging System and saved as .tif files in order to perform band density analysis.

2.4.6 Semi-quantitative Densitometric Analysis

In order to make a comparative and quantitative analysis of target mRNA expression levels, RT-PCR results were analyzed using Bionumerics version 2.0 (Applied Maths, Kortrijk, Belgium). Gel images, in the .tif format, were loaded into the software in order to determine the densities of the RT-PCR product gel bands. Since gel-to-gel variation could potentially occur, in addition to performing each reaction with a set quantity of RNA template, the band densities for each of the four sets of RT-PCR products were normalized to the housekeeping gene ß-actin, which was run on each gel. For both the BALB/c and C3H mouse models, duplicate samples from 6 mice were examined, for each *Mycobacterium tuberculosis* experimental infection group. The H37Rv experimental group was used as a positive and benchmark control.

2.5 Suppression Subtractive Hybridization

2.5.1 Concept

In order to identify key genetic sequence differences present within the bacterial genome of the hypervirulent Type1 but absent from the less virulent laboratory strain H37Rv, a derivative of a subtractive hybridization method was selected in order to conduct a comprehensive survey of the *Mycobacterium tuberculosis* genome. Although subtractive hybridization (SH) will not reveal any details with regard to point mutations (a rare occurrence in *M. tuberculosis*), this method has successfully been used to identify

genetic differences in bacterial pathogens including *Bacillus* species (Radnedge, *et al.*, 2003) and *Porphyromonas gingivalis* (Sawada, *et al.*, 1999). Variations of the subtractive hybridization method have also been effectively applied to a few members of the *Mycobacterium* species (Mahairas, *et al.*, 1996; Jenkin, *et al.*, 2003; Song, *et al.*, 2003).

Subtractive hybridization is a method that uses hybridization of the DNA population of interest (tester) to an excess of the DNA of a reference strain (driver) to physically separate common sequences from unique elements found only within the tester's pool of sequences. Although SH is a robust technique for identifying specific sequences of interest, the method requires multiple rounds of hybridization to produce the desired physical separation of single stranded and double stranded DNA and cannot compensate for the abundance of certain sequences within the DNA populations. In 1996, an improved version of SH was introduced that combined both normalization and subtraction into a single procedure (Diatchenko *et al.*, 1996). The rationale behind the new suppression subtractive hybridization (SSH) method is that following a single round of selective hybridization between tester and driver DNA pools, suppression PCR selectively amplifies and enriches for unique tester sequences (Figure 3). Specifically, since the tester pool is separated into two portions and individually linked to different adaptors, following selective hybridization only sequences that carry both adaptors will exponentially amplify. The remaining combinations of sequences that carry either one type of adaptor or none at all, are either unable to amplify due to a suppression effect caused when a secondary structure forms thus preventing primer annealing or simply undergoes linear amplification (Clontech Laboratories Inc., 2001). Therefore, potentially a 1000-fold enrichment of specific sequences is possible using the SSH technique.

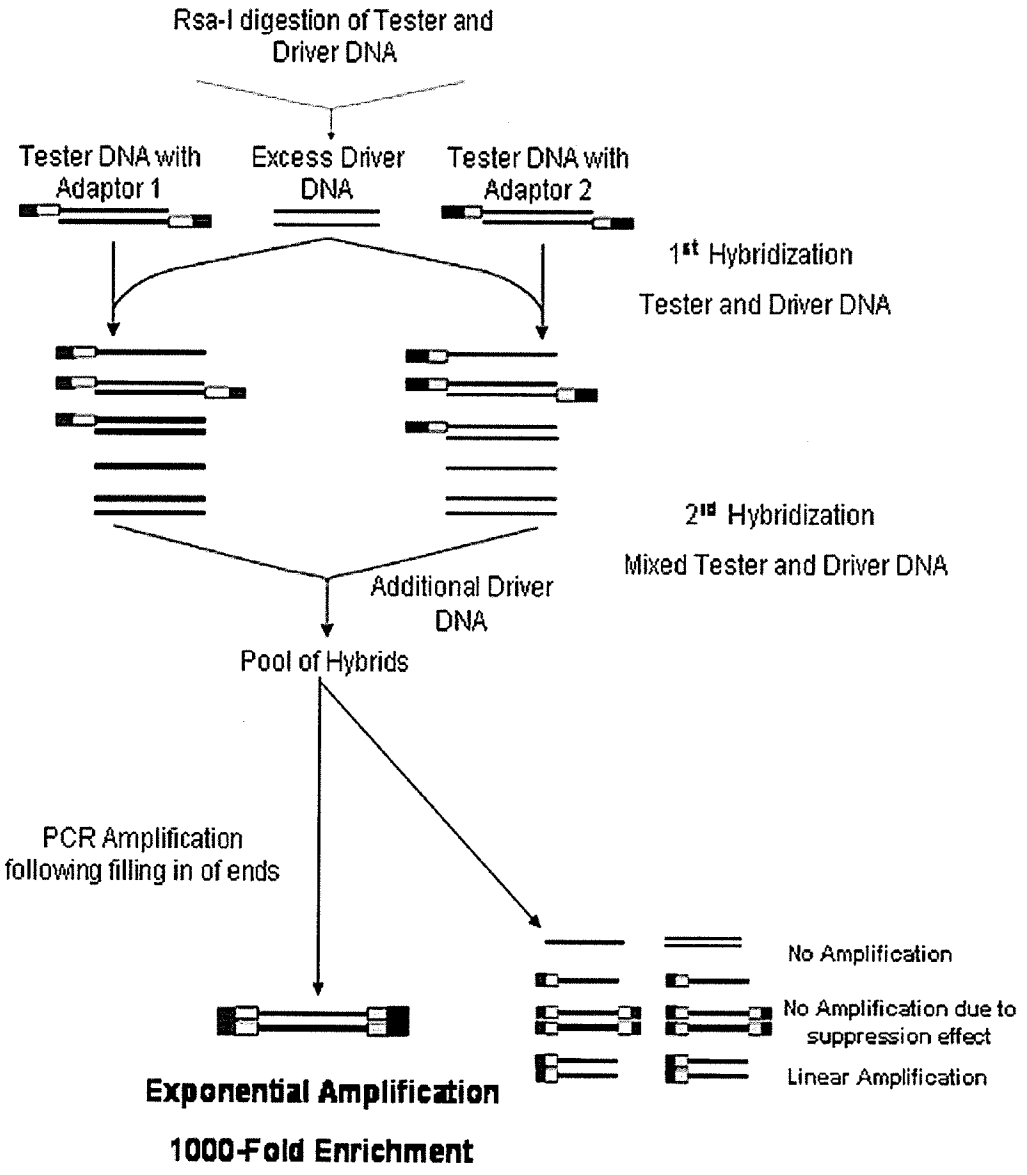

Figure 3. Overview of suppression subtractive hybridization method (adapted from Diatchenko *et al.*, 1996; Clontech Laboratories Inc., 2001). Tester-specific sequences which possess two different adaptors are the only molecules present able to undergo exponential amplification.

2.5.2 Restriction Enzyme Digestion

To identify strain-specific sequences present in *Mycobacterium tuberculosis* Type1, suppression subtractive hybridization was conducted using the Clontech PCR-Select Bacterial Genome Subtraction Kit. All experimental and positive control reactions (*E. coli* genomic DNA provided in the kit), were performed as per manufacturer's instructions with only a few modifications. For all experimental subtractions, *M. tuberculosis* Type1 was used as the tester and *M. tuberculosis* H37Rv was utilized as the driver.

In order to generate short, blunt-ended sequences that can be ligated to adaptors and are optimal for subtraction, tester Type1 DNA was digested with the 4-base-cutting restriction enzyme *Rsa* I. Digestion reactions were prepared as follows: 5 µl 10X *Rsa* I Restriction Buffer, 1.5 µl *Rsa* I (10 U/µl), 2 µg of genomic DNA (variable µl) and a varying amount of water, up to a total of 50 µl. Samples were mixed and then incubated at 37°C for 16 hours. Experimental driver H37Rv DNA, and control driver *E. coli* DNA was also digested with *Rsa* I using the same reaction mixture and incubation conditions.

Additionally, in separate SSH experimental procedures, another 4 base-cutting restriction enzyme, *Alu* I [10 U/µl] (New England Biolabs Inc.) was used to digest both tester and driver DNA and then linked to appropriate *Alu* I specific adaptors.

To confirm that a complete digestion of genomic DNA had occurred, 5 µl of *Rsa* I-digested genomic DNA was electrophoresed on a 1% agarose gel containing 0.002% ethidium bromide in 1% agarose, using 10 mg/ml stock solution. The gel was made with and run in 1X TAE buffer and electrophoresed for 30 minutes at 100 volts. A Ready-

Load™ 1 Kb Plus DNA Ladder (Invitrogen, Appendix 3) and non-digested genomic DNA for both the tester and driver were also loaded on the gels.

Following the termination of the digestion reaction by the addition of 2.5 µl of EDTA, digested tester and driver DNA was then cleaned up to remove traces of the restriction enzyme and diluted to the appropriate concentration prior to adaptor ligation. Briefly, digested DNA was extracted using a multi-step phenol-chloroform-isoamyl alcohol procedure and ethanol-precipitated as per the kit manufacturer's instructions. Pellets were air-dried for 5-10 minutes and resuspended in 6.5 µl sterile water and stored at -20°C. Driver DNA concentrations were maintained at approximately 300 ng/µl while 1.2 µl of tester DNA was diluted with 1.8 µl sterile water. At the same time, control tester DNA for a positive reaction control was also prepared by mixing 1.2µl of *Rsa* I-digested *E. coli* genomic DNA with 1.8 µl of diluted ϕX174/*Hae* III digest DNA.

2.5.3 Ligation of Adaptors

Prior to hybridization, both control (*E. coli*) and experimental (Type1) tester DNA samples were subjected to a ligation reaction. Each tester DNA was separated into two equal pools and individually ligated to one of two adaptors. Each 10 µl ligation reaction was prepared as follows: 1 µl of diluted tester DNA, 2 µl of either Adaptor 1 or Adaptor 2R (10 mM), 2 µl 5X Ligation Buffer, 1 µl T4 DNA Ligase (400 U/µl) and 4 µl of sterile water. In order to produce a negative control, 1.5 µl of each aliquot was combined so that DNA with both adaptors present would be generated and serve as an unsubtracted tester control. All reactions were incubated overnight at 16°C until the ligation reaction was terminated by the addition of 1 µl of 0.2 M EDTA. Samples were then heated for 5

minutes at 72°C to inactivate the ligase. Unsubtracted tester controls were then prepared for PCR amplification by diluting 1 µl into 1 ml of sterile water. All samples were then stored at -20°C.

Ligation reactions that used *Alu* I-digested tester DNA were performed exactly as described for *Rsa* I-digested tester DNA but utilized two different *Alu* I-specific adaptors (Jenkin, *et al.*, 2003).

Table 9. Adaptor sequences used in SSH ligation reactions

Name	Sequence
Rsa I Adaptor 1	5' CTAATACGACTCACTATAGGGCTCGAGCGGCCGCCCGGGCAGGT 3' 3' GGCCCGTCCA 5'
Rsa I Adaptor 2R	5' CTAATACGACTCACTATAGGGCAGCGTGGTCGCGGCCGAGGT 3' 3' GCCGGCTCCA 5'
Alu I Adaptor 1a	5' CTAATACGACTCACTATAGGGCTCGAGCGGCCGCCCGGGCAGGT 3' 3' GGCCCGTCCA 5'
Alu I Adaptor 2	5' CTAATACGACTCACTATAGGGCAGCGTGGTCGCGGCCGAGGT 3' 3' GCCGGCTCCA 5'

2.5.4 Hybridization

The first hybridization step is designed to both normalize and specifically enrich for target sequences. Normalization occurs since more abundant sequences form homo-hybrids and reanneal quicker than sequences of lower occurrence. In addition, the formation of hetero-hybrids of non-target DNA further enriches for specific sequences of interest. For both control and experimental samples, two 4 µl reactions were prepared as follows: 1 µl Adaptor 1-ligated tester DNA or 1 µl Adaptor 2R-ligated tester DNA, 1 µl of 4X Hybridization Buffer (Clontech) and 2 µl of *Rsa* I-digested driver DNA. In experiments conducted using *Alu* I as the restriction enzyme, *Alu* I-digested driver DNA

and one of the two *Alu* I-specific adaptors were substituted in the reaction. Each sample was then incubated in an MJ DNA Engine® Tetrad™ 2 thermal cycler for one and a half minutes at 98°C. *E. coli* positive control samples were then incubated at 63°C for another 90 minutes. Based on the high G+C content of the *Mycobacterium tuberculosis* genome, experimental samples were hybridized at 65°C for the period of 90 minutes.

Immediately following the first hybridization, an additional 300 ng of restriction enzyme cut-driver DNA (1 µl) was mixed with 1 µl of 2X Hybridization Buffer (Clontech) and denatured at 98°C for one and a half minutes. The freshly denatured driver DNA was then simultaneously combined with both samples from the first hybridization step (which were not denatured again and kept in the thermal cycler) and incubated overnight at 63°C and 65°C respectively for the *E. coli* control and *M. tuberculosis* experimental samples. This step was performed to generate tester-specific hybrids, which possessed different adaptors on each end. The following morning, 200 µl of Dilution Buffer (Clontech) was added to the hybridized samples and heated at 63°C for an additional 7 minutes to eliminate any non-specific hybridization prior to storage at -20°C.

2.5.5 PCR Amplification of Tester-specific Sequences

To selectively acquire target sequences, two rounds of amplification were attempted to amplify tester-specific sequences. Initially a brief incubation was performed to fill in the missing strands of adaptors to create the primer binding site within the two adaptor regions at the 5' ends of the target sequences. The first amplification used only one primer to exponentially amplify any sequences that possessed two different adaptors at the 5' ends. The second amplification used nested PCR to further enhance the selection

of tester-specific sequences. All PCR reactions were performed using a MJ DNA Engine® Tetrad™ 2 thermal cycler and were carried out as per manufacturer's guidelines (Clontech) with a few modifications following optimization of template concentration, annealing temperature and cycle parameters. For each subtracted *E. coli* control and *M. tuberculosis* experimental sample along with their corresponding unsubtracted tester controls, a 25 µl reaction was prepared for the first PCR amplification as follows: 2.5 µl 10X BD Advantage™ 2 PCR Buffer, 0.5 µl dNTP (10 mM) mix (Invitrogen), 0.5 µl 50X BD Advantage™ 2 Polymerase Mix (BD Biosciences), 1.0 µl (10 µM) PCR Primer 1, 1 µl of diluted DNA, and 19.5 µl sterile dH_2O. Cycling conditions for the first round of PCR are outlined in Table 10.

Table 10. Primary and secondary SSH PCR cycling parameters

Primary PCR			
Number of Cycles	Time	Temperature	Cycle Type
1	2 min	72°C	Adaptor extension
25-30	30 sec 30 sec 90 sec	94°C 66°C 72°C	Denaturation Annealing Elongation
1	5 min	72°C	Additional elongation
1	∞	4°C	Final cooling
Secondary PCR			
Number of Cycles	Time	Temperature	Cycle Type
12-19	30 sec 30 sec 90 sec	94°C 68°C 72°C	Denaturation Annealing Elongation
1	∞	4°C	Final cooling

Prior to the second round of amplification, 1 µl of primary PCR product was diluted with 19 µl sterile dH_2O. Preparation of the secondary PCR reaction was as follows: 2.5 µl 10X BD Advantage™ 2 PCR Buffer, 0.5 µl dNTP (10 mM) mix

(Invitrogen), 0.5 µl 50X BD Advantage™ 2 Polymerase Mix (BD Biosciences), 1.0 µl (10 µM) each of Nested Primer 1 and Nested Primer 2R, 1 µl of diluted primary PCR product DNA, and 18.5 µl sterile dH_2O. Reaction mixtures were then subjected to cycling conditions as indicated in Table 10 and final PCR products were stored at -20°C. For samples initially digested with *Alu* I, separate primers (as outlined in Table 11) previously employed by *Jenkin et al.* (2003), were used in place of those provided within the Clontech PCR-Select Bacterial Genome Subtraction Kit.

Table 11. SSH primers for amplification of tester-specific sequences

Name	Sequence
Rsa I PCR Primer 1	5' CTA ATA CGA CTC ACT ATA GGG C 3'
Rsa I Nested Primer 1	5' TCG AGC GGC CGC CCG GGC AGG T 3'
Rsa I Nested Primer 2R	5' AGC GTG GTC GCG GCC GAG GT 3'
Alu I Primer 1 (P1)	5' CTA ATA CGA CTC ACT ATA GGG C 3'
Alu I Nested Primer 1 (NP1)	5' TCG AGC GGC CGC CCG GGC AGG T 3'
Alu I Nested Primer 2 (NP2)	5' AGC GTG GTC GCG GCC GAG GT 3'

Primary and secondary PCR products were visualized by performing 2% agarose gel electrophoresis where gels were made with and run in 1X TAE buffer, and contained ethidium bromide for DNA staining. Typically 7 µl was combined with 3 µl of 10X Ficoll DNA tracking dye and run for approximately 40 minutes at 100 volts. Molecular weight markers, either Ready-Load™ 1Kb Plus DNA Ladder (Invitrogen) or Ready-Load™ ϕX174 RF DNA/*Hae* III Fragments (Invitrogen, Appendix 3), were also included

on the gels for approximation of PCR amplicon size for both experimental (*M. tuberculosis*) and control (*E. coli*) subtractions.

Additionally, 25 µl of secondary PCR product was run on 2% agarose gels for 60 minutes at 100 volts in order to clearly separate all products enough so that each band could be excised from the gel. Gel slices were then purified using the Wizard® SV Gel and PCR Clean-Up System (Promega) as per manufacturer's instructions and sequenced using the appropriate primer (Table 11) used during the primary PCR amplification.

2.5.6 Cloning of PCR Products

Since multiple bands were produced as a result of the two amplification reactions, cloning of the PCR products was necessary in order to both facilitate the screening and eventual sequencing of amplicons. Accordingly, PCR products were cloned into the pCR4-TOPO™ vector (Appendix 1) of the TOPO TA Cloning Kit for Sequencing™ (Invitrogen) as per manufacturer's instructions. Briefly, 2 µl of the secondary PCR product was added to the cloning reaction, which was allowed to proceed for 10 minutes. Using the One Shot® Chemical Transformation Protocol, pCR4-TOPO™ was amplified by transformation of chemically competent TOP10 *E. coli* cells. Transformed *E. coli* cells were then plated onto pre-warmed Luria-Bertani (LB) agar plates, pre-incubated for 2 hours with 10 µl of isopropyl-ß-D-thiogalactopyranoside (IPTG) and 50 µl of 5-bromo-4-chloro-3-indoyl-ß-D-galactopyranoside (X-Gal), containing either 50 or 100 µg/ml of ampicillin and incubated overnight at 37°C. Random white colonies were picked into the appropriate 5 ml of LB broth containing either 50 or 100 µg/ml ampicillin, and cultures were again grown overnight at 37°C.

Plasmid DNA was then extracted using the QIAprep® Spin Miniprep Kit™ (Qiagen) as per manufacturer's instructions. To assure that extracted DNA contained an insert, a 20 µl *Eco* RI (Amersham Biosciences) digestion reaction was performed at 37°C for one hour and then samples were visualized on a 1% agarose gel. Samples containing inserts were sequenced (section 2.5.9) using the T3 primer and sequence analysis was conducted using BLAST (section 2.5.10) and DNASTAR software package (DNASTAR, Inc., Madison, WI).

2.5.7 Colony Blot Preparation

In addition to direct sequencing of plasmid DNA containing inserts, a high through-put colony blot method, previously described by Stocki *et al.* (2002), was employed with minor modifications, to screen multiple colonies in a relatively rapid and labour efficient way. Inoculation of 100 µl of plasmid containing *E. coli* cultures (initially grown in 5 ml LB broth) were each individually added to 100 µl of fresh LB broth (containing the appropriate concentration of ampicillin) within a 96-well plate and incubated overnight at 37°C. Duplicate Hybond N^{+} ™ membranes (Amersham) were cut to a suitable size in order to completely cover the area of the 96-well plate and then placed on 1% agarose gels (made with water) in order to wet the membranes. Cultures were then spotted onto each membrane using the Biomek® FX Laboratory Automation Workstation (Beckman Coulter, Inc., Fullerton, CA). H37Rv and Type1 genomic DNA spots were both included on each membrane (just prior to UV crosslinking) to act as positive controls and one well, which only contained fresh LB broth, was spotted to act as a negative control. Membranes were then transferred onto LB agar plates (with the proper

ampicillin concentration) and incubated at 37°C for up to 48 hours or until sufficient colony growth on each membrane was observed.

Once colony growth was adequate, membranes were placed on 3MM filter paper (Whatman) saturated with 10% SDS for 3 minutes. Membranes were then placed onto 3MM filter paper saturated with Denaturation Solution (Appendix 2) for 7 minutes followed by an additional 7 minutes period on filter paper saturated with Neutralizing Solution (Appendix 2). Membranes were then washed vigorously for 2-3 minutes in 2X SSC, air dried for up to 20 minutes and UV crosslinked for 3 minutes using the UVP Transilluminator (Kodak Canada, Toronto, Ontario). Probing of membranes was performed as described in section 2.5.8.

2.5.8 Probe Hybridization and Detection

In order to identify spots on the colony blots representing specific sequences present only within the *M. tuberculosis* Type1 genome, probes produced from genomic DNA of either H37Rv or Type1 were labelled using the ECL Direct™ Nucleic Acid Labelling and Detection System (Amersham). Following overnight hybridization of each membrane with one of the two probes at 42°C, membranes were washed and the detection of the labelled probe was performed. The direct labelling of probe DNA with the enzyme horseradish peroxidase (HRP) enabled the oxidation of the substrate luminol thus allowing the chemiluminescent reaction to be detected on Hyperfilm™ ECL™ (Amersham) following a 30 minute exposure and developed using a Feline 14 Automatic X-Ray Film Processor. All labelling, hybridization, stringency washes and detection steps were carried out as per manufacturer's instructions. Any subtractive hybridization

fragments, which appeared to only hybridize when probed with the *M. tuberculosis* Type1 labelled probe and not the H37Rv probe, were sequenced as described in section 2.5.9 and analyzed for DNA homology using BLAST (section 2.5.10).

To ensure that the ECL Direct™ Nucleic Acid Labelling and Detection System could successfully label and accordingly detect *M. tuberculosis* genomic DNA probes, a control blot consisting of varying amounts of genomic DNA from both *M. tuberculosis* strains was individually probed with one of the two probes. Probe hybridization was performed for 4 hours and an exposure of 10 minutes was conducted.

2.5.9 Sequencing

In order to confirm potential Type1 specific sequences, DNA sequencing was performed in-house by the DNA Core Facility using Applied Biosystems (ABI) 3100 and ABI PRISM® 377 DNA sequencers with Applied Biosystems Big Dye Terminator chemistry, Version 3.0 reaction mix. The T3 primer was used to initiate the sequencing reaction as there is a T3 priming site located within the pCR®4-TOPO vector. Data was collected on Macintosh G4 computers using ABI Data Collection Software, Version 1.1. Data was analyzed using ABI Sequence Analysis Software, Version 3.7, and the DNASTAR software package.

2.5.10 Basic Local Alignment Search Tool (BLAST) Analysis

Sequencing data obtained was also analyzed for DNA Homology using the internet based BLAST software, available through the National Center for Biotechnology Information (NCBI) website (http://www.ncbi.nlm.nih.gov). Comparison of obtained

sequences against *Mycobacterium tuberculosis* H37Rv (accession number NC 000962) was conducted using the BLAST program for homology.

3. RESULTS

3.1 Confirmation of Strain Identity by RFLP

Prior to conducting aerosol infections and survival studies, all *Mycobacterium tuberculosis* strains obtained from the Health Sciences Centre (Winnipeg, MB) were subjected to RFLP analysis to confirm their identity. Although the gel was run for a shorter period of time then described in the RFLP protocol, comparison of obtained fingerprints for each isolate matched patterns previously compiled within the National Reference Centre for Mycobacteriology's RFLP database.

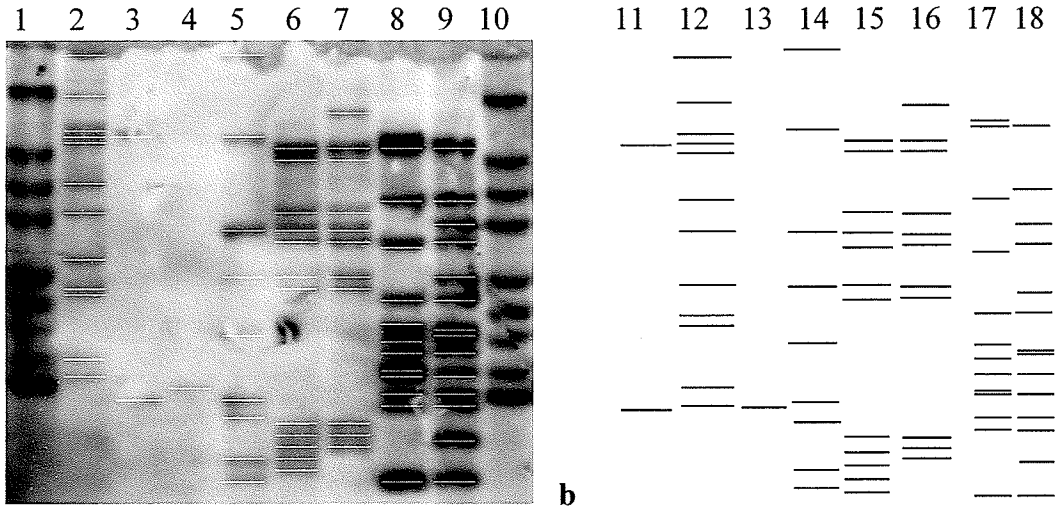

Figure 4a, b. RFLP Patterns of *Mycobacterium tuberculosis* strains.

a. IS*6110* RFLP was performed on *Mycobacterium tuberculosis* strains prior to their use in survival studies. RIVM *M. tuberculosis* reference strain Mt.14323 (lanes 1, 10) was used as a positive control. Clinical isolates (lane 2 – FP1:HSC 2950, lane 3 – FP2:HSC 2936, lane 4 – FP3:HSC 2737, lane 5 – FP5:HSC 2739, lane 6 – FP71:HSC 2353, lane 7 – FP72:HSC 1367) and reference strains (lane 8 - H37Rv:ATCC 27294, lane 9 – H37Ra:ATCC 25177) were tested.

b. RFLP patterns from the NRCM database were generated using Bionumerics version 2.0 and used as a comparison against tested samples (lane 11 – FP2:HSC 2668, lane 12 – FP1:HSC2665, lane 13 – FP3:HSC 2033, lane 14 – FP5:HSC 2032, lane 15 –FP71:HSC 1459, lane 16 – FP72:HSC 1367, lane 17 – H37Rv:ATCC 27294, lane 18 – H37Ra:ATCC 25177).

Each *M. tuberculosis* strain tested produced a unique and clearly distinguishable RFLP pattern in comparison to every other strain examined. The most common isolate FP1 or Type1 (HSC 2950) produced a pattern that indicated the presence of 12 IS*6110* elements. Although HSC 2353 (FP71), another isolate from the province of Manitoba, also produced a 12 band pattern, the arrangement of bands clearly separated it and excluded this strain from being confused with FP1.

Three other common isolates from the province, HSC 2936 (FP2), HSC 2739 (FP5) and HSC 1367 (FP72), also had RFLP analysis performed on them since they were to be used in the subsequent survival and virulence studies. These strains produced distinctive patterns of two, nine and eleven bands respectively. Additionally, one other clinical isolate, HSC 2737 (FP3), along with both the H37Rv (ATCC 27294) and H37Ra (ATCC 25177) reference strains were also tested and displayed results which matched previously observed patterns and established fingerprints (Figure 4).

3.2 Survival of Mice Following Aerosol Infection

In order to confirm the putative hypervirulence observed in *Mycobacterium tuberculosis* Type1 strain, survival studies using C3H, C57BL/6 and BALB/c mice were conducted to compare the virulence of Type1 to that of other common clinical isolates from Manitoba.

In C3H mice, a more susceptible model of TB infection, mice infected with Type1 exhibited a rapid and early mortality. Shortly after the onset of symptoms, all Type1 infected mice succumbed to the disease by day 21. The mean survival time for Type1 infected mice was 20.5 days. Mice infected with Type72, Type5 and Type2 began

to display symptoms of the disease after 22 days. The mean survival times were 32.6, 33.0 and 33.9 days respectively for each strain. Although survival times were similar, the survival profile seen for Type2 and Type5 was different in comparison to Type72 (Figure 5a). In both Type2 and Type5 infected mice, approximately half of the mice succumbed to the disease shortly after the onset of symptoms (days 22-26) while the rest of the mice survived greater than 40 days. H37Rv infected mice showed the longest survival time (52.5 days). Based on these observations, Type1 infected mice showed a significantly earlier mortality when compared to all strains examined ($p \leq 0.0001$). No significant differences in survival were observed between the other clinical strains.

In the BALB/c model, Type1 infected mice began to show disease symptoms at day 23 post-exposure and 11 out of 12 mice had either died or been euthanized due to disease symptoms by day 26 (Figure 5b). The mean survival time for Type1 infected mice was 26.5 days. In contrast, mice infected with either Type5 or Type72 began to present disease symptoms later than Type1 infected mice (day 30), where the majority of animals died or were culled after 50 days (Figure 5b). Mean survival times were 52.3 and 56.3 days for Type72 and Type5, respectively. Mice infected with the Type2 strain displayed a survival profile similar to that seen for H37Rv, where mice did not begin to die until day 76-79 post-exposure. By day 80, the endpoint of the experiment, 7 mice remained for Type2 and 5 mice remained for H37Rv. These mice were assigned a survival time of at least 80 days and thus the estimated survival times for Type2 and H37Rv infected mice were greater than or equal to 70.0 and 73.2 days, respectively. Thus, the mean survival time for Type1 infected mice was significantly shorter than for

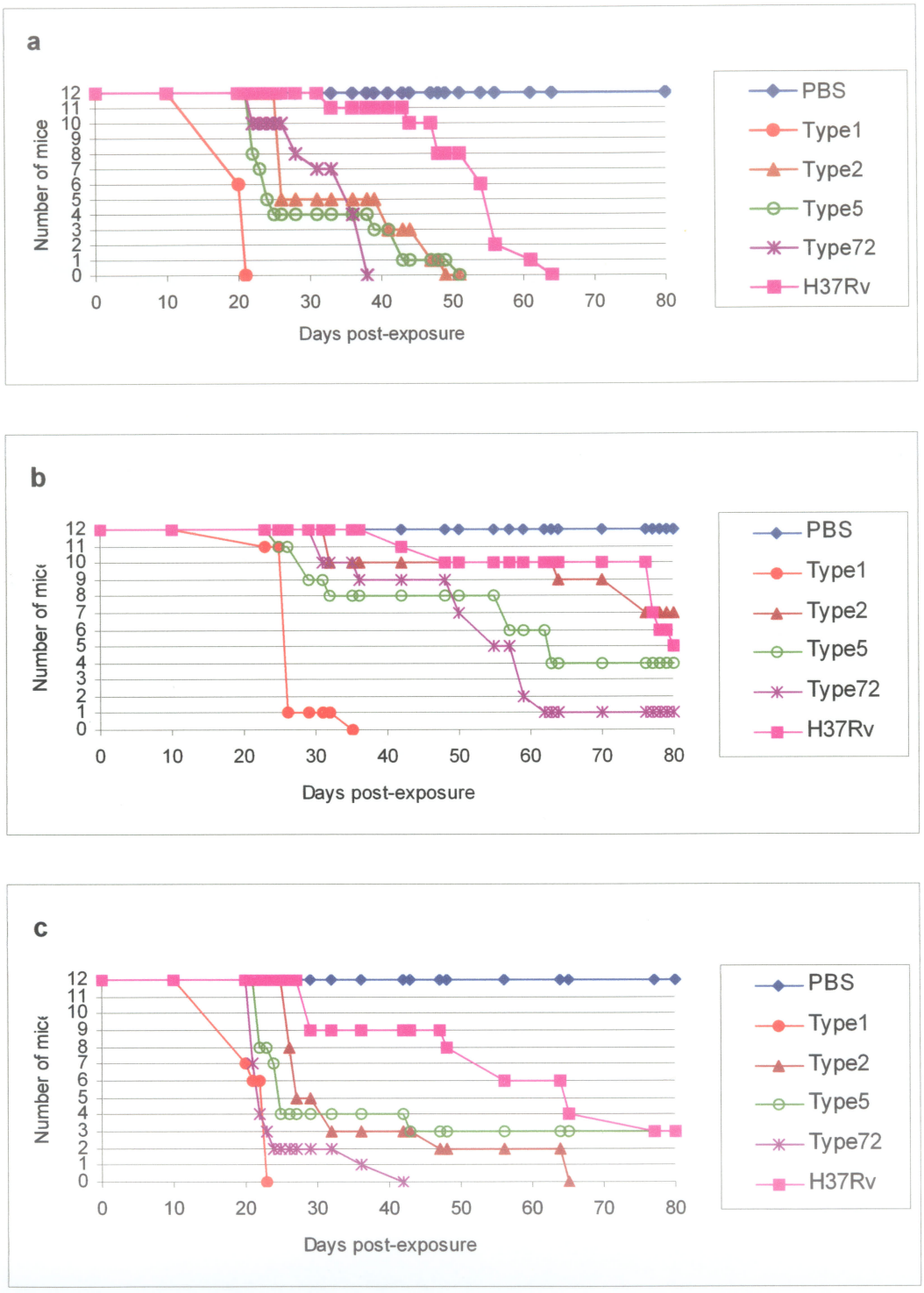

Figure 5a, b, c. Survival of (a) C3H mice, (b) BALB/c mice and (c) C57BL/6 mice (12 mice/group) exposed to aerosols of either PBS (♦), 1.52 x 10^7 CFU/ml *M. tuberculosis* Type1 (♦), 2.6 x 10^7 CFU/ml Type2 (▲), 1 x 10^7 CFU/ml Type5 (o), 2.24 x 10^7 CFU/ml Type72 (*) or 1.28 x 10^7 CFU/ml H37Rv (■) for 30 minutes.

all other strains including Type72 ($p \leq 0.0001$) and Type5 ($p=0.0002$) infected mice. In addition, Type72 infected mice also displayed a significantly shorter survival time than Type2 ($p=0.002$) and H37Rv ($p=0.004$) infected mice.

In the relatively resistance C57BL/6 mouse model, Type1 infected mice again experienced an earlier mortality than mice exposed to aerosols of the other *M. tuberculosis* strains (Figure 5c). Specifically, Type1 infected mice began to exhibit symptoms of disease as early as 20 days post-exposure and by day 23 post-exposure all mice from this experimental group had succumbed to the disease. The mean survival time for Type1 infected mice was 20.8 days. Mice infected with Type5 and Type72 began to demonstrate symptoms of disease by day 21-22 post-exposure while mice infected with either Type 2 or H37Rv developed observable disease symptoms by day 26-27 post-exposure. All mice infected with Type72 or Type2 had either died or been culled by day 42 and 65 post-exposure respectively. However, in the case of Type 5 and H37Rv infected animals, 3 mice for each group remained at the endpoint of the experiment and again these animals were assigned an estimated survival time of 80 days each. Mean survival times were 24.7 and 35.3 days for Type72 and Type2, while estimated survival times for Type5 and H37Rv infected C57BL/6 mice were calculated to be 39.2 and 57.8 days respectively. Again, the mean survival time for Type1 infected mice was significantly shorter than Type72 ($p=0.004$) and also compared to all other strains examined ($p \leq 0.0001$).

Mice infected with the Type72 strain also displayed a significantly earlier mortality compared to Type2 ($p=0.003$), Type5 ($p=0.009$) and H37Rv ($p \leq 0.0001$)

infected mice. Additionally, the survival time of Type2 infected mice was significantly shorter than that of H37Rv infected mice (p=0.002).

In all mouse models, all control mice that were exposed to aerosols of PBS remained healthy with no symptoms throughout the course of the experiment.

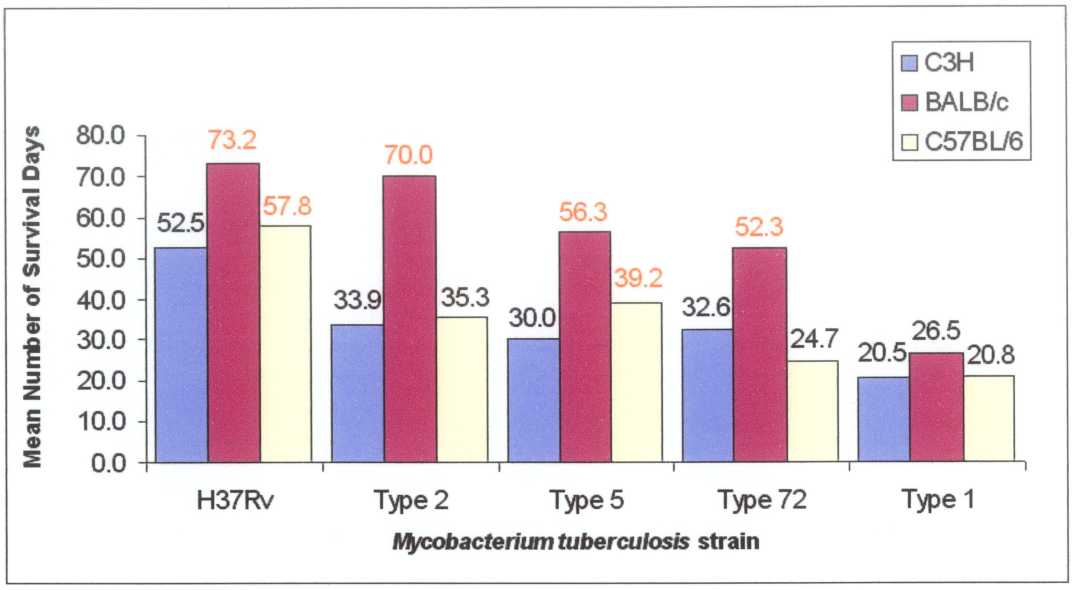

Figure 6. Mean number of survival days for 3 mouse strains. Survival times of mice exposed to aerosols of several different *Mycobacterium tuberculosis* strains. Note: Survival days indicated in orange represent estimated survival times calculated based on the presence of mice that remained viable at the endpoint of the experiment and accordingly each mouse was assigned a survival time of 80 days.

3.3 Growth of *M. tuberculosis* in Infected Lungs at Day 15 Post-exposure

In order to investigate whether a higher growth rate of the Type1 strain in comparison to that of the other isolates was a potential explanation for the enhanced virulence of Type1, the growth of strains in the lungs was evaluated.

At day 15 post-exposure, $\log_{10}$ values from infected lungs of C3H mice for Type1, Type5 and Type72 were 5.52 ± 0.11, 5.51 ± 0.34 and 5.41 ± 0.15, respectively

(Table 12). In contrast, the growth of Type2 from lung samples (4.81 ± 0.28) was less than that seen among other clinical isolates and was closer to the value obtained for H37Rv (4.30 ± 0.29). Therefore, in C3H mice, Type1, Type5 and Type72 displayed a bacterial load 1 $\log_{10}$ higher than that seen in H37Rv.

In BALB/c mice, comparable average $\log_{10}$ values were observed for Type1, Type5 and Type72 in infected lungs: 5.57 ± 0.07, 5.56 ± 0.09 and 5.47 ± 0.12, respectively. Again, as seen in the C3H model, Type2 infected BALB/c mice had a lower bacterial load (5.11 ± 0.27) compared to the other clinical strains and H37Rv had the lowest average $\log_{10}$ value (4.48 ± 0.27) of any of the strains examined (Table 12).

Bacillary loads observed in the lungs of infected C57BL/6 mice were similar to that seen in both other mouse models as $\log_{10}$ values from infected mice were 5.61 ± 0.07, 5.47 ± 0.14 and 5.48 ± 0.13, for Type1, Type5 and Type72 respectively. When examining the growth of Type2 in the lungs of C57BL/6 mice, the observed growth is in complete contrast to that seen in C3H and BALB/c mice. In this case, Type2 infected C57BL/6 mice had a lower bacterial load (4.73 ± 0.23) compared to H37Rv (4.90 ± 0.29).

In all three mouse models, no colonies were detected from all samples taken from mice exposed to aerosols of PBS. In general, in all mouse models, the clinical strains Type1, Type5 and Type72 all obtained levels of growth higher than that of the laboratory strain H37Rv although only in the case of C3H and BALB/c mice was this difference significant. Additionally, Type2 displayed lower growth than that of all other clinical strains, although the number of bacilli in the lungs was not significantly different (less

than 1 $\log_{10}$ difference). Furthermore, with the exception of the C57BL/6 mouse model, H37Rv infected mice had the lowest average $\log_{10}$ values of any of the strains examined.

Table 12. Average $\log_{10}$ value of CFU/ml per 100 mg of lung tissue

Strain	C3H		BALB/c		C57BL/6	
	Average $\log_{10}$ value[a]	SD[b]	Average $\log_{10}$ value[a]	SD[b]	Average $\log_{10}$ value[a]	SD[b]
Type1	5.52	0.11	5.57	0.07	5.61	0.07
Type2	4.81	0.28	5.11	0.27	4.73	0.23
Type5	5.51	0.34	5.56	0.09	5.47	0.14
Type72	5.41	0.15	5.47	0.12	5.48	0.13
H37Rv	4.30	0.29	4.48	0.27	4.90	0.29

[a]Average $\log_{10}$ values are averages from 6 mice per experimental group. Averages were calculated from serial dilutions of lung homogenates prepared from 100 mg of lung tissue at day 15 post-exposure. In all mouse models, lung homogenates from control mice exposed to PBS resulted in no colonies.
[b]SD = Standard deviation (±)

3.4 Histological Analysis of Granulomatous Inflammation in the Lungs

Based on the survival data obtained, histological analysis was performed on lung sections from C3H and BALB/c mice in order to assess lung pathology in an attempt to further characterize the progression and disease manifestation of pulmonary tuberculosis caused by the Type1 strain.

In C3H mice, Type1 infected lungs (Figure 7a) displayed the highest average number of nodules per section (3.62 ± 0.68). Although the number of nodules was lower for each of the other clinical strains, only Type5 and Type72 ($p=0.01$ and $p=0.028$, respectively) were significantly different from Type1 (Table 13). H37Rv infected lungs exhibited the lowest number of nodules, which was significantly lower ($p\leq0.008$) than

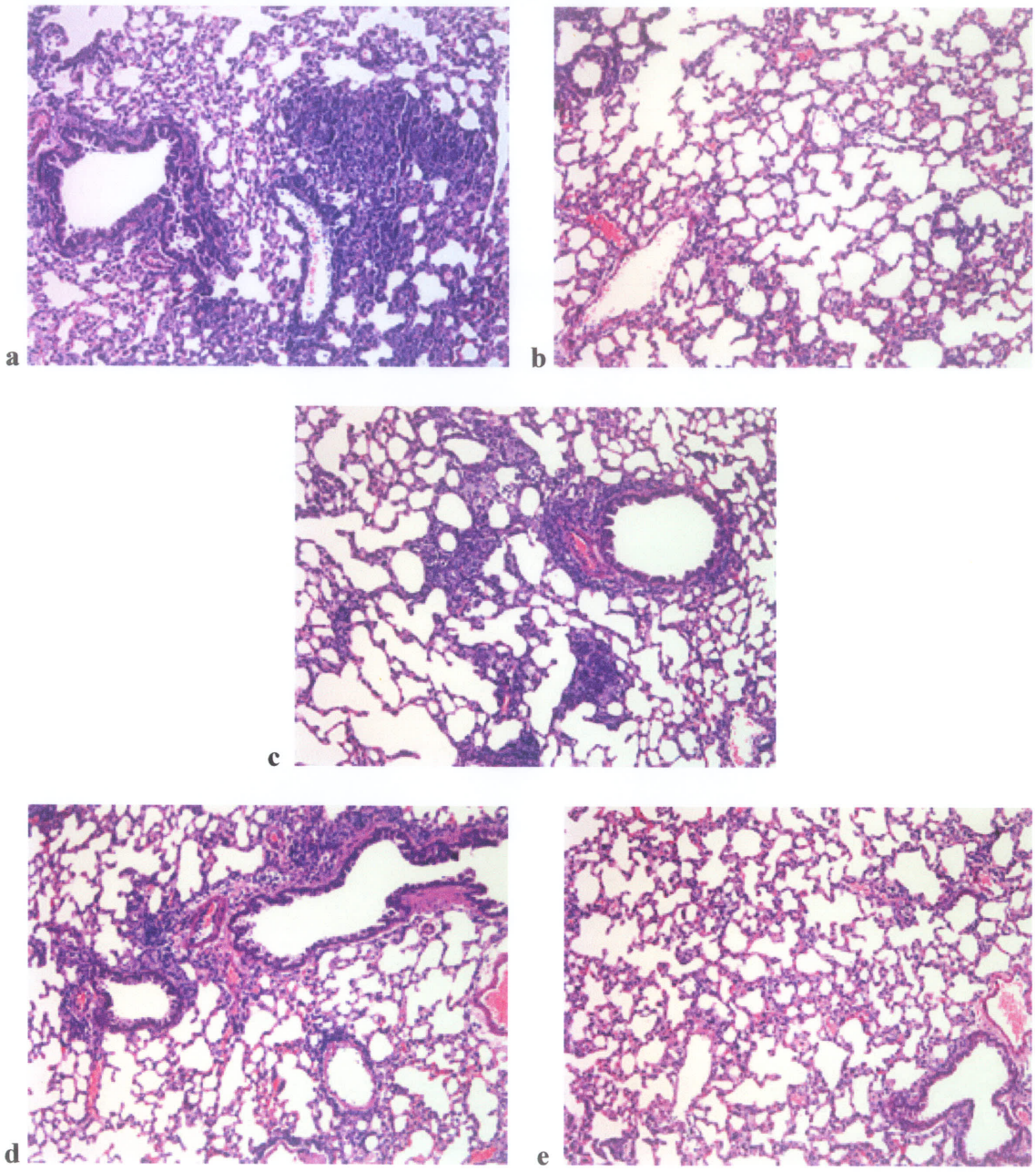

Figure 7. Representative photomicrographs of lung sections. Haematoxylin and eosin stained parasaggittal sections of lung tissue taken from C3H mice infected with *M. tuberculosis* strains (**a**) Type1, (**b**) Type2, (**c**) Type5, (**d**) Type72 and (**e**) H37Rv. Lungs from 6 mice per experimental group per strain of mouse were aseptically removed at day 15 post-exposure. All micrographs are at 100X magnification.

all other strains examined (Table 13).

In C3H mice, nodules from Type1 infected lungs were not only most abundant but also largest in size. The average diameter of a nodular aggregation was 162.29 ± 20.86 μm (Table 13), significantly larger than those from Type2 ($p=0.035$) and Type5 ($p=0.025$) infected lungs. H37Rv infected lungs, in addition to having the least amount of nodules, also possessed significantly smaller nodules ($p\leq0.007$) than any other strain investigated.

In BALB/c mice, the average number of nodules seen in Type1 sections (Figure 8a) was 3.51 ± 0.78, similar to Type2 and Type5 (Table 13). In contrast to the C3H model, Type1 infected lungs from BALB/c mice did not display the highest but instead exhibited the lowest average number of nodules per section among the clinical strains examined. Type72 infected lungs showed the largest number of nodules in BALB/c mice (4.79 ± 0.67), significantly more than all other strains ($p\leq0.013$). Once again, lungs infected with H37Rv displayed the lowest average number of nodules per section, significantly lower than all other strains ($p\leq0.003$). Type1 infected lungs from BALB/c mice had nodules that were similar in size to those seen in C3H mice for this strain (163.44 ± 22.23 μm). Therefore, not only were similar amounts of nodules formed but also the size of these aggregations was comparable. However, in contrast to observations seen for Type1, the size of nodules for all of the other clinical strains was significantly larger in BALB/c mice as compared to C3H mice (Table 13). Type72 infected lungs had the largest nodules (216.62 ± 18.56 μm) which were significantly larger than nodules from any other strain ($p\leq0.009$). Again, in BALB/c mice, H37Rv infected lungs possessed the smallest nodules of all strains examined, although not significantly smaller

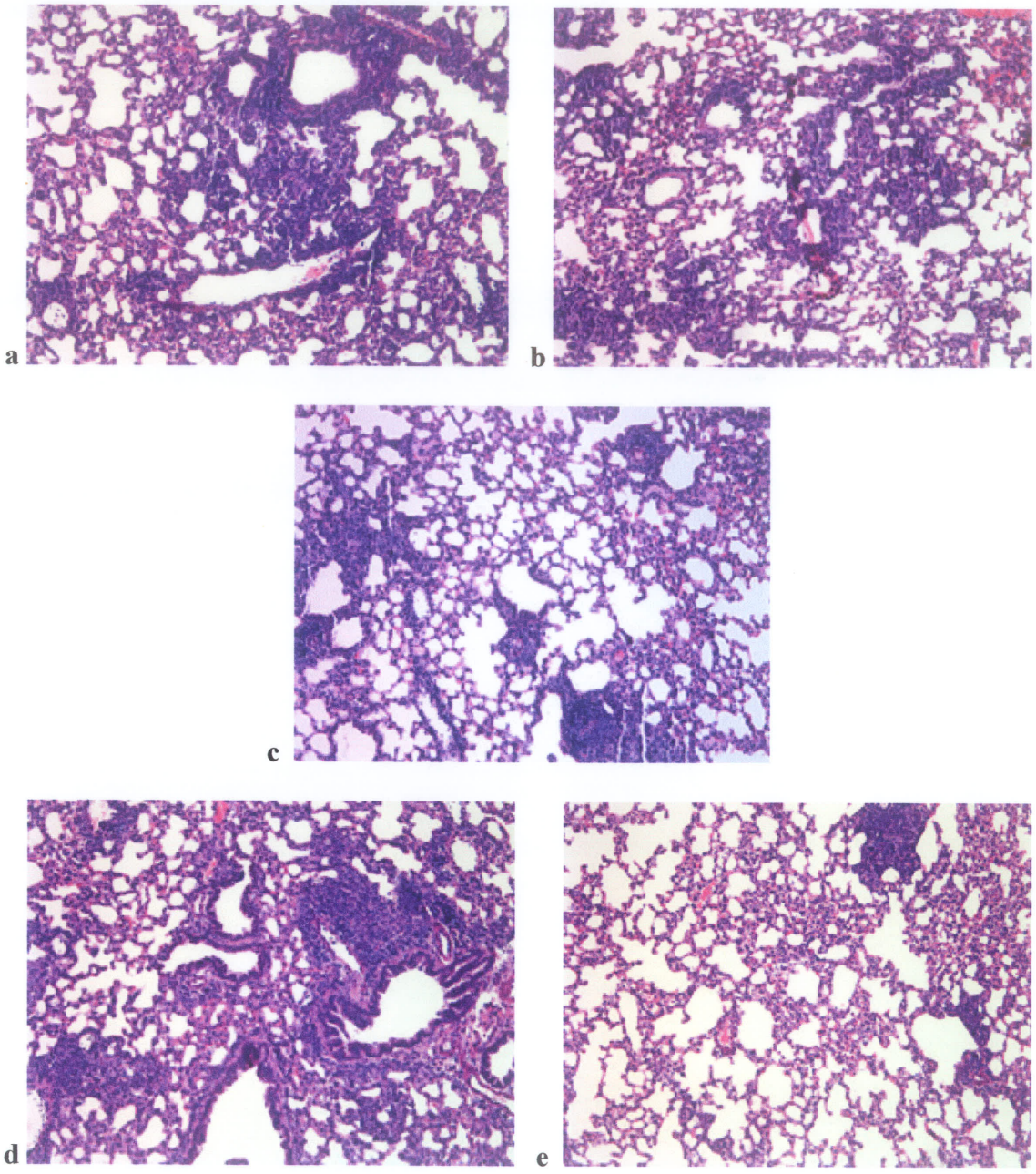

Figure 8. Representative photomicrographs of lung sections. Haematoxylin and eosin stained parasaggittal sections of lung tissue taken from BALB/c mice infected with *M. tuberculosis* strains (**a**) Type1, (**b**) Type2, (**c**) Type5, (**d**) Type72 and (**e**) H37Rv. Lungs from 6 mice per experimental group per strain of mouse were aseptically removed at day 15 post-exposure. All micrographs are at 100X magnification.

Table 13. Histological analysis of nodular formations in lungs of mice

Strain	C3H		BALB/c	
	Average number of nodules per section[a]	Average size (diameter) of a nodule (μm^2)	Average number of nodules per section[a]	Average size (diameter) of a nodule (μm^2)
Type1	3.62 ± 0.68	162.29 ± 20.86	3.51 ± 0.78	163.44 ± 22.23
Type2	2.89 ± 0.48	132.19 ± 19.74	3.52 ± 0.66	178.95 ± 28.68
Type5	2.56 ± 0.62	130.11 ± 18.39	3.77 ± 0.45	175.11 ± 20.59
Type72	2.72 ± 0.74	142.22 ± 27.54	4.79 ± 0.67	216.62 ± 18.56
H37Rv	1.45 ± 0.26	91.34 ± 15.08	2.27 ± 0.38	140.06 ± 34.16

[a]Lungs from 6 mice per experimental group were collected for histological analysis 15 days post-exposure to aerosols of different *M. tuberculosis* strains. Average values ± SD were calculated from 6 mice per experimental group with 25 random sections of lung per mouse.

Sections of lung taken from mice exposed to PBS did not exhibit nodules.

Table 14. Comparison of observed granulomatous inflammation in lungs of mice

Strain	**Average area of lung involved in granulomatous inflammation (μm^2)** [a]	
	C3H	BALB/c
Type1	67238.38 ± 30883.42	71134.41 ± 37433.56
Type2	33936.36 ± 13689.39	81836.07 ± 35190.25
Type5	33053.37 ± 11944.11	90609.22 ± 17467.90
Type72	35881.74 ± 14696.23	159744.23 ± 26105.97
H37Rv	12126.55 ± 3040.30	38755.81 ± 25849.48

[a]Average values ± SD were calculated from 6 mice per experimental group with 25 random sections of lung per mouse taken 15 days post-exposure to aerosols of different *M. tuberculosis* strains.

Lung sections taken from mice exposed to PBS displayed no granulomatous inflammation.

than those seen in Type1 infected lungs (p=0.1).

In both mouse models, all control mice exposed to aerosols of PBS displayed no formation of nodules.

In terms of the total area of lung section occupied by granulomatous inflammation, the clinical strains of *M. tuberculosis* displayed two different patterns in the two mouse models. In C3H mice (Figure 7), lungs infected with Type1 showed the largest area occupied by granulomatous inflammation (67238.38 ± 30883.42 μm^2). Lungs infected with other clinical strains, although not statistically significant, had approximately half as much area involved in granulomatous inflammation compared to Type1 (Table 14).

In BALB/c mice (Figure 8), all clinical isolates except Type1 displayed a significantly larger amount of lung occupied by granulomatous inflammation than observed in C3H mice. In this model, Type72 infected lungs had a significantly larger total area involved in the granulomatous response, 159744.23 ± 26105.97 μm^2, approximately twice as much as any other clinical strain examined ($p \leq 0.0001$ compared with all strains). The total area involved in the granulomatous response in Type1 infected BALB/c mice (71134.41 ± 37433.56 μm^2) was similar and not significantly different (p=0.817) to that observed in C3H mice for this strain of *M. tuberculosis* (Table 14).

In both the C3H and BALB/c models, lungs infected with H37Rv showed the lowest total area occupied by granulomatous inflammation. Visible acid-fast bacilli were only present in lungs of mice exposed to any clinical strains or H37Rv and not in animals exposed to PBS. For all mice exposed to aerosols of PBS, no lung sections revealed any presence of nodules or cellular aggregations.

Therefore, taken together, histological analysis of lung sections at 15 days post-exposure revealed that regardless of which mouse model was being examined, lungs infected with Type1 showed approximately the same average number and size of nodules along with a similar total area involved in the granulomatous response (Table 14). In contrast, lungs infected with any of the other clinical strains exhibited a more numerous and extensive granulomatous response in BALB/c mice compared to the C3H model. Furthermore, even though mice infected with Type1 succumbed to disease earlier in both mouse models, lung histology revealed two differing granulomatous responses in which Type1 was ranked as either producing the most (C3H) or the least (BALB/c) granulomatous inflammation upon infection in contrast to the other clinical strains.

3.5 Semi-quantitative RT-PCR Detection of Cytokine Expression

To investigate the host-parasite relationship, the manifestation of disease caused by Type1 and the magnitude of the host immune response, RT-PCR was performed in order to quantify the expression levels of key cytokines present in the lungs of infected mice.

3.5.1 RNA Integrity

After isolating total RNA via the TRIzol method, random samples from both the C3H and BALB/c mouse strains were examined by denaturing agarose gel electrophoresis to ensure that the isolated RNA would make a satisfactory template for subsequent RT-PCR reactions. Although, only 1 μg of RNA was run on the gel for each sample, generally, if the two appropriate sized bands were observed, the quality of each

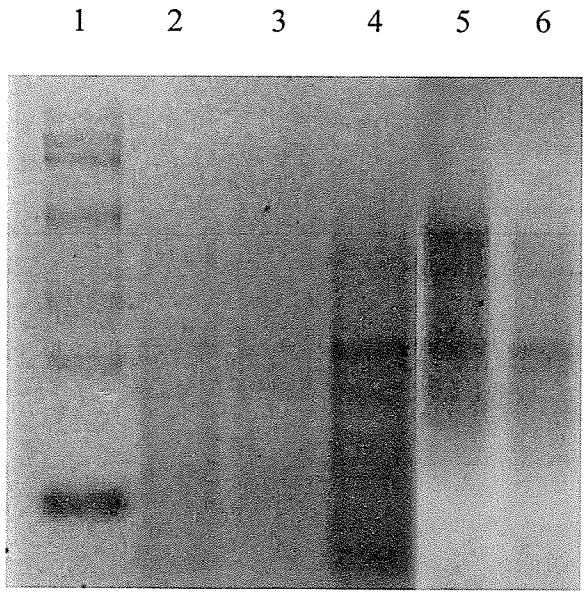

Figure 9. RNA integrity check via denaturing agarose gel electrophoresis. Representative gel image showing random RNA samples that were tested (lane 2 – Type2 C3H mouse #4, lane 3 – Type5 BALB/c Mouse #2, lane 4 – Type72 C3H mouse #3, lane 5 – H37Rv BALB/c mouse #2, lane 6 – Type5 C3H). A 0.24-9.5 Kb RNA Ladder™ (Invitrogen) was also included (lane 1).

sample examined was deemed to be sufficient and usable. Samples (Figure 9, lane 4 and 5) which displayed the presence of two bands with molecular sizes of approximately 1.9 Kb and 4.7 Kb, representing the 18s and 28s rRNA bands respectively, were used as it was likely that these samples did not suffer major degradation during the preparation of the RNA. Any samples that appeared to lack either one or both of these two bands or displayed excess smearing, were discarded and a new round of RNA extraction was performed for these samples.

3.5.2 RT-PCR

After examining RNA integrity by gel electrophoresis, RT-PCR was performed on samples from 6 mice per experimental group for both the C3H and BALB/c mouse

models. For each sample, different primer sets (Table 7) designed to amplify a segment of gene for either IL-5, IL-10, IL-12 p40 and IFN-γ, were employed in order to examine the expression of these four TB important cytokines. For each given cytokine tested, reactions for all 6 samples were performed simultaneously and then run together on the same gel to minimize the possibility of gel-to-gel variation. Duplicate sets of reactions were performed for each experimental group on all cytokines, with the exception of the BALB/c Type2 group that unfortunately failed to yield duplicate data for the IL-5 cytokine. All successful amplifications yielded products whose size matched the corresponding predicted product size as indicated in Table 7. In general, all products obtained (6 in total from each given experimental group) for each duplicate set, displayed bands of similar intensity as gauged by visual observation (Figure 10). In cases where individual bands from one given set were not visually similar to that of the corresponding sample in the duplicate set of reactions for a particular experimental group, the mouse number and cytokine being tested were noted for careful examination during the subsequent quantification steps and excluded if data values drastically differed.

A negative water control was included with each set of six reactions and in each case yielded no amplification product. In addition to performing all reactions with a standard amount of template, positive control reactions using the housekeeping gene β-actin were included to ensure that loading of each sample would be as precise as possible and also to be used in subsequent quantification steps as a normalizing standard.

1 2 3 4 5 6 7 8 9 10 11 12 13 14 15 16 17

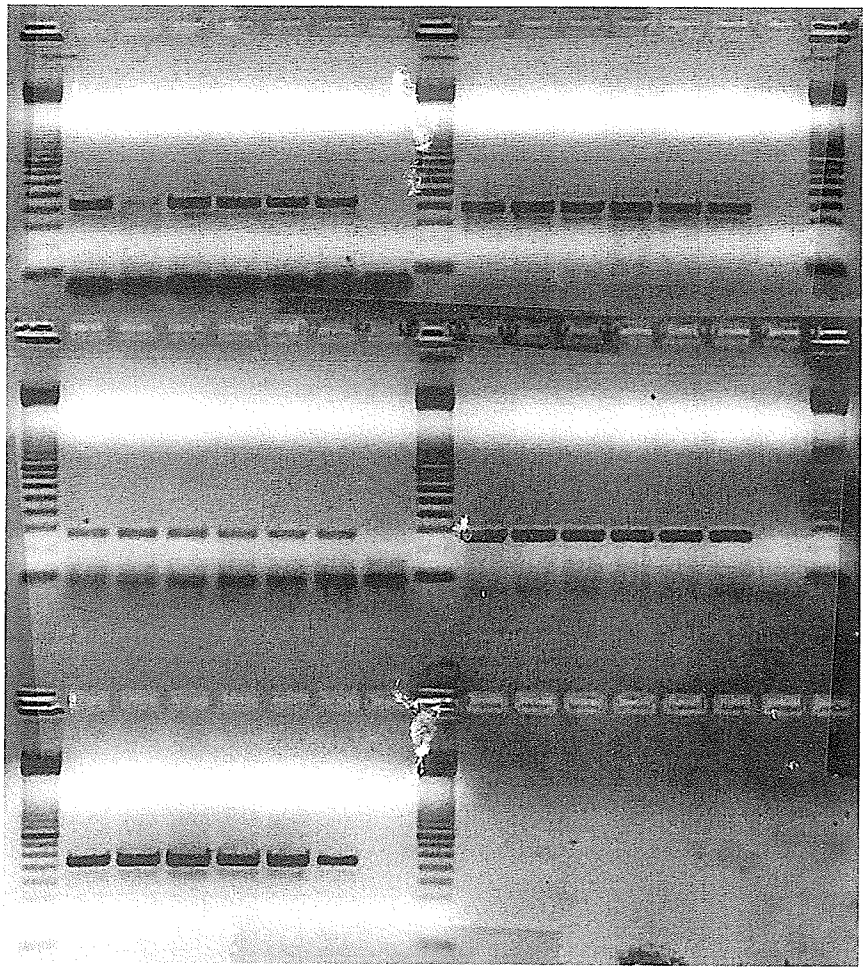

Figure 10. Representative gel image of RT-PCR products. Samples from six BALB/c mice infected with *M. tuberculosis* Type2 were subjected to RT-PCR to examine the expression level of IL-5, IL-10, IL-12 p40 and IFN-γ. Reactions for β-actin were also performed and utilized as a positive control. Water controls were used as negative controls.

Top: Lane 1, 9 & 17 – 100 bp DNA Ladder (Invitrogen), lanes 2-7 – Mice 1-6 IL-12 p40, lanes 10-15 – Mice 1-6 IFN-γ, lanes 8 & 16 – negative water control.

Middle: Lane 1, 9 & 17 – 100 bp DNA Ladder (Invitrogen), lanes 2-7 – Mice 1-6 IL-5, lanes 10-15 – Mice 1-6 IL-10, lanes 8 & 16 – negative water control.

Bottom: Lane 1 & 9 – 100 bp DNA Ladder (Invitrogen), lanes 2-7 – Mice 1-6 β-actin, lane 8 – negative water control.

3.5.3 Semi-quantitative Cytokine Expression Analysis

The relative expression of key cytokines in the lungs of mice infected with various *Mycobacterium tuberculosis* strains was compared by assessing each successful RT-PCR product a numerical value based on the density of each amplification product band. Raw band density values were computer generated based on the number of pixels comprising each band on the gel images. In addition, band densities for control β-actin products were calculated and standardized to a value of 20000 pixels in order to be used as a way to normalize values obtained for every other cytokine. Since a β-actin RT-PCR reaction was performed for each sample, the ratios used to normalize the raw β-actin pixels data to the standard 20000 level, were also applied to the raw data for each of the four cytokine reactions performed on each sample in order to generate adjusted pixel values that could be used for direct comparison, thus minimizing potential gel-to-gel variation. For each experimental infection group, comparative pixel averages were calculated from duplicate data sets comprising up to 6 samples per set (potentially 12 adjusted values per experimental group).

In the C3H mouse model, relative induction of all four cytokines was greatest in H37Rv infected lungs. Lungs infected with this strain exhibited induction levels of 17472.16, 18697.97, 17167.43 and 19055.27 pixels for IFN-γ, IL-12 p40, IL-10 and IL-5 respectively. Excluding H37Rv, the highest induction of IFN-γ and IL-12 p40 was seen in samples from Type2 infected mice (14149.16 and 15992.13). Among the other clinical isolates, average values for IFN-γ were 13648.87, 12002.40 and 11187.31 while values of IL-12 p40 were 13862.16, 8509.40 and 10229.56 for Type1, Type 72 and Type5 infected mice respectively. Correspondingly, when examining the calculated data obtained for

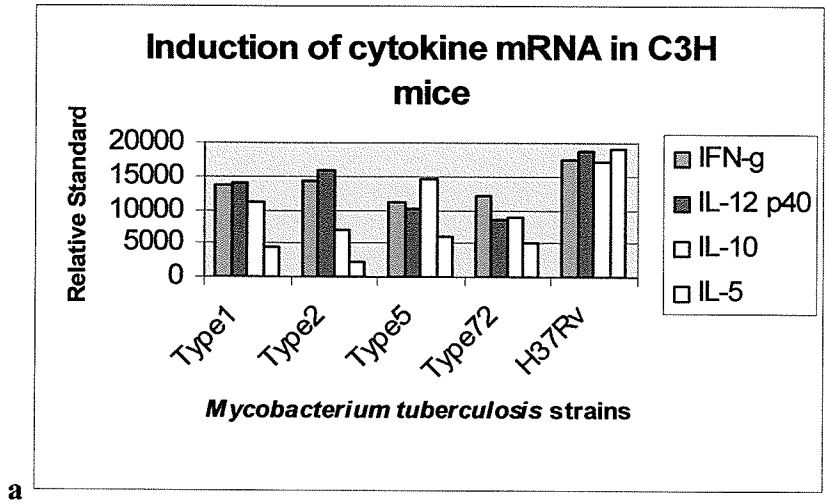

a

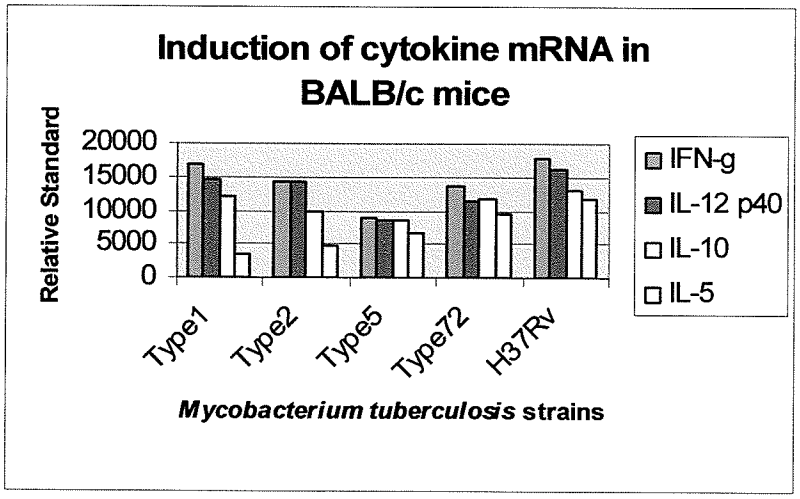

b

Figure 11. Normalized average band densities based on pixel data values. RT-PCR band densities representing induction of several key tuberculosis cytokines in the lungs were calculated following infection with various *M. tuberculosis* strains. Average pixel values for each cytokine were normalized to pixel data obtained for the housekeeping gene β-actin.

anti-inflammatory cytokines, mice infected with Type2 displayed the lowest relative induction of IL-10 and IL-5 (7115.17 and 2122.82). Amongst the clinical isolates, no other obvious associations between pro and anti-inflammatory cytokines were evident. Type5 infected mice induced the largest relative amount of IL-10 and IL-5, 14741.04 and 6101.62, higher than that observed for Type1 (11100.62 and 4438.25) and Type72 (9006.24 and 5184.07).

Again, in BALB/c mice, the highest relative induction of all four cytokines was observed in mice infected with the laboratory strain H37Rv. However, in comparison to values seen for these cytokines in C3H mice, average cytokine induction levels were generally lower in BALB/c mice with the exception of IFN-γ values. Average pixel values were 17638.12, 16285.65, 12918.24 and 11646.55 for IFN-γ, IL-12 p40, IL-10 and IL-5 respectively.

Unlike the situation observed in C3H mice, induction of three of the four cytokines among mice infected with clinical isolates was highest in Type1 infected mice. Relative expression levels for IFN-γ (16708.77), IL-12 p40 (14452.54) and IL-10 (12095.14) were observed in Type1 infected lungs. When examining the expression levels of IFN-γ and IL-12 p40 among the other clinical isolates, average values for Type2, Type72 and Type5 infected mice were 14266.49, 13658.44 and 8975.18 as well as 14315.45, 11561.93 and 8440.08 for the two cytokines respectively.

Data values obtained for the other two cytokines revealed that Type72 displayed the highest expression of anti-inflammatory cytokines among the clinical isolates. Although the expression level of IL-10 was slightly less than that seen in Type1 infected lungs (11669.01 compared to 12095.14), Type72 did display a higher expression

compared to Type2 (9971.68) and Type5 (8586.25). In the case of the cytokine IL-5, Type72 exhibited an average expression level of 9545.69 pixels, greater than all other clinical isolates examined. Average values for IL-5 were 3436.32, 2342.27 and 6570.14 for Type1, Type 2 and Type5 infected BALB/c mice respectively.

3.6 Identification of Strain-specific Virulence Factors

In order to further investigate the hypervirulence of the Type1 strain, the suppression subtractive hybridization method was employed in order to identify strain-specific virulence factors present within the bacterial genome of Type1 but absent from the laboratory strain H37Rv. Since microarray technology and strategies fail to identify sequences present in test isolates in relation to known reference strains, the hybridization technique was chosen since it utilized an adaptor-ligation PCR-based strategy to selectively isolate then enrich for sequences only present within the test isolates genome.

3.6.1 Primary and Secondary PCR

Following successful digestion, ligation and hybridization procedures, subtracted target DNA was subjected to two individual PCR amplifications as described in section 2.5.5. The first amplification step was successfully performed using one primer (Table 11) that was capable of binding to a section within each of the adaptors. This allowed amplification of certain types of products yet prevented the amplification of undesired products due to the creation of panhandle-like structures, which suppress exponential amplification (Figure 3). Subtracted experimental primary PCR products generally were

difficult to visually observe while unsubtracted experimental primary PCR products produced a smear of DNA with few if any distinguishable DNA bands being observed.

To ensure that experimental products were genuine and that the subtractions via hybridization did indeed successfully occur, control experiments involving genomic *E. coli* DNA and ϕX174/*Hae* III digest DNA, were performed simultaneously. Subtracted and unsubtracted target *E. coli* DNA were subjected to the same PCR conditions as were experimental *M. tuberculosis* samples and yielded expected products. As with the unsubtracted experimental sample, primary PCR products from unsubtracted *E. coli* target DNA produced a DNA smear while the control subtracted *E. coli* sample and the PCR control subtracted DNA (provided in the Clontech kit) produced matching banding patterns, which displayed faint bands of 1.3, 1.1, 0.9 and 0.6 Kb (Figure 12a).

To further amplify and enrich for tester-specific sequences in addition to reducing any background PCR products, primary PCR products were used as a template along with nested primers (Table 11) so that a secondary PCR reaction could be performed as described previously (section 2.5.5). Secondary PCR products from unsubtracted samples (both experimental and control) again produced DNA smears similar to that seen with the primary PCR products. Secondary PCR products generated from subtracted *E. coli* control samples again displayed bands of 1.3, 1.1, 0.9 and 0.6 Kb, which were clear and strong unlike those seen following the first PCR amplification. These bands corresponded to fragments of the *Hae* III-digested ϕX174 DNA known to be present (1 copy per *E. coli* genome) following subtraction of the prepared *E. coli* control samples. In contrast to what was observed for experimental samples following the primary PCR amplification, PCR products generated following the secondary PCR reaction produced numerous,

distinct DNA bands (Figure 12c). In total, 11 bands could be clearly observed on the agarose gels following electrophoresis. Product sizes ranged from as high as 2 Kb to as low as fragments of 150-200 bp. The same PCR product banding pattern for *M. tuberculosis* experimental samples was observed following each separate subtraction experiment performed. Water controls were included for each set of PCR amplifications and served as negative PCR controls.

3.6.2 Isolation and Screening of Individual Target Sequences

As a result of the two rounds of successful amplification that produced an array of bands of differing size, rather than a single product, several methods were employed to screen potential candidates in an attempt to identify Type1 specific sequences isolated by the SSH technique.

3.6.2.1 Direct Sequencing of PCR Products

Since 11 distinguishable bands had been observed following electrophoresis, each band was cut directly out of the agarose gel and purified using the Wizard® SV Gel and PCR Clean-Up System (Promega). Each purified product was then concentrated and sent to the DNA Core Facility to sequence each product using the same primers that were used in the amplification steps (section 2.5.5). Unfortunately, sequence data for each of the products submitted, revealed a sequence identity of at least 98% to that of sequences contained within the H37Rv reference strain and thus indicated that they were not specific to the Type1 genome.

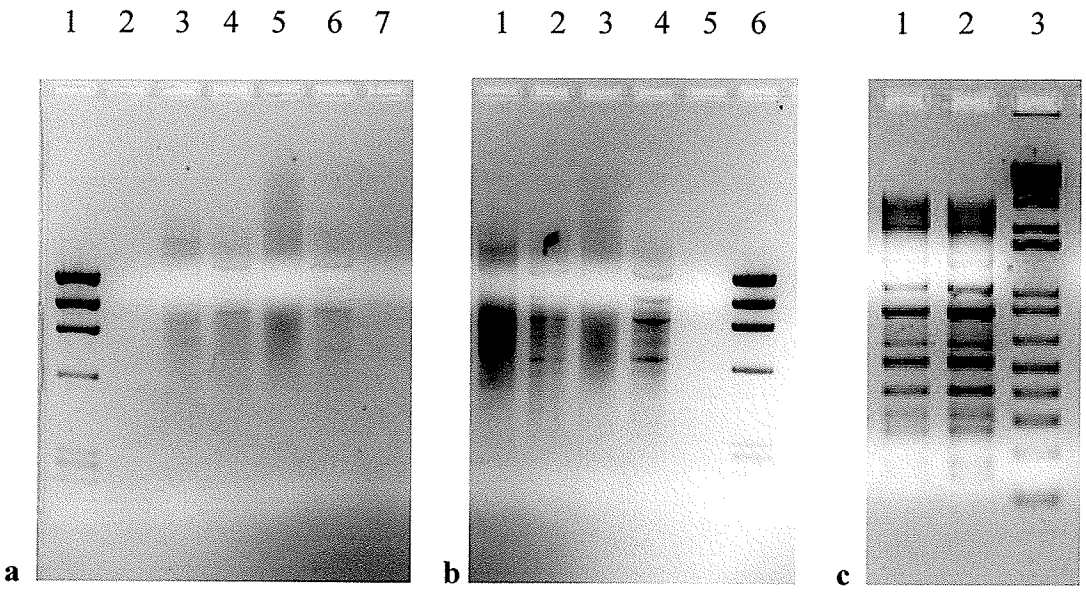

Figure 12. Suppression subtractive hybridization PCR products. Primary and secondary PCR amplifications were performed on subtracted *M. tuberculosis* target DNA as well as subtracted *E. coli* DNA, which was used as a positive experimental control. PCR was also performed on unsubtracted target DNA for both *M. tuberculosis* and *E. coli* and utilized as a negative experimental control. Water controls were also included as negative PCR reaction controls.

a: Lane 1 – ϕX174 RF DNA/*Hae* III Fragments DNA Ladder (Invitrogen), lane 2 – subtracted *M. tuberculosis* primary PCR product, lane 3 – unsubtracted *M. tuberculosis* primary PCR product, lane 4 – subtracted *E. coli* positive control primary PCR product, lane 5 – unsubtracted *E. coli* positive control primary PCR product, lane 6 – PCR control subtracted *E. coli* control primary PCR product, lane 7 – water control.

b: Lane 1 – unsubtracted *M. tuberculosis* secondary PCR product, lane 2 – subtracted *E. coli* positive control secondary PCR product, lane 3 – unsubtracted *E. coli* positive control secondary PCR product, lane 4 – PCR control subtracted *E. coli* control secondary PCR product, lane 5 – water control, lane 6 – ϕX174 RF DNA/*Hae* III Fragments DNA Ladder (Invitrogen).

c: Lane 1 – subtracted *M. tuberculosis* secondary PCR product (1 in 19 dilution), lane 2 – subtracted *M. tuberculosis* secondary PCR product (1 in 9 dilution), lane 3 – 1Kb Plus DNA Ladder (Invitrogen).

3.6.2.2 Cloning and Sequencing of Plasmid DNA

Secondary PCR products were also cloned into the pCR4-TOPO™ vector provided in the TOPO TA Cloning Kit for Sequencing™ to facilitate the attempt to directly identify individual sequences contained within the array of PCR products generated. Following propagation of the vector and extraction of plasmid DNA (as described in section 2.5.6), random clones were selected for restriction digestion analysis to determine if the majority of clones did contain inserts. Approximately, 1 out of every 6 clones was subjected to *Eco* RI restriction digestion prior to sending a larger number of clones to DNA Core for sequencing. From the 10 clones tested, 9 displayed at least two bands, one representing the cut vector (approximately 4 Kb) and the other band representing an insertion consisting of either a partial fragment or a complete PCR product. In the case of clone 33 (Figure 13, lane 7), two bands were present including one that was larger than the one representing the cut vector. Sequence data revealed that this was not a large PCR product but rather an artefact of a damaged agarose gel well and in reality just an empty vector since sequencing showed a 99.8% similarity to the cloning vector. Among the other clones tested, digestion products or fragments observed had a range of sizes from as low as less than 400 bp to as high as approximately 3 Kb, not drastically different to the sizes of SSH generated PCR products (Figure 12c).

Based on the high percentage of clones observed that successfully contained inserts, a total of 63 clones were picked and sent to DNA Core for direct sequencing using the T3 priming site located on the vector. Unfortunately, no clones were identified as containing Type1 specific sequences. Rather, from the 63 clones tested, 4 clones were identified as being empty vectors (99% similarity), 4 clones yielded poor, unusable data

while the remaining 55 clones all displayed a sequence similarity of at least 95.9 %, to both the reference sequence of H37Rv and also to the published sequence of the American clinical outbreak isolate CDC1551.

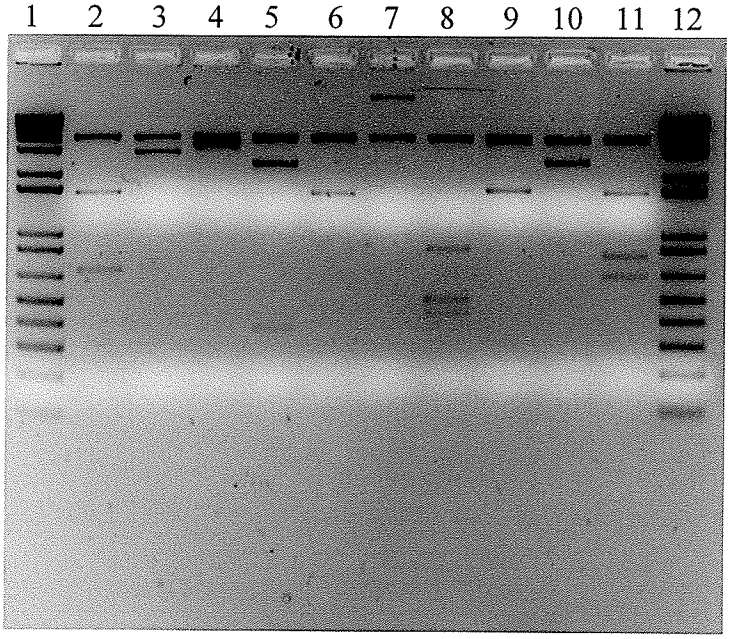

Figure 13. *Eco* RI restriction digestion of PCR product containing clones. Random clones were assessed to determine the likelihood of an insertion being present.

Lane 1 & 12 – 1Kb Plus DNA Ladder (Invitrogen), lane 2 – clone 3, lane 3 – clone 17, lane 4 – clone 41, lane 5 – clone 27, lane 6 – clone 22, lane 7 – clone 33, lane 8 – clone 11, lane 9 – clone 37, lane 10 – clone 56 and lane 11 – clone 48.

3.6.2.3 High-throughput Screening via Colony Dot Blots

In order to avoid performing an excessive amount of the more expensive and time-consuming task of sequencing individual clones, a colony dot blot approach was undertaken in an attempt to screen a larger number of clones to identify potential candidates for further investigation and subsequent sequencing. Duplicate blots containing 92 colony spots were prepared as described in section 2.5.7. To ensure that

each blot was functional and capable of producing accurate results, several control spots were included on each blot. A total of three positive controls were included, two spots of Type1 genomic DNA, and a single spot of H37Rv genomic DNA. Additionally, to ensure that each of the two probes only bound to actual clones, a negative control spot consisting strictly of LB culture media was employed.

ECL labelled probes made from *M. tuberculosis* Type1 genomic DNA or H37Rv genomic DNA (section 2.5.8), were initially tested on controls blots containing varying amounts of genomic DNA of each strain to determine that both the hybridization and detection of each probe could be carried out successfully. When each control blot was probed with one of the two probes, each spot of the corresponding matching strain produced a clear strong signal. Additionally, a weaker cross-hybridization was observed as sure enough; the probe was also able to bind to the other similar *M. tuberculosis* strain. Accordingly, a similar phenomenon was detected when the other *M. tuberculosis* strain was used as the probe.

A total of 6 complete 96 spot colony blots were prepared in duplicate and then each blot was individually probed with either the H37Rv probe or the Type1 probe. In all instances, every positive control spot was easily detected following probing. In general, a similar cross-hybridization reaction was observed in comparison to control blots where the non probe-matching *M. tuberculosis* positive control was also detected when probed, although the signal detected was lower. All LB media controls failed to yield a detectable signal.

When examining all the blots following chemiluminescent detection, 19 individual spots were initially identified as clones that potentially contained Type1

specific sequences since the Type1 probe was observed to have successfully bound to these spots while the H37Rv probe apparently was unable to bind (Figure 14). All of the 19 clones were then prepared and sent to DNA Core to determine the sequence of each of the inserts contained within the vectors. Subsequently, DNA homology analysis, using the internet based BLAST software, as described in section 2.5.10, revealed that sequence data obtained from each of the 19 clones showed a sequence homology of at least 98.4% when compared to the reference sequence of *Mycobacterium tuberculosis* H37Rv (accession number NC 000962).

Overall, a total of 552 colonies were investigated using the colony dot blot approach. Although, a handful of clones were initially identified as target candidates, not a single one was confirmed to possess Type1 specific sequences. Therefore, a combined total of 615 individual clones, (from both colony blots and direct sequencing) were examined and unfortunately yielded no Type1 specific sequences.

Based on the unsuccessful results obtained using the restriction enzyme *Rsa* I in the SSH procedure, an attempt to conduct the same procedure while substituting *Alu* I and the appropriately associated adaptors and primers (Table 9 and 11) was undertaken. Preliminary primary and secondary PCR reactions were performed on *Alu* I generated samples using the same conditions as *Rsa* I samples but failed to yield a similar type of PCR product pattern as previously described (Figure 12c). Instead, a DNA smear was observed and therefore, the initial *Alu* I SSH work was abandoned.

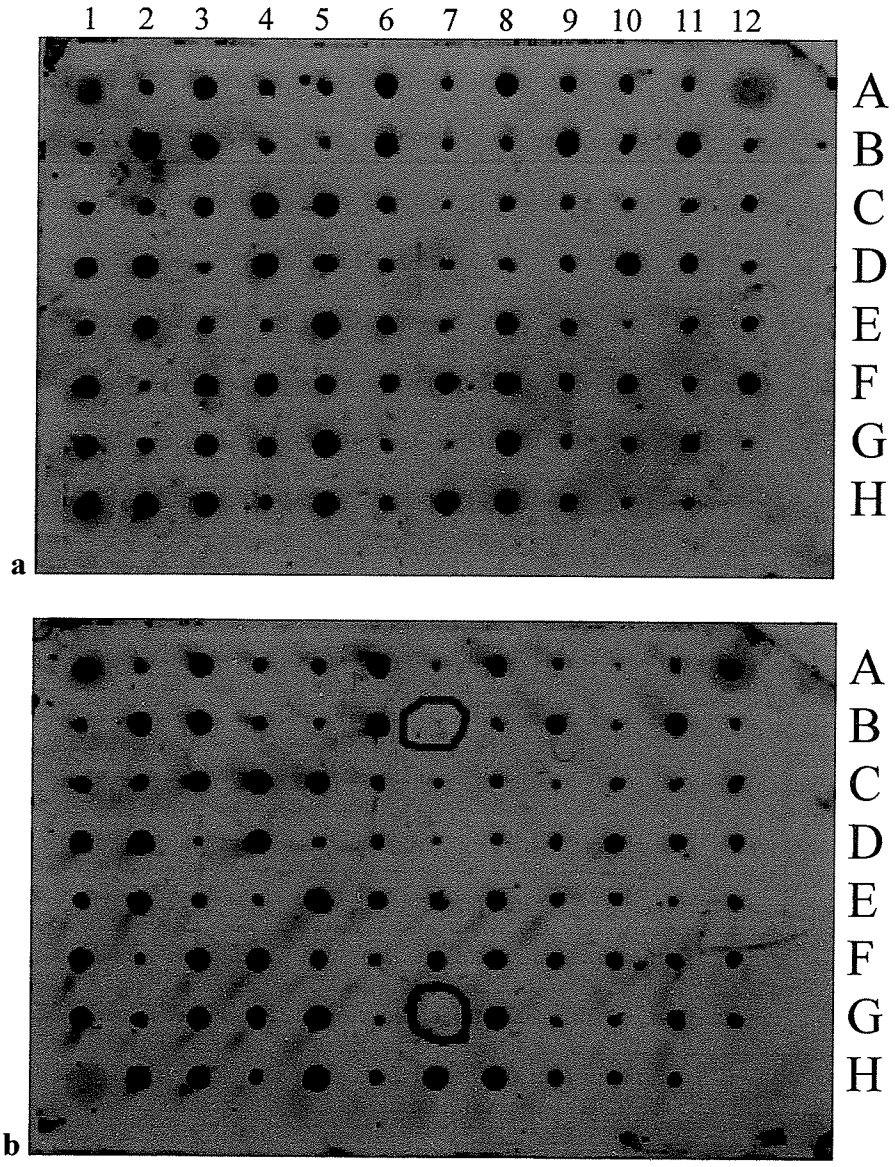

Figure 14. Representative SSH colony dot blots. Duplicate blots were probed with either the *M. tuberculosis* Type1 (a) or H37Rv probes (b). Individual clones such as 7B and 7G, which were detected when probed with Type1 but not H37Rv were singled out as potential candidates and sent for sequencing. On each blot, spots A1 and H1 were genomic Type1 DNA, spot A12 was genomic H37Rv DNA while H12 was the LB media control spot.

4. DISCUSSION

After several decades of decline in the number of TB cases, developed countries, including Canada, still face TB as a major health problem as the number of infections have ceased to decline and have even increased in some areas (Health Canada Health Protection Branch and LCDC, 1998). The main focus of this project was to investigate one group of isolates from Manitoba which share the same RFLP pattern, designated fingerprint Type1, and attempt to account for the overwhelming dominance of this isolate within the province as it accounts for 25.8% of total cases of TB. Additionally, since this group of isolates is predominant among the treaty-status population (Blackwood, *et al.*, 2003), further attention with regards to this strain is warranted. Limited knowledge concerning Type1 has made it difficult to account for its widespread occurrence within the province. While socio-economic factors play a significant role in the spread of the Type1 strain, the exact reason for the dominance of this strain in different communities in Manitoba, despite the fact that many other strains circulate in these locales, remains unknown. In recent times, suggestions such as environmental factors, the genetic make-up of the host and the host-bacterium interaction have been postulated to explain why certain clinical isolates are able to establish themselves and subsequently become dominant in a given community. Although each suggestion may play a role, the idea that some strains may possess specific bacterial virulence factors that confer an increased virulence to that strain has been the primary focus or hypothesis explored (Valway, *et al.*, 1998). Recently, Manca and colleagues (1999, 2001) examined two clinically important *M. tuberculosis* isolates from the United States: CDC1551 and HN878. CDC1551, an outbreak isolate from the Kentucky/Tennessee border, was originally described to have

"increased virulence" and the ability to grow substantially faster than the laboratory strain Erdman (Valway, *et al.*, 1998). However, upon examination *in vitro* and *in vivo*, CDC1551 was not deemed to be more virulent than other *M. tuberculosis* isolates in terms of growth but rather it was capable of inducing a more vigorous host response (Manca, *et al.*, 1999). From this initial study, HN878, a strain isolated from an outbreak in Houston, was shown to cause an unusually early death in an experimental mouse model when compared with other clinical isolates and in contrast to CDC1551, was suggested to be hypervirulent, possibly by failing to induce a Th1-type host response (Manca, *et al.*, 2001). Presented with these suggestions of hypervirulent clinical isolates and the possibility that such a phenomenon was occurring with the Type1 strain in Manitoba, the primary goal of this research project was to examine and further characterize the Type1 strain by focusing the investigation on any strain-specific bacterial virulence factors that could modulate the host's immune response thus favouring survival of the organism in an attempt to provide the basis for an explanation of the overwhelming dominant position of Type1 in the province.

Survival Comparison of Type1 and Other Clinical Isolates

Initial *in vitro* experiments using the *M. tuberculosis* Type1 strain supported the hypothesis of hypervirulence through strain-specific bacterial factors occurring here in Manitoba (Sharma, *et al.*, 2003). In comparison to H37Rv, Type1 induced significantly lower amounts of pro-inflammatory cytokines (IL-1β and IFN-γ) in infected macrophage cell lines (U937 and THP-1). Similar levels of anti-inflammatory cytokines (IL-4 and IL-10) were observed in Type1, H37Rv or H37Ra infected cultures (Sharma, *et al.*, 2003).

Taken together, this implied that the Type1 strain might down-regulate the protective response against infection.

Our research group's preliminary *in vivo* experiments using BALB/c mice had shown a significant decrease in survival times of Type1 infected mice in comparison to H37Rv infected mice (NRCM unpublished data). Cytokine profiles generated at progressive time intervals demonstrated a transition from a Th1 to a Th2-type immune response in Type1 infected BALB/c mice, which suggested that Type1 has the ability to modulate the host's immune response thus potentially favouring the pathogen. Furthermore, when lung histology was examined, the establishment of disease was observed to have occurred sooner following infection with Type1 as nodule formation occurred around 7 days for Type1 compared to 14 days for H37Rv. As well, the granulomatous response was significantly larger and more severe in Type1 infected mice (NRCM, unpublished data).

To further characterize the Type1 strain in terms of the progression and manifestation of pulmonary tuberculosis associated with it, the first step in the project strategy was to compare the Type1 strain against three other common clinical isolates from Manitoba, Type2, Type5 and Type72 as well as H37Rv, following aerosol infection in the relatively resistant C57BL/6, BALB/c and susceptible C3H mouse models. These mouse models were selected as previous investigations have shown their differing genetic make-up, immunity and tolerance to challenge with *M. tuberculosis* (Medina and North, 1998; Kelley and Collins, 1999; Chackerian, *et al.*, 2001).

As virulence is defined as the relative capacity of a pathogen to overcome the body's defences and the extent to which a given *M. tuberculosis* strain is able to cause

pathology and ultimately death in a given period of time (Mitchison, *et al.*, 1961; *Merriam Webster's Collegiate Dictionary*, 1998), survival results suggested that the Type1 strain in Manitoba does indeed possess an apparent enhanced or hypervirulence. In each of the mouse models tested, mice infected with Type1 succumbed to disease significantly earlier than all other *M. tuberculosis* strains examined. Furthermore, the general trend exhibited by the other clinical strains studied, regardless of which mouse model was used, was that these strains displayed an intermediate average period of survival compared to Type1 and H37Rv.

Although the results obtained from the survival studies provided a clear confirmation to the previous suggestion of hypervirulence with regards to the Type1 strain, survival times obtained in this project may seem shorter in comparison to other publications (Medina and North, 1998; Chackerian, *et al.*, 2001). The observed shorter survival times are believed to have been attributed to a slightly higher initial amount of bacilli present in the lungs (100-250 compared to 50-100) and to Humane Endpoint Criteria that may have been too stringent. Since a larger initial load may simply speed up the overall course of disease progression for each of the strains, the shorter survival times do not change the fact that Type1 infected mice succumbed to disease earlier than all other strains tested in each of the three mouse models. Additionally, since this survival study involved euthanization of animals based on endpoint criteria rather than a true mortality study and given that all mice were treated the same with respect to euthanization criteria, no alteration to the observed pattern showing that Type1 succumbed first, followed by the other clinical strains than H37Rv, would be expected.

Accordingly, since these two factors neither jeopardized nor lessened the observed hypervirulence of Type1, all data was not only deemed acceptable but also exceptional.

Therefore, based on survival times that show that Type1 causes earlier mortality, not only is this strain hypervirulent compared to H37Rv, but Type1 also possesses enhanced virulence compared to other common clinical isolates from Manitoba.

Growth of the Organism is Not Responsible for Enhanced Virulence

Given that the results obtained from the survival studies confirmed that enhanced virulence was a property of the Type1 strain, the purpose of the subsequent colony forming unit (CFU) assays was to determine whether the enhanced virulence of Type1 was attributed to a higher growth rate of this particular strain. Past studies have suggested that the growth rate of mycobacteria may provide a strong indication of the virulence of the organism (Silver, *et al.*, 1998). In order to directly judge the significance of the growth of Type1 in the lungs compared to other isolates, lung bacillary loads were evaluated 15 days post-exposure. Growth was assessed at this time point, since previous experiments conducted by Dr. Meenu Sharma demonstrated that average CFU counts were only significantly greater for Type1 compared to H37Rv at 14 days post-exposure (NRCM unpublished data). In the C3H and BALB/c mouse models, Type1, along with Type5 and Type72, exhibited colony counts greater than 1 $\log_{10}$ higher in both models compared to H37Rv. Again, in the case of C57BL/6 mice, bacillary loads for Type1, Type5 and Type72 were greater than that of H37Rv infected mice but not in terms of statistical significance. Bacillary loads, although lower, were comparable between Type2

and H37Rv, especially in C57BL/6 mice. Differences in bacillary loads between clinical isolates in each mouse model were insignificant.

Therefore, as a result of the colony forming unit data, the perceived enhanced virulence of the Type1 strain cannot be attributed to a higher growth rate of the isolate as the difference in average $\log_{10}$ counts between Type1 and all other clinical strains studied was less than 1 $\log_{10}$ difference. Thus, in accordance with North *et al.* (1999), results from this portion of the project show that the growth rate of mycobacteria in mice alone is an unreliable indicator of mycobacterial virulence.

Histological Analysis of Lung Sections

The purpose of the histological analysis of lung sections was to assess lung pathology in order to further characterize the progression and disease manifestation of pulmonary tuberculosis caused by Type1 in comparison to the other clinical isolates. Accordingly, based on the shorter than expected survival times obtained for C57BL/6 mice, all subsequent work was carried out solely on samples taken from C3H and BALB/c mice in order to assure that the generated data genuinely represented the disease state and progression rather than being overly influenced by a potentially pre-mature culling of the animals.

Histological analysis of lung sections revealed that two distinct situations were evident between the C3H and BALB/c mouse models in terms of the total area of the lung involved in the granulomatous response following Type1 infection. In order to calculate a numerical value for the granulomatous response, nodules or nodular formations were defined as visual, inflammatory aggregations composed of neutrophils,

monocytes/macrophages, lymphocytes, epithelioid cells and including associated cellular debris (Figures 7, 8). In both models, Type1 infected lungs displayed similar numbers and size of nodular formations, along with approximately the same amount of total area of lung being occupied by granulomatous inflammation at 15 days post-exposure. Again, day 15 was chosen as the time point of interest since previous observations made by Dr. Meenu Sharma noted that infection with Type1 results in an earlier onset of disease compared to H37Rv, progressing from mild to severe between days 14 and 21 post-exposure (NRCM unpublished data). In C3H mice, Type1 infected mice displayed the largest amount and size of nodules of any strain examined. Furthermore, the total area occupied by nodules and cellular aggregation was nearly double to that seen in mice infected with any of the other clinical strains. These observations suggested that in C3H mice, Type1 causes earlier mortality in mice by inducing a vigorous host response in the alveoli of the lungs that is detrimental to the host. Accordingly, when examining the other clinical isolates and H37Rv, the clinical isolates exhibited an intermediate average number of survival days as well as an intermediate amount of total area involved in the granulomatous response in comparison to Type1 and H37Rv. Fittingly, H37Rv had the smallest total area involved and C3H mice infected with this strain survived the longest.

Contrary to what was observed in C3H mice, Type1 infected BALB/c mice did not display the most extensive and robust inflammatory response of all strains investigated, even though mice infected with Type1 still experienced the earliest mortality in comparison to other clinical strains and H37Rv. In the BALB/c model, Type72 infected mice displayed the largest total area of granulomatous inflammation and mice infected with this strain succumbed to disease earlier than the other strains

investigated excluding Type1. Type5, Type2 and H37Rv followed this trend whereby an increasing amount of nodules and cell aggregations corresponded to relatively earlier mortality. In BALB/c mice, bacillary loads in Type1 infected lungs were again equally high, but unlike the situation in C3H mice, Type1 infected lungs displayed neither the highest average number nor the largest nodules. As a result of inducing both smaller and fewer nodules, Type1 infected lungs in BALB/c mice showed the smallest total area of granulomatous inflammation of any of the clinical isolates. Despite this, Type1 still caused the earliest mortality of mice of any *M. tuberculosis* strain investigated. As a result of the differing situation seen in BALB/c mice compared to that of C3H mice, another suggested explanation derived from the granulomatous inflammation data was that perhaps in BALB/c mice, Type1 is acting similarly to HN878, as observed by Manca *et al.* (2001), in an immunomodulating fashion. Based on previous *in vivo* experiments conducted at the NRCM, which demonstrated that an early transition from a Th1 to a Th2-type immune response occurs soon after infection with Type1 (NRCM unpublished data), the suggestion that the Type1 strain may actually be modulating the host's capacity to mount a protective Th1-type response was considered and investigated.

RT-PCR Generated Cytokine Profiles

Tuberculosis can best be described as an interactive battle, which pits the host response against the parasite with the outcome being either the control or progressive development of the disease. As with other infectious agents, the human immune response to tuberculosis can be considered like a double-edged sword, which works towards the elimination of pathogens but also may be harmful to host cells (Barnes, *et al.*, 1993b).

As revealed by histological analysis, the Type1 strain demonstrated two distinct granulomatous inflammation patterns when examined in the two different mouse models. Therefore, it was necessary to investigate these different host-parasite relationships in an attempt to associate the observed inflammation and manifestation of disease caused by Type1 with the extent of the host immune response by evaluating cytokine mRNA levels from lung homogenates.

To assess the strength or degree of the host response to infection with the various *M. tuberculosis* strains, 4 cytokines were chosen to be examined using RT-PCR, based on their significance in disease progression or containment as outlined in Figure 1. IFN-γ was chosen as one of two pro-inflammatory cytokines to be studied for two major reasons. First, IFN-γ is the principal mediator of macrophage activation and since it is widely believed that mycobacterial infections are primarily controlled via the activation of such macrophages through type 1 cytokine production by T-cells (Fenton, *et al.*, 1997; Seah, *et al.*, 2000), accordingly IFN-γ which is central to these processes was deemed a logical cytokine to examine. Additionally, IFN-γ was selected because of its importance in tuberculosis disease control. IFN-γ importance has been well cited in the literature, especially with respect to mice with disruptions of the IFN-γ gene (GKO knockouts), which are more susceptible to *M. tuberculosis* infection than wild-type mice (Cooper, *et al.*, 1993; Flynn, *et al.*, 1993). The second "protective" cytokine chosen was IL-12. This cytokine was selected based on the fact that it favours the development of Th1-like responses, down-regulates Th2 responses by antagonizing IL-10, enhances IFN-γ production and cytotoxic activity of both NK and T-cells along with its ability to up-regulate NO and H_2O_2 release (Fulton, *et al.*, 1996; Jyothi, *et al.*, 2000), all vital activities

of tuberculosis disease control. Perhaps more importantly, IL-12 or specifically IL-12 p40 was chosen as this portion of the heterodimer is the inducible chain (Schoenhaut, *et al.*, 1992) and therefore would provide better insight to the induction of the protective response generated as a result of the *M. tuberculosis* infection. In order to examine cytokines that counter the effects of the protective cytokines that were to be studied, IL-5 and IL-10 were selected for examination. IL-10 was chosen based on the understanding that its secretion can down-regulate the Th1 response and that it can suppress the activation of macrophages thus inhibiting important microbicidal activity (North, 1998; Jung, *et al.*, 2003) while IL-5 was examined based on its presence during a Th2 response and its ability to push the nature of the immune response to a more humoral rather than cell-mediated response (*Tuberculosis: Pathogenesis, Protection, and Control*, 1994).

Based on the observed histological analysis results, it was hypothesized that the two distinct granulomatous inflammation patterns could be linked accordingly to specific theorized cytokine levels or patterns. In C3H mice, it was observed that Type1 infected mice not only displayed an earlier mortality but also the greatest amount of inflammation of all the strains examined while in BALB/c, Type1 still caused the earliest mortality but actually produced the lowest inflammation of all the clinical isolates tested. These observations suggested that Type1 causes earlier mortality in C3H mice by inducing a vigorous, unspecific host response in the alveoli of the lungs that is detrimental to the host but potentially Type1 may actually be acting in an opposite fashion in BALB/c mice by modulating the host's capacity to mount a protective Th1-type response.

Based on this suggested logic, it was expected that levels of IL-12 p40 and IFN-γ would be much greater in Type1 infected C3H mice compared to all other strains tested

within the C3H model. In fact, levels of these two cytokines were actually lower than seen in both Type2 and H37Rv infected C3H mice (Figure 11) even though each of these experimental groups had inflammation levels much lower than that observed for Type1 infected mice and survived longer. Since no clear profile of abundant protective cytokines was obtained, the hypothesis of a vigorous host response occurring within the alveoli of the lungs causing detrimental damage to the host was unfortunately not confirmed and remains unresolved. When examining the levels of IL-5 and IL-10 for Type1 infected C3H mice, the obtained profile displayed intermediate levels of these cytokines in comparison to the other strains tested in this mouse model and accordingly it was impossible to make a clear association linking the levels of these cytokines to both the observed survival time and plentiful amount of granulomatous inflammation observed in Type1 infected mice.

Again, in the same fashion as with the C3H model, when examining the protective cytokine levels for Type1 infected BALB/c mice, the hypothesized profiles were not observed. As a result of the lower amount of granulomatous inflammation observed in Type1 infected BALB/c mice, if indeed the proposed modulation of the immune system was occurring, it was hypothesized that lower values of the protective cytokines would be detected and potentially there would also be an up-regulation of non-protective or Th2-type cytokines. In reality, levels of both IFN-γ and IL-12 p40 were not only greater for Type1 infected mice in comparison to all other clinical strains examined in the BALB/c mouse model but also were greater than levels detected in the C3H model for this particular strain of *M. tuberculosis*. Therefore, no clear association between the observed lack of granulomatous inflammation seen in Type1 infected BALB/c mice in

comparison to other clinical *M. tuberculosis* strains and any apparent modulation or down-regulation of protective cytokines can be concluded. Additionally, in contrast to recent findings by *Freeman et al.* (2006), which demonstrated an up-regulation of Th2-type cytokines including IL-5, IL-10 and IL-13 in infected cells from more virulent *M. tuberculosis* strains, no drastic up-regulation of IL-10 was noticed from Type1 samples (only slightly greater than Type72) compared to other clinical strains in BALB/c mice. Furthermore, levels of IL-5 detected from Type1 infected BALB/c mice were lower than all other strains examined. Therefore, when taken together, levels observed for both protective and non-protective cytokines fail to show a relationship with the idea of a proposed modulation of the immune system taking place in the BALB/c mouse model when infection with the Type1 strain is occurring.

The failure to correlate levels of important cytokines associated with stages of disease progression and ultimately survival may in fact be a reflection of the complexity of the host-parasite immune interaction seen in tuberculosis disease. As seen in Figure 1 and as often described throughout the literature, a broad spectrum of cytokines and factors may contribute to antimycobacterial immune defences (Boom, *et al.*, 1991; Barnes, *et al.*, 1993a). Through discussion with members of Gilla Kaplan's laboratory at The Rockefeller University in New York, it was interpreted that the relatively low number of cytokines examined could at least somewhat account for the lack of a clear correlation between the results seen in the survival and histological studies and that provided by the cytokine data. To emphasize this point, work conducted by Kaplan's group, a leader in *M. tuberculosis* virulence studies, focused on more than 20 different cytokines and chemokines. Unfortunately, the scope of such an endeavour would have

been far too great based on the number of overall samples and the availability of manpower. Consequently, our data remains inconclusive with regard to linking an immunological explanation to the survival and granulomatous responses observed in both the C3H and BALB/c mouse models.

Strain-specific Virulence Factors

Although survival data from all three mouse models provided the basis for the confirmation of the hypervirulence of *M. tuberculosis* Type1, the unanswered explanation for the hypervirulent nature of this strain remained. It is widely believed within the tuberculosis research community that *M. tuberculosis* possesses a remarkable lack of diversity observed at the nucleotide level (Cole and Barrell, 1998; Brosch, *et al.*, 2001). Accordingly, in order to identify potential bacterial virulence factors as the source of Type1's hypervirulence, the focus of such as an investigation had to be oriented around insertions and deletions.

Over the past few years, new technological breakthroughs and insights into genomic comparison as well as enhancements in sequencing procedures and equipment have opened the door for researchers to examine various bacteria more completely at the gene level. Following the publication of the complete genome sequence of *M. tuberculosis* H37Rv (Cole, *et al.*, 1998) and the development of readily obtainable ORFmer sets of this reference strain, DNA microarray technology has provided mycobacterial researchers with an instrument to conduct high-throughput whole-genome comparisons between species and even between individual strains of a given species. Within the mycobacterial domain, several research teams have proven that microarray

technology can successfully identify deleted regions in comparison to reference strains. Among the most notable studies, *Behr et al.* (1999) identified 16 regions of deletions (totalling 129 ORFs) among BCG strains in comparison to *M. bovis* while *Kato-Maeda et al.* (2001), were able to detect 25 small-scale genomic deletions among 19 clinical isolates of *M. tuberculosis* in comparison to H37Rv.

Recently, a microarray project of this nature was undertaken by Kym Blackwood-Antonation at the NCRM in an initial attempt to examine the Type1 strain in comparison to H37Rv at the genomic level. From this study, only 20 putatively deleted ORFs were detected in the Type1 strain. This was particularly interesting since it was the lowest amount detected in comparison to several other clinical isolates from the province of Manitoba that were tested against H37Rv (NRCM unpublished data). As seen with other studies, most of the deleted ORFs were clustered into specific regions.

Perhaps the most intriguing discovery made from Blackwood-Antonation's study was the identification of the deletion of part of the ESAT-6 family of genes (NRCM unpublished data). The presence of the ESAT-6 protein, a protein often studied with regard to vaccine development, has generally been linked to virulent *M. tuberculosis* and *M. bovis* strains whereas its absence is often associated with avirulent strains (Harboe, *et al.*, 1996). Therefore, it seemed out of place for coding genes of such a protein to be missing in a hypervirulent strain such as Type1.

Although such microarray work on the Type1 strain does begin to expand the insight into this strain and perhaps lay the foundation for potential sources to explain the hypervirulent nature of the strain, two important facts could not be underestimated or ignored. First, deletions of genes generally reflect the loss of ancestral genes that are no

longer essential for the survival of the organism and accordingly any accumulation of these deletions generally diminishes the virulence of the organism (Kato-Maeda, *et al.*, 2001) as exemplified by the progressive attenuation of the *M. bovis* BCG strains (Behr, *et al.*, 1999; Behr, 2001). Secondly, a major limitation of microarray work is that deletion analysis can only identify deletions relative to a reference strain that has been completely sequenced, thus any extra or strain-specific sequences present would remain hidden using this technique (Pym and Brosch, 2000; Brosch, *et al.*, 2001).

It has been noted that considerable dissimilarity in gene content can not only occur between species of the same genus but in fact significant variation has been seen between strains of the same species where on average strain-specific gene content has ranged from 6-25% (Nesbo, *et al.*, 2002). In order to complement Blackwood-Antonation's microarray study and to investigate potential insertions occurring within the Type1 genome, subtractive hybridization, an attractive technique with the ability to identify regions present in a given strain but absent in another closely related strain, was attempted. Specifically, suppression subtractive hybridization (SSH) was chosen as this method had previously been shown to be both an effective and relatively cost effective method for identifying differing nucleotide sequences between genomes. In terms of technical requirements and labour intensive issues, SSH offers many advantages compared to standard subtraction hybridization methods or even other techniques like differential display. A major advantage of the procedure is that SSH eliminates the requirement of multiple rounds of hybridization and the need for physical separation of single stranded and double stranded DNA molecules by combining both normalization of sequence abundance and subtraction into a single procedure (Diatchenko, *et al.*, 1996;

Byers, *et al.*, 2000). Additionally, since this improved version of subtractive hybridization is a suppression PCR-based DNA subtraction technique, this method eases both the molecular obstacles and demands encountered in standard subtractive hybridization by allowing the procedure to be performed starting with a small initial amount of sample genomic DNA and yet still selectively amplify and obtain a 1000-fold enrichment for unique strain-specific sequences (Diatchenko, *et al.*, 1996; Clontech Laboratories Inc., 2001).

As with almost every scientific procedure, SSH does not escape without having at least one major drawback. Despite significantly reducing the overall time needed to obtain potential sequences of interest, the entire search for strain-specific sequences remains technically demanding as SSH still requires further procedures to be performed including dot blots, cloning and sequencing in order to validate that potential sequences are indeed strain-specific (Byers, *et al.*, 2000).

Based on the perceived advantages of the SSH method, *M. tuberculosis* Type1 was subjected to this procedure in an attempt to pinpoint some potential sequences to be screened and validated as Type1 specific virulence factors. Using the SSH procedure, an abundance of PCR product was successfully obtained that was believed to have contained multiple heavily enriched sequences unique to the Type1 strain.

Initially, direct screening of gel-purified PCR products was selected as the first validation method to be attempted, as it was believed to be an easy way to quickly identify a few Type1 specific sequences. Based on the agarose gel images obtained that displayed 11 clear and prominent DNA bands (Figure 12c), it was assumed that direct sequencing of such bands would reveal Type1 sequences that had been greatly enriched

for during the two-step PCR amplification. Despite the fact that the control experiments utilizing *E. coli* and the ϕX174 RF DNA/*Hae* III fragments had generated the expected agarose gel DNA banding patterns and were confirmed through sequencing, regrettably, each of the 11 bands examined turned out to be sequences common to both *M. tuberculosis* H37Rv and Type1.

The creation of multiple clones, using the SSH-generated PCR products, was then undertaken as the second validation method with the belief that potentially any unique Type1 sequences present within the PCR products were just not abundant enough to be visually observed on the agarose gels. At random, 63 clones were selected and sequenced. Again, as with the first validation method, not a single clone was confirmed as being exclusively unique to the Type1 genome.

Although each of the first two screening methods had failed to yield a single confirmable Type1 specific sequence, a third higher-throughput system of screening was employed to more rapidly test a larger number of generated clones. Chemiluminescent detectable colony blots representing a total of 552 colonies were produced and probed. From these blots, finally 19 individual spots were singled out as clones that potentially contained only Type1 specific DNA. Unfortunately, following subsequent sequencing and analysis, every one of the 19 clones was eliminated and discounted as a Type1 specific clone.

Overall, 615 individual clones in addition to 11 purified PCR products were unsuccessfully examined and yielded no confirmable Type1 specific sequences. Despite the understanding that the SSH procedure is not entirely effective, data from various SSH studies cited in the literature report an effectiveness of >50% of clones being tester-

specific (Stocki, *et al.*, 2002; Winstanley, 2002; Radnedge, *et al.*, 2003). Therefore, the lack of a single confirmed Type1 specific clone was totally unexpected. A possible explanation for the lack of success achieved in this study may potentially be the number of clones tested. Based on the large genome size of *M. tuberculosis*, the small size of cloned inserts and the likelihood of duplicate clones, it is entirely possible that several thousand clones would have to be examined rather than the mere 615 tested in this study in order to find any confirmable Type1 specific clones. In addition, as seen in Blackwood-Antonation's microarray studies, despite testing approximately 4000 open reading frames, only 20 deletions were detected. Thus it can be rationalized that the chances of detecting an insertion in *M. tuberculosis* Type1 might be of the same magnitude.

When conducting SSH experiments, it is almost certain that a proportion of clones will result in false positives. In addition to the handful of clones that were initially identified as target candidates, purified PCR products examined using the gel purification and direct sequencing screening method were also later shown to be false positives. A plausible explanation for the occurrence of such false positives detected in this study has been described by *Agron et al.* (2002), who recognized that during SSH, false positives may arise from sequences who manage to remain single-stranded long enough to eventually hybridize with complementary strands present within the tester DNA thus producing an amplifiable product even though the experimental hybridizations are carried out in the presence of excess driver DNA.

The failure to identify any strain-specific sequence using the SSH technique and consequently the inability to associate any bacterial factors as potential sources of

Type1's hypervirulence was both unfortunate and unexpected based on the successfulness of this technique as a useful and powerful tool as cited throughout the literature for many other bacterial pathogens. Although SSH has been successfully utilized in a few cases with other mycobacterial species (Mahairas, *et al.*, 1996; Jenkin, *et al.*, 2003; Song, *et al.*, 2003), this technique has yet to be successfully used in *M. tuberculosis* virulence studies. At the time that this part of the project was being conducted, only a single laboratory worldwide, the Azhikina research group, was attempting to use the SSH approach as a viable and reproducible instrument to facilitate the comparison of *M. tuberculosis* genomes. Through personal communications with Tatyana Azhikina, lead project investigator at the Laboratory of Structure and Functions of Human Genes from the Ovchinnikov Institute of Bioorganic Chemistry in Moscow, Russia, it was revealed that their research group had encountered numerous difficulties using SSH and had abandoned the procedure in lieu of a new RFLP based enhanced version of subtractive hybridization which recently has been described in the literature and applied to comparison of clinical *M. tuberculosis* strains.(Azhikina, *et al.*, 2006; Gvozdevskii, *et al.*, 2006).

Future Directions

At the outset of this project, several specific tasks were outlined with the overall goal of achieving two main objectives which included the confirmation of the putative hypervirulence observed in *Mycobacterium tuberculosis* Type1 strain and the identification of strain-specific bacterial virulence factors that may be a potential source and explanation for the apparent enhanced virulence of the Type1 strain.

Survival studies in three differing mouse models each confirmed the hypervirulence of the Type1 strain in comparison to other common clinical isolates from the province of Manitoba while assessment of lung samples further characterized the pulmonary tuberculosis disease brought about by Type1. Although histological analysis did reveal two distinct granulomatous responses in C3H and BALB/c mice, evaluation of cytokine mRNA levels from lung homogenates proved inconclusive and prevented a clear correlation between the measured host immune responses and the observed disease manifestation from being declared. A quantitative RT-PCR method may also be a better mechanism than the semi-quantitative approach utilized in this project. Future immunological studies will be required in order to generate a more complete and detailed examination of the multiple components and factors involved in tuberculosis disease progression or control. Specifically, studies of a greater scope that measure levels of abundantly more cytokines, chemokines and other immunological markers, including examination at more than one time point, than those performed during this current project as well as additional granuloma composition investigations, should be conducted.

In this study, the search for a feasible rationale to explain the hypervirulent nature of the Type1 strain was focused on the identification of strain-specific virulence factors. Unfortunately, suppression subtractive hybridization proved to be quite ineffective and ultimately disappointing as it failed to yield even a single confirmable clone containing unique Type1 sequences. Further Type1 studies must remain focused towards finding potential sources of Type1's hypervirulence. Additional subtractive hybridization experiments, whether it be of the SSH nature or some other alternative variety, should be attempted testing larger numbers of clones.

In recent years, several other types of experimental procedures have been cited throughout mycobacterial literature, which potentially may facilitate the search for specific bacterial factors responsible for the hypervirulence of Type1. Work conducted involving DNA electrophoresis, has demonstrated that two-dimensional bacterial genome display (2DBGD) is a novel yet feasible alternative approach to performing whole-genome comparative analysis between *M. tuberculosis* strains (Dullaghan, *et al.*, 2002; Malloff, *et al.*, 2002).

Even though potential insertions and deletions of unique sequences have been the primary suggestions as to how Type1 has developed its enhanced virulence, it is entirely possible that changes in regulation or expression of genes common to many *M. tuberculosis* isolates may prove to be the real reason behind Type1's hypervirulence and epidemiological dominance in Manitoba. Previously, Graham and Clark-Curtiss (1999) utilized the SCOTS (selective capture of transcribed sequences) technique as a method of examining *in vitro* gene expression levels while *Talaat et al.* (2004) used a microarray based approach to profile *in vivo*-expressed genes of *M. tuberculosis* during the course of infection in mice. Each of these two separate methods may be utilized for future expression profiling studies.

Although the studies conducted in this project and the potential future studies previously mentioned focus on bacterial factors and the interaction that occurs between the bacteria and a given host, information concerning the susceptibility of various population groups within the province of Manitoba and social risk factors which may influence them, are lacking. Comprehensive epidemiological studies examining the relationship between the Type1 strain and various socio-economic factors such as

poverty, old age, malnutrition and overcrowding should be undertaken. Studies of this nature will strengthen the knowledge pertaining to the Type1 strain by adding a host component to any explanation with regard to the dominance of Type1 within Manitoba.

Research Impact

The re-emergence of tuberculosis as an important public health issue worldwide, even within many developed countries, has heightened the need for a better understanding into the genetics and pathogenesis of the organism. The work conducted during this project and subsequently reported in this manuscript focusing on a clinical isolate was much overdo. Throughout the literature, a lack of studies utilizing and characterizing clinical isolates and instead relying on hardly virulent laboratory adapted strains has hampered both the understanding of *M. tuberculosis* pathogenesis and the development of new vaccine candidates.

The confirmation of the hypervirulent nature of the Type1 strain in addition to the discovery of distinctive granulomatous responses occurring in differing genetic backgrounds during this study, has provided researchers and health officials with both a plausible rationalization into the phenomenal epidemiological dominance of this strain and also a clear and alarming warning with respect to the outbreak potential of such a strain, especially among the treaty-status population of this province.

Although specific bacterial virulence factors involved in the hypervirulence of Type1 remain unknown, this study has shown the need to expand such investigative studies in order to unlock the key fundamentals of pathogenesis for Type1 as well as all

other *M. tuberculosis* strains. Identification of prospective Type1 virulence factors will surely generate additional studies aimed at resolving the host-parasite interaction.

Immunological data presented in this manuscript, although inconclusive, has again demonstrated the complexity of the disease progression or control balance observed following tuberculosis infection. Further research into the possible pathogen derived immunomodulation by the Type1 strain is essential in order to build a stronger foundation for the pursuit of new and improved therapeutic strategies and public health control measures in the province of Manitoba.

Taken together, it should be noted that previous work, including this project, on the Type1 strain in Manitoba has only scratched the surface with respect to many of this strain's mysteries and characteristics due to the difficulty of manipulating this organism and that to date, many questions and suggestions remain unresolved awaiting discovery.

Appendix 1

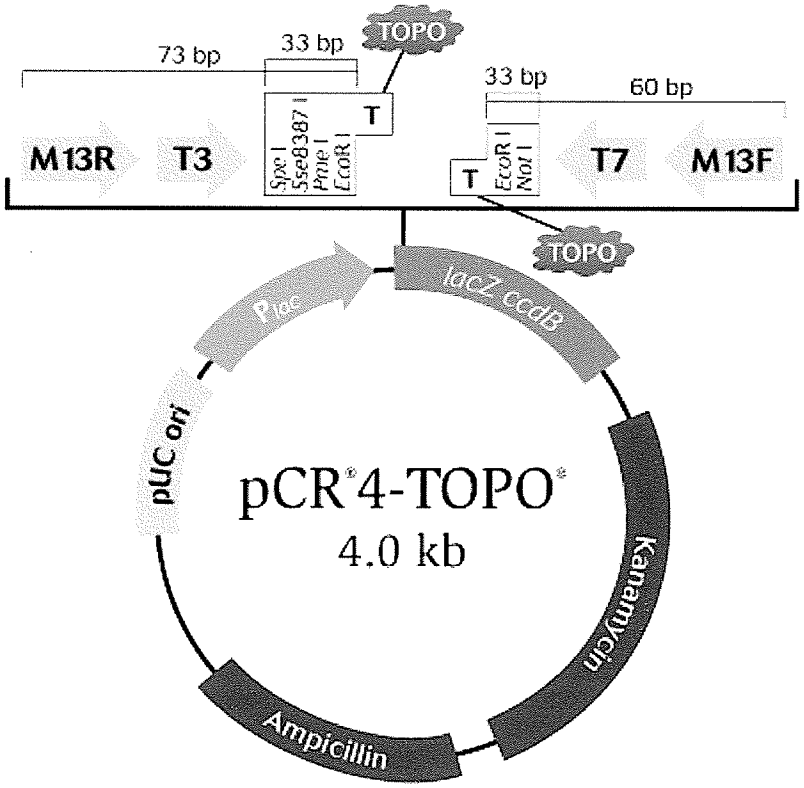

Figure 15. pCR4-TOPO™ vector (Invitrogen Corporation, 2003). Sequencing of cloned inserts was accomplished using the T3 primer and corresponding T3 primer binding site located within the vector.

Appendix 2 - Recipes

Section 2.1.1 – Middlebrook 7H10 media plates (in house recipe)

volume/mass	chemical
19.47g	Middlebrook 7H10 Agar Base
900 ml	dH_2O
5 ml	Glycerol

Suspend Agar base (19.47 g) in 900 ml distilled water then add 5 ml glycerol and dissolve completely. Sterilize by autoclaving then cool to 45°C to pour plates. Keep in dark at 2-8°C.

Section 2.1.1 – Middlebrook 7H9 media (in house recipe)

volume/mass	chemical
4.7 g	Middlebrook 7H9 Broth
2 ml	Glycerol B
900 ml	dH_2O
100 ml	Middlebrook ADC enrichment

Add all ingredients except Middlebrook ADC enrichment and mix well. Autoclave for 15 minutes. Cool to 45°C, then aseptically add ADC supplement. Aseptically dispense appropriate volume into desired container. Store at 2-8°C.

Section 2.2.2 – 10X TE Buffer (in-house recipe)

volume/mass	chemical
15.76 g	100mM Tris-HCl (pH 8.0)
3.72g	10 mM EDTA
Up to 1L	dH_2O

Dissolve everything in slightly less than 1L of water and then adjust the volume to 1 L by adding water. Ensure pH 8.0 is obtained. Autoclave. Store at room temperature. To use as a buffer (1X TE), make a 1:10 dilution with H_2O.

Section 2.2.4 – 10X TBE Buffer (in-house recipe)

volume/mass	chemical
108 g	Tris base
55 g	Boric Acid
20 ml	0.5M EDTA
Up to 1L	dH_2O

Dissolve everything in slightly less than 1L of water and then adjust the volume to 1 L by adding water. If white clumps begin to precipitate in the solution, place the bottle in hot water until the clumps dissolve. The solution can be stored at room temperature. To use as a buffer (1X TBE), dilute the 10X stock by adding 900 ml water to 100ml 10X TBE.

Section 2.4.2 – 10X FA gel buffer
(www.qiagen.com/literature/BenchGuide/pdf/1017778_BenchGuide_chap_3.pdf#45)
1 L total volume in 18 MΩ H_2O:

volume	chemical
41.9 g	3-(N-morpholino) propane-sulfonic acid (MOPS)
6.8 g	sodium acetate•H_2O
20 ml	0.5 M EDTA, pH 8.0

pH to 7.0 with NaOH.
Treat entire volume with 0.1% diethyl pyrocarbonate (DEPC) at 37°C overnight.
Autoclave for 15 minutes.
Dilute to 1X in DEPC-treated H_2O.

Section 2.4.2 – 5X RNA loading buffer
(www.qiagen.com/literature/BenchGuide/pdf/1017778_BenchGuide_chap_3.pdf#45)
10 ml total volume in DEPC-treated H_2O:

volume/mass	chemical
80 µl	0.5 M EDTA
750 µl	37% formaldehyde
2 ml	glycerol
3.084 ml	formamide
4 ml	10X FA gel buffer
to desired colour	bromophenol blue

Section 2.4.5 – 50X TAE Buffer (in-house recipe)

volume/mass	chemical
242 g	Tris base
18.6 g	EDTA
57.1 ml	Glacial Acetic Acid
Up to 1L	dH_2O

Add the Tris base to the EDTA in about 400 ml of water. Mix well. Adjust to pH 8.0 with Acetic Acid, then bring up to 1L with H_2O. To use as a buffer (1X TAE), dilute the stock 50X.

Section 2.5.7 - Denaturation Solution (in-house recipe)

final concentration	chemical
1.5 M	NaCl
0.5 M	NaOH

Section 2.5.7 - Neutralizing Solution (in-house recipe)

final concentration	chemical
1.5 M	NaCl
0.5 M	Tris·Cl, pH 7.0

Appendix 3 - Ladders

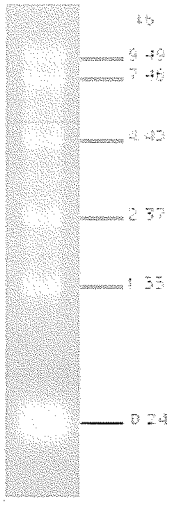

0.24-9.5 Kb RNA Ladder
3 µg/lane (formaldehyde-treated)
1.2% agarose gel
stained with ethidium bromide

Figure 16. Invitrogen 0.24-9.5 Kb RNA Ladder™

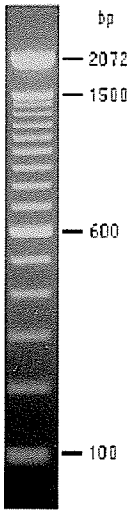

100 bp DNA Ladder
0.5 µg/lane
2% agarose gel stained with ethidium bromide.

Figure 17. Invitrogen 100 bp DNA Ladder

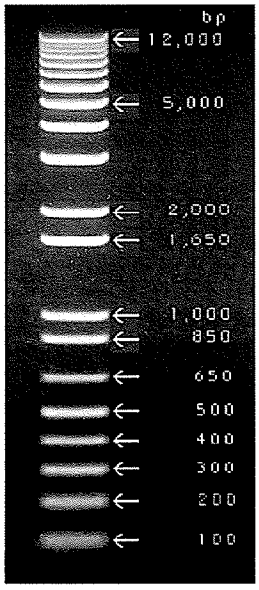

1 Kb Plus DNA Ladder
0.7 µg/lane
0.9% agarose gel
stained with ethidium bromide

Figure 18. Invitrogen Ready-Load™ 1 Kb Plus DNA Ladder

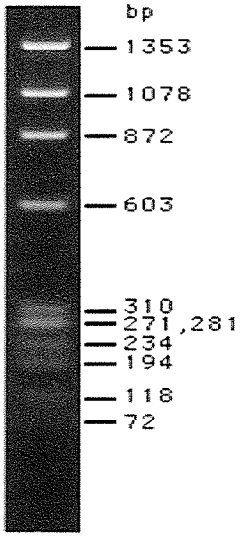

ϕX174 RF DNA/*Hae* III Fragments
0.75 µg/lane
1.5% agarose gel
stained with ethidium bromide

Figure 19. Invitrogen Ready-Load™ ϕX174 RF DNA/*Hae* III Fragments

Reference List

1. Bench Guide (RNA). Qiagen Literature General Molecular Biology Protocols Online. 2003
   Ref Type: Electronic Citation

2. 1993. Bergey's Manual of Determinative Bacteriology, 9th Ed. Williams & Wilkins, New York. p. 597-603.

3. 1967. Carleton's Histological Technique, 4th ed. OUP; London: p. 129.

4. Clontech PCR-Select Bacterial Genome Subtraction Kit User Manual. Protocol# PT3170-1, Version# PR17129. 2001. Clontech Laboratories Inc.
   Ref Type: User Manual

5. Invitrogen 2005-06 Online Product Catalogue. 2006. Invitrogen Corporation
   Ref Type: Catalogue

6. 1968. Manual of Histological Staining Methods of the Armed Forces Institute of Pathology, 3rd Ed. McGraw-Hill, New York; p. 219-220.

7. 1998. Merriam Webster's Collegiate Dictionary, 10th Ed. Mish F C., ed. Merriam-Webster, Springfield, MA.

8. Proceedings of the National Consensus Conference on Tuberculosis Dec 3-5 1997. Health Canada Health Protection Branch and LCDC. Online. 1998.
   Ref Type: Online Citation

9. Topo TA Cloning® Kit for Sequencing. Version L. 2004. Invitrogen Corporation.Online 2003.
   Ref Type: User Manual

10. 1996. Tuberculosis. William N. Rom & Stuart Garay, Little Brown & Company Inc, New York, USA.

11. Tuberculosis in Canada 1998. Health Canada, Population and Public Health Branch. Online 1998.
    Ref Type: Online Citation

12. Tuberculosis in Canada 2001. Health Canada, Population and Public Health Branch. Online 2001.
    Ref Type: Online Citation

13. 1994. Tuberculosis: Pathogenesis, Protection, and Control. ASM Press, Washington, DC, USA.

14. **Abebe F, T. Mustafa, A. H. Nerland, and G. A. Bjune.** Cytokine profile during latent and slowly progressive primary tuberculosis: a possible role for interleukin-15 in mediating clinical disease. Clin Exp Immunol. 2006, **143(1)**:180-92.

15. **Agron P. G., M. Macht, L. Radnedge, E. W. Skowronski, W. Miller, G. L. Andersen.** Use of subtractive hybridization for comprehensive surveys of prokaryotic genome differences. FEMS Microbiol Lett. 2002; **211(2)**:175-82.

16. **Azhikina .T, N. Gvozdevsky, A. Botvinnik, A. Fushan, I. Shemyakin, V. Stepanshina, M. Lipin, C. Barry III, and E. Sverdlov.** A genome-wide sequence-independent comparative analysis of insertion-deletion polymorphisms in multiple Mycobacterium tuberculosis strains. Res Microbiol. 2006; **157(3)**:282-90.

17. **Barnes P. F., J. S. Abrams, S. Lu, P. A. Sieling, T. H. Rea, and R. L. Modlin.** Patterns of cytokine production by mycobacterium-reactive human T-cell clones. Infect Immun. 1993a; **61**(1):197–203.

18. **Barnes P. F., D. Chatterjee, J. S. Abrams, S. Lu, E. Wang, M. Yamamura, P. J. Brennan, and R. L. Modlin.** Cytokine production induced by Mycobacterium tuberculosis lipoarabinomannan. Relationship to chemical structure. J Immunol. 1992a; **149(2)**:541-7.

19. **Barnes P.F., C. L. Grisso, J. S. Abrams, H. Band, T. H. Rea, and R. L. Modlin.** Gamma delta T lymphocytes in human tuberculosis. J Infect Dis. 1992b; **165(3)**:506-12.

20. **Barnes P.F., S. Lu, J. S. Abrams, E. Wang, M. Yamamura, and R. L. Modlin.** Cytokine production at the site of disease in human tuberculosis. Infect Immun. 1993b; **61(8)**:3482-9.

21. **Behr M. A.** Comparative genomics of BCG vaccines. Tuberculosis. 2001; **81(1-2)**:165-8.

22. **Behr M. A., M. A. Wilson, W. P. Gill, H. Salamon, G. K. Schoolnik, S. Rane, P. M. Small.** Comparative genomics of BCG vaccines by whole-genome DNA microarray. Science. 1999; **284**:1520-3.

23. **Blackwood K. S., A. Al-Azem, L. J. Elliott, E. S. Hershfield, and A. M. Kabani.** Conventional and Molecular Epidemiology of Tuberculosis in Manitoba, BMC- Infect Dis 2003; **3**:18.

24. **Boom W. H., R. S. Wallis, and K. A. Chervenak.** Human Mycobacterium tuberculosis-reactive CD4+ T-cell clones: heterogeneity in antigen recognition, cytokine production, and cytotoxicity for mononuclear phagocytes. Infect Immun. 1991; **59(8)**:2737–2743.

25. **Brosch R., A. S. Pym, S. V. Gordon, and S. T. Cole.** The evolution of mycobacterial pathogenicity: clues from comparative genomics. Trends Microbiol. 2001; **9(9)**:452-8.

26. **Byers R. J., J. A. Hoyland, J. Dixon, and A. J. Freemont.** Subtractive hybridization - genetic takeaways and the search for meaning. Int J Exp Pathol. 2000; **81(6)**:391-404.

27. **Camus J-C., M. J. Pryor, C. Médigue, and S. T. Cole.** Re-annotation of the genome sequence of *Mycobacterium tuberculosis* H37Rv. Microbiology. 2002; **148**:2967-73.

28. **Chackerian A. A., T. V. Perera, and S. M. Behar.** Gamma interferon-producing CD4+ T lymphocytes in the lung correlate with resistance to infection with Mycobacterium tuberculosis, Infect Immun 2001; **69**:2666-2674.

29. **Cole S. T., and B. G. Barrell.** Analysis of the genome of Mycobacterium tuberculosis H37Rv. Novartis Found Symp. 1998; **217**:160-72.

30. **Cole S. T., R. Brosch, J. Parkhill, T. Garnier, C. Churcher, D. Harris, S. V. Gordon, K. Eiglmeier, S. Gas, C. E. Barry III, F. Tekaia, K. Badcock, D. Basham, D. Brown, T. Chillingworth, R. Connor, R. Davies, K. Devlin, T. Feltwell, S. Gentles, N. Hamlin, S. Holroyd, T. Hornsby, K. Jagels, A. Krogh, J. McLean, S. Moule, L. Murphy, K. Oliver, J. Osborne, M. A. Quail, M. A. Rajandream, J. Rogers, S. Rutter, K. Seeger, J. Skelton, R. Squares, S. Squares, J. E. Sulston, K. Taylor, S. Whitehead, and B. G. Barrell.** Deciphering the biology of Mycobacterium tuberculosis from the complete genome sequence, Nature 1998; **396**:190.

31. **Collins F M.** Protection against mycobacterial disease by means of live vaccines tested in experimental animals, *In* G.P. Kubica and L.G. Wayne ed., The mycobacteria: a sourcebook, part B. Marcel Dekker, Inc., 1984; pp.787-839.

32. **Comstock G. W.** Epidemiology of tuberculosis. Am Rev Respir Dis. 1982; **125**:8-15.

33. **Cooper A. M., D. K. Dalton, T. A. Stewart, J. P. Griffin, D. G. Russell, and I. M. Orme.** Disseminated tuberculosis in interferon gamma gene-disrupted mice. J Exp Med. 1993; **178(6)**:2243-7.

34. **Cousins D. V., R. Bastida, A. Cataldi, V. Quse, S. Redrobe, S. Dow, P. Duignan, A. Murray, C. Dupont, N. Ahmed, D. M. Collins, W. R. Butler, D. Dawson, D. Rodriguez, J. Loureiro, M. I. Romano, A. Alito, M. Zumarraga, and A. Bernardelli.** Tuberculosis in seals caused by a novel member of the Mycobacterium tuberculosis complex: Mycobacterium pinnipedii sp. nov. Int J Syst Evol Microbiol. 2003; **53**:1305-14.

35. **Crick D. C., S. Mahapatra, and P. J. Brennan.** Biosynthesis of the arabinogalactan-peptidoglycan complex of Mycobacterium tuberculosis. Glycobiology. 2001; **11(9)**:107R-118R.

36. **Dannenberg A. M., Jr.** Immune mechanisms in the pathogenesis of pulmonary tuberculosis. Rev Infect Dis. 1989; **11**:S369-78.

37. **Diatchenko L., Y. F. Lau, A. P. Campbell, A. Chenchik, F. Moqadam, B. Huang, S. Lukyanov, K. Lukyanov, N. Gurskaya, E. D. Sverdlov, and P. D. Siebert.** Suppression subtractive hybridization: a method for generating differentially regulated or tissue-specific cDNA probes and libraries. Proc Natl Acad Sci U S A. 1996; **93(12)**:6025-30.

38. **Dolin P. J., M. C. Raviglione, and A. Kochi**. Global tuberculosis incidence and mortality during 1990-2000, Bull World Health Organ 1994; **72**:213-220.

39. **Dullaghan E. M., C. A. Malloff, A. H. Li, W. L. Lam, and R. W. Stokes.** Two-dimensional bacterial genome display: a method for the genomic analysis of mycobacteria. *Microbiology* 2002; **148**:3111-3117.

40. **Fenton M. J., and M. W. Vermeulen.** Immunopathology of tuberculosis: roles of macrophages and monocytes. Infect Immun. 1996; **64(3)**:683–690.

41. **Fenton M. J., M. W. Vermeulen, S. Kim, M. Burdick, R. M. Strieter, and H. Kornfeld.** Induction of gamma interferon production in human alveolar macrophages by Mycobacterium tuberculosis. Infect Immun. 1997; **65(12)**:5149-56.

42. **Firmani M. A., and L. W. Riley.** Mycobacterium tuberculosis CDC1551 is resistant to reactive nitrogen and oxygen intermediates in vitro. Infect Immun. 2002; **70(7)**:3965–3968.

43. **Fleischmann R. D., D. Alland, J. A. Eisen, L. Carpenter, O. White, J. Peterson, R. DeBoy, R. Dodson, M. Gwinn, D. Haft, E. Hickey, J. F. Kolonay, W. C. Nelson, L. A. Umayam, M. Ermolaeva, S. L. Salzberg, A. Delcher, T. Utterback, J. Weidman, H. Khouri, J. Gill, A. Mikula, W. Bishai, W. R. Jacobs Jr, J. C. Venter, and C. M. Fraser.** Whole-genome comparison of Mycobacterium tuberculosis clinical and laboratory strains, J Bacteriol 2002; **184**: 5479-5490.

44. **Flynn J. L., J. Chan, K. J. Triebold, D. K. Dalton, T. A. Stewart, and B. R. Bloom.** An essential role for interferon gamma in resistance to Mycobacterium tuberculosis infection. J Exp Med. 1993; **178(6)**:2249-54.

45. **Freeman S., F. A. Post, L. G. Bekker, R. Harbacheuski, L. M. Steyn, B. Ryffel, N. D. Connell, B. N. Kreiswirth, and G. Kaplan.** Mycobacterium tuberculosis H37Ra and H37Rv differential growth and cytokine/chemokine induction in murine macrophages in vitro. J Interferon Cytokine Res. 2006; **26(1)**:27-33.

46. **Fulton S. A., J. M. Johnsen, S. F. Wolf, D. S. Sieburth, and W. H. Boom.** Interleukin-12 production by human monocytes infected with Mycobacterium tuberculosis: Role of phagocytosis. Infect Immun. 1996; **64(7)**:2523–2531.

47. **Gazzinelli R. T., S. Hieny, T. A. Wynn, S. Wolf, and A. Sher.** Interleukin 12 is required for the T-lymphocyte-independent induction of interferon gamma by an intracellular parasite and induces resistance in T-cell-deficient hosts. Proc Natl Acad Sci U S A. 1993; **90(13)**:6115–6119.

48. **Graham J. E., and J. E. Clark-Curtiss.** Identification of *Mycobacterium tuberculosis* RNAs synthesized in response to phagocytosis by human macrophages by selective capture of transcribed sequences (SCOTS). Proc Natl Acad Sci U S A. 1999; **96(20)**:11554–11559.

49. **Gvozdevskii N. A., T. L. Azhikina, and E. D. Sverdlov.** Deletion-insertion differences between the genomes of Mycobacterium tuberculosis highly virulent strain HN878 and less virulent strain CDC1551. Zh Mikrobiol Epidemiol Immunobiol. 2006; **1**:10-5.

50. **Happel K. I., E. A. Lockhart, C. M. Mason, E. Porretta, E. Keoshkerian, A. R. Odden, S. Nelson, and A. J. Ramsay.** Pulmonary interleukin-23 gene delivery increases local T-cell immunity and controls growth of Mycobacterium tuberculosis in the lungs. Infect Immun. 2005, **73(9)**:5782-8.

51. **Harboe M., T. Oettinger, H. G. Wiker, I .Rosenkrands, and P. Andersen.** Evidence for occurrence of the ESAT-6 protein in Mycobacterium tuberculosis and virulent Mycobacterium bovis and for its absence in Mycobacterium bovis BCG. Infect Immun. 1996; **64(1)**:16–22.

52. **Hernandez-Pando R., H. Orozco, K. Arriaga, A. Sampieri, J. Larriva-Sahd, and V. Madrid-Marina.** Analysis of the local kinetics and localization of interleukin-1 alpha, tumour necrosis factor-alpha and transforming growth factor-beta, during the course of experimental pulmonary tuberculosis, Immunology 1997; **90**:607-617.

53. **Jenkin G. A., T. P. Stinear, P. D. R. Johnson, and J. K. Davies.** Subtractive hybridization reveals a type I polyketide synthase locus specific to Mycobacterium ulcerans. J Bacteriol. 2003; **185(23)**:6870-82.

54. **Jung Y. J., L. Ryan, R. LaCourse, and R. J. North.** Increased interleukin-10 expression is not responsible for failure of T helper 1 immunity to resolve airborne Mycobacterium tuberculosis infection in mice. Immunology. 2003; **109(2)**:295-9.

55. **Jyothi M. D., S. K. Garg, and N. B. Singh.** Mechanisms involved in protective immune response generated by secretory proteins of Mycobacterium habana against experimental tuberculosis. Scand J Immunol. 2000; **51**:502-510.

56. **Kapur V., T. S. Whittam, and J. M. Musser.** Is Mycobacterium tuberculosis 15,000 years old? J Infect Dis. 1994; **170(5)**:1348-9.

57. **Kato-Maeda M., J. T. Rhee, T. R. Gingeras, H. Salamon, J. Drenkow, N. Smittipat, and P. M. Small.** Comparing Genomes within the Species *Mycobacterium tuberculosis.* Genome Res. 2001; **11(4)**:547-54.

58. **Kaufmann S. H. E.** New issues in tuberculosis. Ann Rheum Dis. 2004, **63**:50-56.

59. **Kaufmann S. H. E., S. T. Cole, V. Mizrahi, E. Rubin and C. Nathan.** Mycobacterium tuberculosis and the host response. J Exp Med. 2005, **201(11)**:1693-7.

60. **Kelley C. L. and F. M. Collins.** Growth of a highly virulent strain of Mycobacterium tuberculosis in mice of differing susceptibility to tuberculous challenge. Tuber Lung Dis. 1999; **79(6)**:367-70.

61. **Khader S. A., J. E. Pearl, K. Sakamoto, L. Gilmartin, G. K. Bell, D. M. Jelley-Gibbs, N. Ghilardi, F. deSauvage, and A. M. Cooper.** IL-23 compensates for the absence of IL-12p70 and is essential for the IL-17 response during tuberculosis but is dispensable for protection and antigen-specific IFN-gamma responses if IL-12p70 is available. J Immunol. 2005, **175(2)**:788-95.

62. **Kochi A.** The global tuberculosis situation and the new control strategy of the World Health Organization, Tubercle 1991; **72**:1-6.

63. **Mahairas G. G., P. J. Sabo, M. J. Hickey, D. C. Singh, and C. K. Stover.** Molecular analysis of genetic differences between Mycobacterium bovis BCG and virulent M. bovis. J Bacteriol. 1996; **178(5)**:1274-82.

64. **Malloff C.A., R. C. Fernandez, E. M. Dullaghan, R. W. Stokes, W. L. Lam.** Two-dimensional display and whole genome comparison of bacterial pathogen genomes of high G+C DNA content. Gene. 2002; **293**:205-11.

65. **Manabe Y. C., A. M. Dannenberg Jr., and W. R. Bishai.** What we can learn from the Mycobacterium tuberculosis genome sequencing projects. Int J Tuberc Lung Dis. 2000; **4(2)**:S18-23.

66. **Manca C., L. Tsenova, C. E. Barry III, A. Bergtold, S. Freeman, P. A. Haslett, J. M. Musser, V. H. Freedman, and G. Kaplan.** Mycobacterium tuberculosis CDC1551 induces a more vigorous host response in vivo and in vitro, but is not more virulent than other clinical isolates, J Immunol 1999; **162**:6740-6746.

67. **Manca C., L. Tsenova, A. Bergtold, S. Freeman, M. Tovey, J. M. Musser, C. E. Barry III, V. H. Freedman, and G. Kaplan.** Virulence of a Mycobacterium tuberculosis clinical isolate in mice is determined by failure to induce Th1 type immunity and is associated with induction of IFN-alpha /beta, Proc Natl Acad Sci USA 2001; **98**:5752-5757.

68. **Masaki S., G. Sugimori, A. Okamoto, J. Imose, and Y. Hayashi.** Effect of Tween 80 on the growth of Mycobacterium avium complex, Microbiol Immunol 1990; **34**:653-663.

69. **Medina E. and R. J. North**. Resistance ranking of some common inbred mouse strains to Mycobacterium tuberculosis and relationship to major histocompatibility complex haplotype and Nramp1 genotype, Immunology 1998; **93**:270-274.

70. **Mitchison D. A., A. L. Bhatia, S. Radhakrishna, J. B. Selkon, T. V. Subaiah, and J. B. Wallace**. The virulence in the guinea pig of tubercle bacilli isolated before treatment from south Indian patients with pulmonary tuberculosis., WHO 1961; **25**:285-312.

71. **Nesbo C. L., K. E. Nelson, and W. F. Doolittle.** Suppressive subtractive hybridization detects extensive genomic diversity in Thermotoga maritima. J Bacteriol. 2002; **184(16)**:4475-88.

72. **North R. J.** Mice incapable of making IL-4 or IL-10 display normal resistance to infection with Mycobacterium tuberculosis. Clin Exp Immunol. 1998; **113(1)**:55-8.

73. **North R. J., L. Ryan, R. LaCource, T. Mogues, and M. E. Goodrich.** Growth rate of mycobacteria in mice as an unreliable indicator of mycobacterial virulence, Infect Immun 1999; **67**:5483-5485.

74. **Pym A. S., and R. Brosch.** Tools for the Population Genomics of the Tubercle Bacilli. Genome Res. 2000; **10(12)**:1837-9.

75. **Radnedge L., P. G. Agron, K. K. Hill, P. J. Jackson, L. O. Ticknor, P. Keim, and G. L. Andersen.** Genome Differences That Distinguish *Bacillus anthracis* from *Bacillus cereus* and *Bacillus thuringiensis.* Appl Environ Microbiol. 2003; **69(5)**:2755–2764.

76. **Raja A.** Immunology of tuberculosis. Indian J Med Res. 2004, **120(4)**:213-32.

77. **Raviglione M. C., D. E. Snider Jr., and A. Kochi.** Global epidemiology of tuberculosis. Morbidity and mortality of a worldwide epidemic, JAMA 1995; **273**:220-226.

78. **Ryffel B, C. Fremond, M. Jacobs, S. Parida, T. Botha, B. Schnyder, and V. Quesniaux.** Innate immunity to mycobacterial infection in mice: critical role for toll-like receptors. Tuberculosis. 2005, **85(5-6)**:395-405.

79. **Sawada K., S. Kokeguchi, H. Hongyo, S. Sawada, M. Miyamoto, H. Maeda, F. Nishimura, S. Takashiba, and Y. Murayama.** Identification by subtractive hybridization of a novel insertion sequence specific for virulent strains of Porphyromonas gingivalis. Infect Immun. 1999; **67(11)**:5621-5.

80. **Schoenhaut D. S., A. O. Chua, A. G. Wolitzky, P. M. Quinn, C. M. Dwyer, W. McComas, P. C. Familletti, M. K. Gately, and U. Gubler.** Cloning and expression of murine IL-12. J Immunol. 1992; **148(11)**:3433-40.

81. **Schwebach J R, A. Casadevall, R. Schneerson, Z. Dai, X. Wang, J. B. Robbins, and A. Glatman-Freedman.** Expression of a Mycobacterium tuberculosis arabinomannan antigen in vitro and in vivo, Infect Immun 2001; **69**:5671-5678.

82. **Seah G. T., G. M. Scott, and G. A. Rook.** Type 2 cytokine gene activation and its relationship to extent of disease in patients with tuberculosis. J Infect Dis. 2000; **181(1)**:385-9.

83. **Sharma M. K., A. Al-Azem, J. Wolfe, E. Hershfield, and A. Kabani.** Identification of a predominant isolate of Mycobacterium tuberculosis using molecular and clinical epidemiology tools and in vitro cytokine responses, BMC-Infect Dis 2003; **3**:3.

84. **Silver R. F., Q. Li, and J. J. Ellner.** Expression of virulence of Mycobacterium tuberculosis within human monocytes: Virulence correlates with intracellular growth and induction of tumor necrosis factor alpha but not with evasion of lymphocyte-dependent monocyte effector functions, Infect Immun 1998; **66**:1190-1199.

85. **Smith. I.** Mycobacterium tuberculosis pathogenesis and molecular determinants of virulence. Clin Microbiol Rev. 2003; **16(3)**:463-96.

86. **Song C-H., J-S. Lee, H-J. Kim, J-K. Park, T-H. Paik, and E-K Jo.** Interleukin-8 is differentially expressed by human-derived monocytic cell line U937 infected with Mycobacterium tuberculosis H37Rv and Mycobacterium marinum. Infect Immun. 2003; **71(10)**:5480-7.

87. **Sreevatsan S., X. Pan, K. E. Stockbauer, N. D. Connell, B. N. Kreiswirth, T. S. Whittam, and J. M. Musser.** Restricted structural gene polymorphism in the *Mycobacterium tuberculosis* complex indicates evolutionarily recent global dissemination. Proc Natl Acad Sci U S A. 1997; **94(18)**:9869–9874.

88. **Stenger S., and R. L. Modlin.** T cell mediated immunity to Mycobacterium tuberculosis. Curr Opin Microbiol. 1999; **2(1)**:89-93.

89. **Stocki S. L., L. A. Babiuk, N. A. Rawlyk, A. A. Potter, and B. J. Allan.** Identification of genomic differences between Escherichia coli strains pathogenic for poultry and E. coli K-12 MG1655 using suppression subtractive hybridization analysis. Microb Pathog. 2002; **33(6)**:289-98.

90. **Sudre P., G. ten Dam, and A. Kochi.** Tuberculosis: a global overview of the situation today, Bull World Health Organ 1992; **70**:149-159.

91. **Talaat A. M., R. Lyons, S. T. Howard, and S. A. Johnston.** The temporal expression profile of *Mycobacterium tuberculosis* infection in mice. Proc Natl Acad Sci U S A. 2004; **101(13)**:4602–4607.

92. **Valway S. E., M. P. C. Sanchez, T. F. Shinnick, I. Orme, T Agerton, D. Hoy, J. Scott Jones, H. Westmoreland, and I. M. Onorato.** An outbreak involving extensive transmission of a virulent strain of Mycobacterium tuberculosis, N Engl J Med 1998; **338**:633-638.

93. **van Soolingen D., P. E. de Haas, P. W. Hermans, and J. D. van Embden.** DNA fingerprinting of Mycobacterium tuberculosis. Methods Enzymol. 1994; **235**:196-205.

94. **Winstanley C.** Spot the difference: applications of subtractive hybridisation to the study of bacterial pathogens. J Med Microbiol. 2002; **51(6)**:459-67.

95. **Wozniak T. M., A. A. Ryan, J. A. Triccas, and W. J Britton.** Plasmid interleukin-23 (IL-23), but not plasmid IL-27, enhances the protective efficacy of a DNA vaccine against Mycobacterium tuberculosis infection. Infect Immun. 2006 **74(1)**:557-65.